CONSERVATION OF 19TH AND EARLY 20TH CENTURY OIL PAINTINGS: STUDIES OF PIGMENT DISCOLOURATION BY SCANNING ELECTRON MICROSCOPY

By

Rachel Elizabeth White

SUBMITTED IN FULFILLMENT OF THE
REQUIREMENTS FOR THE DEGREE OF
DOCTOR OF PHILOSOPHY
AT THE
UNIVERSITY OF TECHNOLOGY, SYDNEY
AUSTRALIA
2007

Certificate

I certify that the work in this thesis has not previously been submitted for a degree nor has it been submitted as part of requirements for a degree except as fully acknowledged within the text.

I also certify that the thesis has been written by me. Any help that I have received in my research work and the preparation of the thesis itself has been acknowledged. In addition, I certify that all information sources and literature used are indicated in the thesis.

Production Note:
Signature removed prior to publication.

Signature of Author

For Lawson

Table of Contents

List of Figures

List of Tables

Nomenclature

Table 1: List of symbols and abbreviations

amu	atomic mass units
BSE	backscattered electrons
DTG	Differential Thermogravimetric Analyses
$E_\circ$	Electron beam energy
ESEM	Environmental Scanning Electron Microscope
nA	nanoamps
nm	nanometre
SEM	Scanning Electron Microscope
T	Torr
TG	Thermogravimetric Analyses
WOF	width of field
XRD	X-ray Diffraction

Abstract

The discolouration of artistic oil paintings due to pigment interaction has been a concern for artists and painting conservators since the early 1800s. Since then there has been considerable speculation on the origin and mode of this discolouration. This project sought to determine what discolouring interactions between pigments exist in historic oil paintings and to understand the mechanisms involved. The discolouring pigment system was studied using x-ray diffraction, thermal analysis, x-ray microanalysis techniques and hydration experiments using an Environmental Scanning Electron Microscope.

A discolouring chemical interaction between cadmium yellow (a cadmium sulfide pigment) and malachite (basic copper carbonate) was identified. The darkening reaction between copper containing pigments and the range of cadmium sulfide pigments was established to be the only discolouring that occurs between artistic pigments investigated in this work. This interaction occurs due to copper ions being mobile in the drying oils used for oil painting. The copper ions are taken up by the oil medium and transported throughout the oil layer to adjoining paint layers. Any cadmium sulfide present in the oil painting will undergo ion exchange at its surface with the copper ions in the medium to produce copper sulfide. The copper-cadmium ion exchange was found to continue until the cadmium sulfide is completely converted to copper sulfide. For the combination of cadmium yellow and malachite it was established that the discolouring copper sulfide was covellite, CuS.

Acknowledgements

I acknowledge my gratitude for the guidance, knowledge and assistance of my principal supervisor Associate Professor Matthew Phillips and my great appreciation of the assistance and support of my co-supervisors Dr Paul Thomas and Dr Richard Wuhrer.

Special thanks are due to Katie McBean and Mark Berkahn for their invaluable help and support over the course of this project. Jean Paul Guerbois, Dr Norman Booth and Anthea Harris are acknowledged for their extensive technical assistance. I would like to express my gratitude to Paula Dredge from the Art Gallery of New South Wales for providing samples and images along with her ongoing assistance with all facets of painting conservation. Thanks also to the friendly and helpful staff at Parkers - Sydney Fine Art Supplies in the Rocks.

The friendship, support and assistance I received throughout from Kin Friolo, Katie McBean, Dr Brian Reedy, Dr Scott Morgan and Victor Lo has been greatly appreciated. Thank you to my proof readers, Dr Ross White, Dr John Miles and Lawson Goulter for their valuable input.

Finally, I'd like to recognise my family and thank them for their continued love and support.

Chapter 1

Introduction

1.1 Pigment interaction in historic oil paintings

The discolouration of a paint layer due to chemical interaction of pigments is one of numerous processes that can affect the appearance of an oil painting. These processes can arise from the materials and methods used to construct the paint film or the environment the painting is exposed to after it is completed.

Oil painting has had a long and varied history with painting methods and materials constantly changing over time. The use of drying oils for artistic paintings became common across Europe in the seventeenth century (Doerner 1984, Mayer 1991). Since that time, the importance of a high level of craftsmanship associated with paintings deteriorated and was overridden by artistic concerns. The catalyst for this shift was the Industrial Revolution during the late eighteenth and much of the nineteenth centuries. Commercial manufacturing freed artists from the production of their materials and scientific advances provided a broad range of new artistic resources (Mayer 1991). Over time these developments eroded the skills that artists required to construct a permanent paint layer.

Writers on artistic technique in the nineteenth century were concerned with the visual permanence of oil paintings (Carlyle 2001). These concerns included the yellowing of the paint layer, the darkening effect of air pollution and changes in pigments (Carlyle 2001). The discolouration due to chemical interaction was a particular concern, and centred around the role of lead in darkening of paint layers (Carlyle 2001). Much of the literature at the time suggested that paints containing lead and copper would darken when in contact with sulfide-containing paints (Section 2.3). The origin for these problems was shifted between the new pigments (Mayer 1991), the artists and their colourmen (Carlyle 2001), who produced and provided materials.

1.2 Motivation

The motivation for this project stemmed from the examination of historic Australian oil paintings by scanning electron microscopy to determine the pigments used and paint application methods to establish an appropriate conservation strategy for these works (Dredge *et al.* 2003). As part of the studies, a tiny fragment of crumbling paint from a lower region of *Summer*, a painting by the Australian artist Phillips Fox, was observed to have discolouration between a yellow paint layer and a green paint layer. This project was initiated to study the sources of discolouration by pigment interaction and to examine these discolourations via novel scanning electron microscopic and x-ray mapping techniques. This involved the use of both conventional and Environmental (or low vacuum) Scanning Electron Microscopes. X-ray mapping and scatter diagram analysis techniques were used to study the progress of pigment interaction for the first time. The Environmental Scanning Electron Microscope (ESEM) allows experiments to be performed and monitored at a microscopic level, and the opportunity exists to examine any pigment interactions *in-situ*. In addition, potential risks for modern oil paintings, as well as the restoration and conservation of existing works, were investigated.

Scanning electron microscopy (SEM) and Environmental scanning electron microscopy (ESEM) are becoming standard instrumentation for the study of artistic and historic conservation objects. These forms of visualisation and microanalysis are part of a vast array of scientific techniques that are being applied to art and historic objects (Lahanier 1991). ESEM is particularly useful in the examination of samples from conservation objects as samples do not need to be prepared by drying and applying a conductive coating required for conventional SEM (Doehne & Stulik 1990, Barnes 1991, Stulik & Doehne 1991). This allows precious samples to

be easily examined by other techniques. The ESEM has been used to study cross-sections of paint fragments for pigment identification (Bower *et al.* 1994). The use of ESEM as an experimental tool for studying the degradation processes that occur in conservation objects is a growing field. This technique provides new information on how these processes occur at a microscopic level and provides greater understanding of the material and its behaviour. Studies to date include: the examination of the effect of deliquescence and recrystallisation of salts in the Dead Sea Scrolls (Wallert 1996), cracking of paper (Grön & Beghello 1996) and albumen photographs (Messier & Vitale 1993), humidity cycling in adobe building materials (Doehne & Stulik 1991), and the corrosion of lead by air pollutants (Doehne & Stulik 1991). In this project, the ESEM is used for the first time to examine chemical interactions between oil paint pigments that produce discolouring effects in artistic oil paintings.

1.3 Thesis structure

This thesis begins with a comprehensive examination of the relevant literature pertaining to the discolouration of oil paintings from the nineteenth and early twentieth centuries. This led to the identification of potentially discolouring pigment combinations that will be tested experimentally.

The products of any ensuing interaction will be characterised and the mechanism of discolouration examined. The progress of these interactions will be investigated in detail using a variety of characterisation and microanalysis techniques. The SEM techniques that were employed in this work are detailed including the innovative use of x-ray mapping and scatter diagram analysis under conventional (high vacuum) SEM. The *in-situ* capabilities of the ESEM will be exploited in an attempt to visualise interactions as they occur.

Observations made of the interaction are depicted and inferences from the characterisation experiments are drawn to create a model for pigment interaction. The scanning electron microscopic techniques developed for the analysis of the interaction system are described and their success determined. These studies will expand the SEM experimentation techniques available to conservators and scientists for the examination of pigment processes.

Finally conclusions relevant to conservators, restorers and modern oil painters will be included to further the understanding of historic oil paintings.

1.4 Publications

Publications arising from this work:

Rachel White, Matthew R. Phillips, Paul Thomas and Richard Wuhrer, *In-situ Investigation of Discolouration Processes Between Historic Oil Paint Pigments*, Microchimica Acta, EMAS/IUMAS Special Issue, volume 121, no. 1-2, pages 310-322, 2006.

R.E. White, P.S. Thomas, M. R. Phillips and R. Wuhrer, *A DSC Study of the Effect of Lead Pigments on the Drying of Cold Pressed Linseed Oil*, Journal of Thermal Analysis and Calorimetry, volume 80, pages 237-239, 2005.

1.4.1 Proceedings and prizes

Proceedings and prizes arising from this work:

R.White, M.R. Phillips, P. Thomas and R. Wuhrer, *In-situ investigation of discolouration processes between historic oil paint pigments*, Third meeting of the International Union of Microbeam Analysis Societies (IUMAS-3), May 2005, Florence, Italy. Student prize for presentation in the Young Scientist's session and Australian Microbeam Analysis Society student bursary.

R.White, M.R. Phillips, P. Thomas and R. Wuhrer, *Discolouration processes of artistic oil paint pigments - in-situ ESEM investigations*, AMAS VIII - The eighth biennial symposium of the Australian Microbeam Analysis Society, February 2005, Melbourne, Victoria. Australian Microbeam Analysis Society student bursary.

Rachel White, Matthew Phillips, Paul Thomas, Richard Wuhrer and Paula Dredge, *Interactions between pigments in 19th and early 20th century oil paintings - in-situ studies using the Environmental Scanning Electron Microscope*, Microscopy and Microanalysis 2004, August 2004, Savannah, Georgia, USA. Microbeam Analysis Society Distinguished Scholar Award.

R. White, M.R. Phillips, P. Thomas, P. Dredge and R. Wuhrer, *In-situ ESEM studies of chemical interactions between artistic oil paint pigments*, Australian Conference on Microscopy and Microanalysis (ACMM) 18, February 2004, Geelong, Victoria. Australian Microbeam Analysis Society student bursary.

R. White, M.R. Phillips, P. Thomas, P. Dredge and R. Wuhrer, *Conservation of 19th and Early 20th Century Oil Paintings In situ Studies Using the Environmental Scanning Electron Microscope* AMAS VII - The seventh biennial symposium of the Australian Microbeam Analysis Society, February 2003, Melbourne, Victoria. Australian Microbeam Analysis Society student bursary.

Chapter 2

Discolouring interactions of historic oil paint pigments

2.1 Discolouration of artistic pigments

Since the mid nineteenth century artists have been aware of problems associated with pigment discolouration in oil paintings. These problems coincided with the development of synthetic manufacture of chemicals and the production of new pigments during the Industrial Revolution, which spanned the late eighteenth and the nineteenth centuries. Discolouration of paint layers was detected relatively quickly and many writers concerned with artistic materials and methods, such as Church (1892) and Standage (1892), warned artists of the dangers of incompatible pigments. In an era when artists were exploring new methods of expression, as in the Impressionist movement, the new bright pigments being produced were considered essential colours (Ives 1996) and the warnings were not always heeded. Compounding this problem was the anecdotal and at times conflicting information artists received from various manuals and handbooks (Gettens & Sterner 1941). The discolouration of oil paint layers due to pigment interaction became one of the many problems found in oil paintings from this period until many of the problematic pigments, like emerald green, fell out of use due to their toxicity or were replaced by other formulations (Fiedler & Bayard 1997). Even at the date of this study there is still considerable conflicting opinion (Mayer 1991, Ives 1996, Fiedler & Bayard 1997) on which nineteenth century pigments interact and which do not.

2.2 Oil painting

Oil painting has been a major art form since the sixteenth century. It gradually took over from tempera painting (an egg-yolk based medium) and from the seventeenth century onwards, it was the predominant form of painting (Mayer 1991). The relative ease of the construction of an oil painting and the relatively minor variance between wet and dry colour made it a popular technique that is still in use today. Over the centuries the technique has evolved, changing with innovations by artists as well as the availability of new materials and production methods.

The construction of an oil painting consists of a number of layers of different materials. Firstly, the support on which the design is to be painted must be prepared. The support is generally a wooden frame or board with canvas stretched over it, although artists have used all manner of materials from wood panels to sheets of metal or paper to achieve their desired effects. This support is then treated by applying a ground layer, which provides a suitable degree of absorbency and "tooth" (roughness) to allow the chromatic paint layer to be applied with ease. The ground layer is generally made up of chalk or gypsum, occasionally with the addition of some white lead pigment, mixed with glue. This layer is sometimes covered with a layer of white paint (usually a lead white pigment mixed with drying oil) to produce a whiter surface on which to begin painting. Originally artists produced their own canvases but as the nineteen century progressed, pre-prepared canvases became available from art suppliers.

Coloured paints were produced by combining pigments with a drying oil. This can be done by hand by simply grinding a pigment into a drying oil (usually linseed oil) until the desired consistency is obtained. The amount of oil required to bring a pigment to an appropriate painting consistency varies between pigments. Most artists' texts, including Doerner (1984) and Mayer (1991), contain tables of oil absorption by

pigments. These list the amount of drying oil required to blend the pigment into a usable paint. The quantity of oil required is expressed as a percentage of the quantity of the pigment. For example, 10 to 15% oil to pigment is required to produce Naples Yellow (lead antimony oxide) paint; this means 10 to 15 weight of oil to 100 weight of pigment is used (Mayer 1991). A list of the oil absorption values (obtained from Mayer (1991)) for pigments being discussed in this work is included in Table 2.1. It is important to achieve the correct ratio of drying oil and pigment as excessive oil can lead to wrinkling of the paint and too little oil will not bind the pigment properly and result in crumbling (Mayer 1991).

Table 2.1: Oil absorption values

Pigment	Oil absorption value (% oil by weight)
Cadmium yellow	16 to 30%
Lead white	11 to 15%
Vermillion	10 to 16%
Emerald green	around 13%

The handling and drying properties of a paint can be altered by additives. These include solvents, like turpentine, waxes and resins. These formulations along with alternative drying oils (in place of linseed oil) are too numerous to discuss here. Each combination of these various pigment binding media has been developed since oil painting began to suit the needs of artists in creating particular visual effects. During the nineteenth century, the production of paints moved from being the domain of the artist to a commercially available product sold in tubes and pouches. All of the

various materials used by artists, specifically during the nineteenth century, are well documented in various instructional and reference texts of the era, including Standage (1892), Church (1892), Doerner (1984) (originally published in the 1920s) and Gettens & Stout (1966) (reprint of the 1942 edition). A recent and comprehensive collection of information relating to the materials and techniques of English nineteenth century oil painting is presented in *The Artist's Assistant* by Carlyle (2001).

The technique involved in placing down the chromatic layers of paint to produce a picture is individual to both artists and particular schools of painting, such as impressionism or cubism. However, there were some basic rules, which are still true today, to be taken into account to ensure a stable paint film after the painting is dry. For example, the flexibility of the paint layers is important as the painting of a less flexible layer (also known as a lean layer) over a more flexible (or fat) layer will result in the cracking of the top layer as the painting dries and flexes. The process of creating a good quality oil paint film in a painting is detailed by many artistic technique authors (Doerner 1984, Mayer 1991).

After the painting is completed it is allowed to dry. This drying is the oxidation of the drying oils within the paint film which solidifies the paint layers. The process is autoxidative and occurs between the drying oil and atmospheric oxygen to produce peroxy compounds which then form complex molecules by linking the various glyceride molecules present in the oil (Nylén & Sunderland 1965). The cross-linking solidifies the paint from the surface of the painting inwards as the oxygen migrates through the paint. Drying can be accelerated by pigments or drying agents, that contain lead, manganese or cobalt compounds which catalyse the autoxidation process (Nylén & Sunderland 1965). Over time the paint film ages and other processes begin to occur in the paint film. Depolymerisation and chain scission occur which result in shrinkage of the paint film (Nylén & Sunderland 1965). The complex processes involved in paint film drying are examined in detail by Wexler (1964) as well as Nylén

& Sunderland (1965). After the painting has been allowed to dry fully, a process that may take several years depending on the thickness of the paint layers, it is varnished. This was done to protect the paint layers from atmospheric pollution as well as to saturate colours and produce even gloss across the painting (Carlyle 2001). As with all painting materials there is a myriad of different varnish formulations that have been used (Gettens & Stout 1966, Doerner 1984, Mayer 1991).

Oil painting enjoyed a period of excellence during the seventeenth and early eighteenth centuries where paintings were produced with great care and many works have survived in good condition to this day (Mayer 1991). However, as the Industrial Revolution progressed, the preparation of artistic materials was increasingly outsourced as artists became more concerned with artistic expression than craftsmanship (Mayer 1991). Innovations allowed the preparation of artistic paints in pouches or tubes where previously artists had to blend the oil and pigment by hand prior to painting. New colourful pigments became available, a byproduct of scientific advancements in this era. The combination of these factors has subsequently been observed to result in many of the problems associated with oil paintings of the nineteenth and early twentieth centuries. The poor condition of modern oil paintings compared to those of previous eras was a concern for artists and art writers during the nineteenth century (Mayer 1991, Carlyle 2001). A number of nineteenth century artistic manuals (such as Doerner (1984)) include sections on replicating the methods of the Old Master painters. Changes in the way artistic materials were being prepared was a part of this concern (Doerner 1984). There was well founded suspicion (Townsend *et al.* 1995) that materials, especially paints, were being vitiated by the manufacturers. There was significant discussion in England at the time on who was responsible for the decline in quality of artists' materials - the artists or the colourmen who provided them (Carlyle 2001). The fault was shifted between the incompetent use of materials by the artist to ineffective preparation and even substitution of pigments

by the colourmen and their manufacturers (Carlyle 2001).

Stability issues in oil paintings stem from three main causes - the materials used to produce the painting, the method of applying the paint and the environment in which the painting is stored after it has been completed. A painting is composed of a number of layered materials - a support, the ground layers, the pigmented paint layers and the varnish. An individual pigmented paint layer can be composed of a number of pigments and the drying oil, as well as waxes and turpentine, used to alter the working properties of the paint. The long term stability of each of these materials, in each of the layers, will effect the lifetime of the artwork. For example, the choice of a hot-pressed linseed oil over a cold-pressed linseed oil will lead to accelerated embrittlement of the paint film (Mayer 1991). Interactions between materials need to be avoided to preserve the desired appearance of the painting. Although oil painting is a more flexible artistic technique than tempera painting, oil paintings need to be constructed with some thought to long term stability. Lack of adhesion, cracking, flaking and wrinkling of the final paint film can all be caused by inappropriate creation of the ground and paint layers (Mayer 1991). Over the centuries many artistic theory texts have gone to great lengths to inform artists of the proper way to create a durable paint film including instructions to avoid discolourations in the paintings (Carlyle 2001). Detailed descriptions of the proper process can be found in Doerner (1984) and Mayer (1991). The environment to which a painting is exposed can significantly undermine the stability of the materials. Fluctuations in temperature and humidity can lead to a multitude of problems and are a cause of cracking and lack of adhesion (Mayer 1991). Exposure to ultra-violet light causes premature embrittlement of the paint layer, resulting in flaking (Mayer 1991).

2.3 Discolouration of oil paintings

Discolouration is one of the many disfiguring problems that can occur in oil paintings and can significantly affect the intended appearance. It can be caused by chemical interaction between pigments, the interaction between the painting and the environment and by the aging of the paint layer. Yellowing of oil paint as it dries and ages occurs to greater or lesser extent with all drying oils (Nylén & Sunderland 1965, Mayer 1991) and this can affect the appearance of light coloured paints. Lineolic acid (a triglyceride found in varying amounts in all drying oils used for painting), in the presence of moisture and lack of light, produces the greatest yellowing colour. Of all the drying oils used in paintings, linseed oil is the most common and has the highest lineolic acid content and, hence, the greatest propensity to yellow. The yellowing effect can be minimised by careful selection of drying oil other than linseed oil, such as poppy or walnut oil (Mayer 1991).

Some discolouration of pigments occurs on exposure to the environment. Hydrogen sulfide present in the atmosphere, as a byproduct of fossil fuel burning, is noted as a potential source of discolouration in pigments (Standage 1892, Carlyle 2001). This is especially significant in watercolour paintings, manuscripts and murals as there is little or no binding medium to protect the pigment particles from the air (Gettens *et al.* 1993b). The discolouration occurring between lead white pigment and hydrogen sulfide was well known to early writers (Standage 1892). Recently lead- and copper-containing pigments have been shown to convert to lead sulfide and copper sulfide on contact with hydrogen sulfide gas (Smith & Clark 2002). In some cases the dark discolouration product of lead sulfide can be converted to lead sulfate and its white appearance restored (Gettens *et al.* 1993b, Mayer 1991). There is little evidence to suggest that hydrogen sulfide will darken pigments bound in paint layers, particularly those that have dried to some degree. The discolouration of vermillion

pigment (mercury sulfide, HgS) in paint layers is often mistaken as a chemical interaction with lead white pigment (basic lead carbonate, $PbCO_3.Pb(OH)_2$) (Gettens & Sterner 1941). This darkening is caused by conversion of red vermillion (also known as cinnabar) to the black metacinnabar structure, a less dense cubic structure than the hexagonal red cinnabar (Gettens *et al.* 1993a). The presence of impurities in the pigment, such as thiosulfate, leads to instability of the red pigment (Gettens *et al.* 1993a) and the presence of chloride ions in a moist environment can accelerate discolouration by catalysis of the transformation to the black structure (Spring & Grout 2002). Copper sulfides are also produced as corrosion products on copper and bronze objects in anoxic conditions (Scott 2002).

The discolouration of an oil paint layer due to chemical interaction between pigments is a complex problem to investigate. Since the late nineteenth century, the darkening effect that interaction between pigments has on paint layers has been reported regularly in artistic texts (Church 1892, Standage 1892), art material dealers' catalogues (Gettens & Sterner 1941) and in artists' notes (Standage 1892, Fiedler & Bayard 1986, Carlyle 2001).

Several texts indicate different combinations of pigments that darken when in contact and omit other combinations highlighted in other texts. Church (1892) refers to both malachite and emerald green being darkened on contact with cadmium yellow but there is no mention of darkening with verdigris (a copper acetate pigment) which Standage (1892) indicates is "more fugitive and liable to change" than emerald green or malachite. Even recent texts omit interactions cited in previous texts. Mayer (1991) mentions the potential for cadmium yellow pigments to be discoloured by lead-containing pigments but overlooks the discolouration with the copper-containing pigments which are still in use today. Overall the general consensus is that lead- and copper-containing pigments will react with sulfur-containing pigments in oil paint (and other media) to produce a dark discolouration of that region of paint. This dark

discolouration between pigments is a permanent colour change but in some cases it can be removed mechanically (Salvadó *et al.* 2003). The occurrence of this particular type of discolouration between two incompatible pigments in specific paintings is not well reported. This may be due to the discolouration not being sufficiently disfiguring to draw attention to itself or because the regions affected are small or deep enough within the painting not to cause noticable visual change. A John Peter Russell oil painting is reported to be suffering discolouration due to the incompatible combination of cadmium yellow and emerald green (Ives 1996). Another oil painting, *Summer* (Figure 2.1), by the Australian artist Phillips Fox has sections of paint discoloured by this same interaction. The discolouration interface between layers of cadmium yellow and emerald green paint is visible on the optical micrograph in Figure 2.2. This discolouration was discovered in a tiny fragment of crumbling paint from a lower section of the painting, beneath the feet of the character. That region of the painting did not show any noticable discolouration. It is uncertain if pigment discolouration plays a role in the instability of an oil paint layer.

Gettens & Sterner (1941) studied a number of pigment combinations to determine which were incompatible. They found that a mixture of emerald green and cadmium yellow paints was the only combination that discoloured, and concluded that pigment incompatibility was rare. Their definition for a chemical pigment interaction was a mixture of two pigments that "undergo double decomposition which results in complete or partial change for both pigments in the chemical sense and alteration in the original tone of the mixture". Lead white, one of the pigments most commonly declared as incompatible, was reported not to produce discolouration. Its reputation to discolour was attributed to the presence of lead acetate (also white) in the pigment from the manufacturing process or the conversion of vermillion to its black morphology (Gettens & Sterner 1941). The suggestion is that incompatibility between pigments could have been due to impurities in pigments (Gettens &

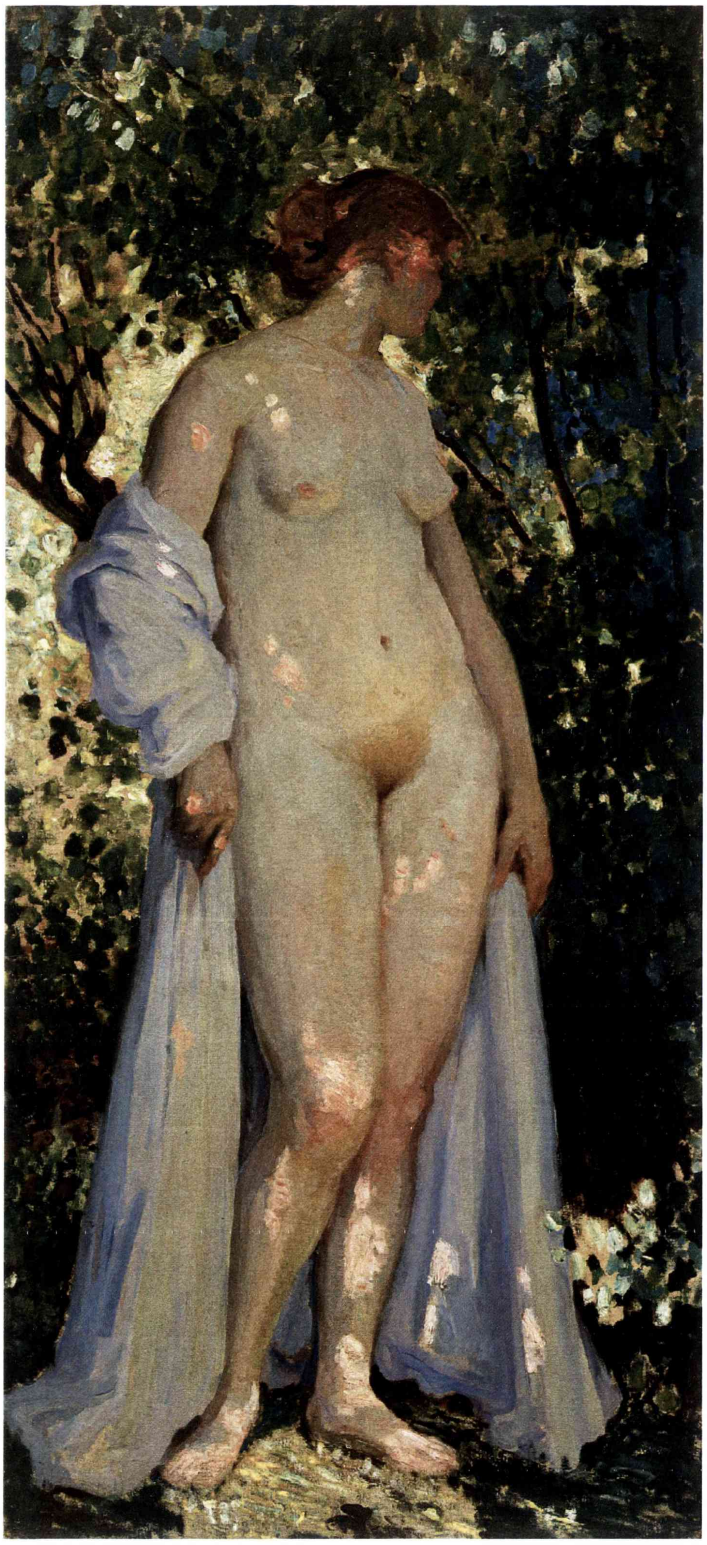

Figure 2.1: *Summer* by Phillips Fox, 1912. Art Gallery of New South Wales, Sydney, Australia (reproduced with permission).

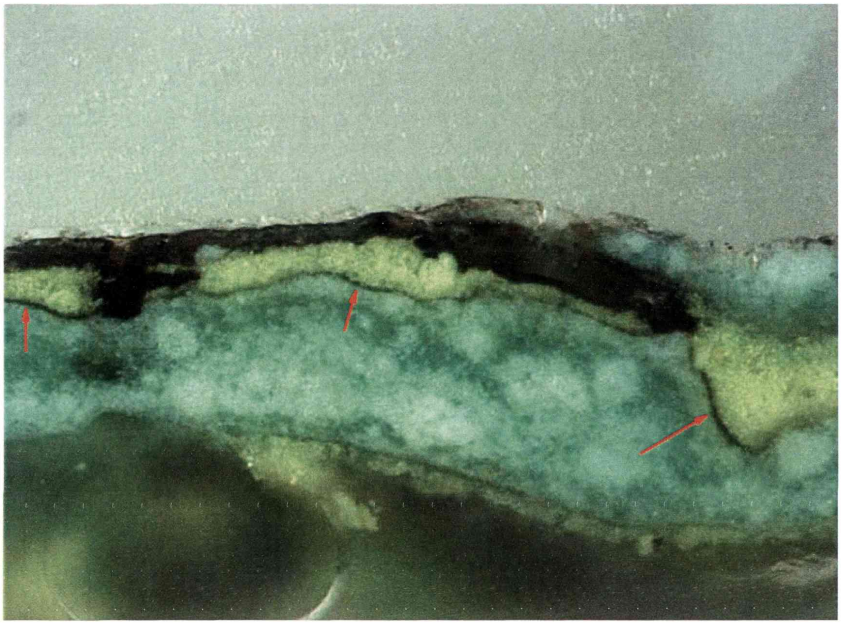

Figure 2.2: Optical micrograph of the cross-section of a paint fragment taken from the lower region of Phillip Fox's *Summer* (1912), showing the darkened interface between cadmium yellow and emerald green paints (reproduced with permission).

Sterner 1941, Fiedler & Bayard 1986) resulting from early manufacturing methods. It is unclear if adulterated pigments played a role in the determination of incompatible pigment combinations. However, due to the fairly common practice of adulteration and substitution of pigments and paints during the late nineteenth century (Townsend *et al.* 1995, Carlyle 2001), artists may have unwittingly created discolouring mixtures.

The darkening combination of emerald green and cadmium yellow was well known to many writers (Church 1892, Gettens & Sterner 1941, Doerner 1984) and artists (Standage 1892, Fiedler & Bayard 1986). Emerald green was an extremely popular pigment in the 19th century. It was rapidly taken up as an artists' pigment soon after it was developed in the early 1800s and continued to be used as an artists' pigment until the mid 20th century. This is despite its toxicity and incompatibility being well known from its early use (Fiedler & Bayard 1997). An example of this chemical interaction was reported to be observed in John Peter Russell's 1891 oil painting *Vue d'Antibes* (Ives 1996). A micrograph of a paint layer fragment cross-section shows a darkened region at the interface between emerald green and cadmium yellow paint layers (Ives 1996). Ives (1996) indicates that the fragment was taken from a region of the painting where an upper layer of paint had been weakened and lost due to this interaction between cadmium yellow and emerald green. As a result, foreground areas of the painting suffered loss of paint and discolouration. It is suggested by Ives (1996) that more than one deterioration process may be occurring. However this apparent eruption of the underlayer of cadmium yellow may be due to chalking of that pigment which is known to occur in paintings that do not contain emerald green or other potentially darkening pigments (Leone *et al.* 2005).

Russell is said to have used the combination of emerald green and cadmium yellow pigments extensively in his paintings (Ives 1996). However, there is no indication in the literature that his paintings have widespread regions of discoloured paint. It may be that these regions of the combination of these pigments are small, or that due

to the style of painting (wet paint over dry, as opposed to wet paint over wet), the interface of dark discolouration would not be large enough or close enough to the surface to affect the outward appearance of the paint layer.

2.4 Chemistry of pigment interaction

There is little recent literature discussing the processes of pigment discolouration in oil paintings. Research on an oil painting by Joan Miró, a surrealist artist, showing spots of dark discolouration offers extensive discussion on the production of copper sulfides in oil paint (Salvadó *et al.* 2003). The painting examined was a cadmium sulfide-pigmented oil painting over a copper plate (treated with garlic and coated with a lead white ground layer). The black spots present on the surface of the painting were found to be copper sulfides by x-ray diffraction (Chalcocite-Q($Cu_{1.95}S$), Roxbyite (Cu_7S_4) and Yarrowite (Cu_9S_8)). These spots were produced by copper ions being extracted from the support by forming free fatty acid salts with the drying oil and diffusing through the paint layers to the cadmium sulfide paint layers and forming dark coloured copper sulfides. The intermediary lead white oil paint layer was ruled out as a cause of the discolouration, as its fatty acid salts are stable and not mobile, but its presence was not an obstruction to the copper ion diffusion (Salvadó *et al.* 2003).

The mobility of copper ions in drying oil paint films is known to occur by the formation of complexes with the fatty acids (Gunn *et al.* 2002). This extraction of copper ions occurs when a copper-containing pigment is in contact with the complexing compounds in the oil or if the complexing compounds are in adjacent paint layers to the pigment (Gunn *et al.* 2002). The progress of the discolouration slows as the oil paint film dries, the oil becomes more viscous as it dries and the diffusion of copper ions is slowed until the drying process is finished (Salvadó *et al.* 2003). The fact that potentially discolouring ions move freely throughout a paint film while it is drying means that the suggestion by a number of writers (Gettens & Sterner 1941, Mayer 1991, Ives 1996) that "locking" pigments into oil by careful grinding of the pigment with the drying oil (in an attempt to coat each particle with the oil to

protect it) is not correct for copper pigments. This technique would be ineffective in preventing or slowing discolouration due to pigment interaction in such cases as the oil is a transport medium for the copper ions.

The mechanism proposed by Salvadó *et al.* (2003) for the discolouration between copper ions and cadmium sulfide pigment is based on a study of the binding of copper to non-stoichiometric nanoparticles of cadmium sulfide (Isarov & Chrysochoos 1997). Cadmium sulfide is a sparingly soluble compound in aqueous solution, with a solubility product (K_{sp}) of 800 x 10^{-28}M (Lide 1993-1994). However, this is significantly higher than that of copper sulfide (6 x 10^{-37}M for cupric sulfide and 2.26 x 10^{-48}M for cuprous sulfide) (Lide 1993-1994). The low solubility of copper sulfides compared to that of cadmium sulfide results in an exchange of copper ions for cadmium ions in the structure (Isarov & Chrysochoos 1997):

$$(CdS)_n + Cu^{2+} \longrightarrow Cd_{n-1}CuS_n + Cd^{2+}$$

Small particles of copper sulfides, Cu_xS (where x = 1 to 2), are formed on the outside of cadmium sulfide particles as copper(II) ions replace cadmium ions in the lattice (Isarov & Chrysochoos 1997). Salvadó *et al.* (2003) suggested that a mechanism similar to this solid state mechanism occurs in drying oils with copper ions being transported to the cadmium sulfide pigments as free fatty acid salts.

2.4.1 Copper sulfide production

The presence of copper sulfide as the discolouring entity in paintings has long been speculated (Church 1892, Standage 1892, Gettens & Sterner 1941). However virtually no systematic chemical analyses and spectroscopic studies have been carried out on such discoloured paintings. In contrast, the production of copper sulfide from contact between cadmium sulfide and copper ions is a well-known process in the manufacture

of solar cells. There has been extensive analysis of the system carried out in that context.

Cadmium sulfide-copper sulfide thin film solar cells were developed in the mid-1950s as a low cost, low weight flexible alternative to silicon solar cells (Stanley 1975). Although they were not adopted as mainstream photoelectric devices, there has been extensive research into their creation and function. During production of the solar cells copper sulfide is topotaxially formed on the surfaces of a cadmium sulfide substrate (Stanley 1975). This creates a heterojunction between the n-type CdS semiconductor substrate and the thin p-type Cu_xS layer (van Overstraeten & Mertens 1986).

The heterojunction is produced by several methods, the main technique being the Clevite process and its variations. In this process, cadmium sulfide surfaces are dipped into a heated copper chloride chemiplating solution, producing a layer of copper sulfide on the cadmium sulfide surface (Green 1986). This conversion from cadmium sulfide to copper sulfide occurs by an ion exchange reaction (Buckley & Woods 1974):

$$CdS + 2Cu^{+} \longrightarrow Cu_2S + Cd^{2+}$$

This copper sulfide layer is polycrystalline (te Velde 1975). The rate of growth of the copper sulfide layer into the surface of the cadmium sulfide is limited by the diffusion of copper ions through the copper sulfide layer to the cadmium sulfide surface (Buckley & Woods 1974). The passage of copper (towards the interface) and cadmium (away from the interface) ions occurs through numerous tiny gaps in the copper sulfide, produced by the slight difference in crystal structure between the cadmium sulfide and copper sulfides as the copper sulfide layer forms (te Velde 1975). The exchange can continue until the cadmium sulfide is completely replaced by copper sulfide unless removed from the chemiplating solution.

Solid-state reactions are another technique used to produce the copper sulfide

layer (te Velde & Dieleman 1973). Here cuprous chloride vapour is deposited onto a cadmium sulfide crystal surface and reacts entirely to produce copper sulfide on heating by (te Velde & Dieleman 1973):

$$CdS + 2Cu_xCl_2 \longrightarrow Cu_xS + CdCl_2$$

The optimum stoichiometry of the copper sulfide layer for solar cell performance is chalcocite, Cu_2S (te Velde & Dieleman 1973). Obtaining this ideal stoichiometry is a complicated process. Other copper sulfide phases can be formed when copper ions of different oxidation states are used and chemiplating conditions are altered (Russell & Woods 1978). These phases include chalcocite (Cu_2S), djurleite ($Cu_{1.96}S$) and covellite (CuS). The formation of covellite occurs in the presence of cupric ions (Russell & Woods 1978). Cupric ions present in cuprous chemiplating process have also been associated with djurleite formation (Stanley 1975) and other sulfur-rich copper sulfides (te Velde & Dieleman 1973). The non-ideal covellite phase has also been detected at the grain boundaries of vapour deposited cadmium sulfide crystallites (Bhide *et al.* 1981) despite the use of the Clevite process to produce the ideal chalcocite phase. Hence, the cuprous chloride used in the Clevite process must be free of any cupric ions. To ensure this, the cuprous chloride is washed in hydrochloric acid to remove any Cu^{2+} ions (Hadley-Jr & Tseng 1977). Monovalent cuprous chloride is also required for the formation of the desirable copper sulfide in solid-state production method (te Velde 1975).

The phase diagram for the Cu-S system, in Figure 2.3 (Roseboom-Jr 1966), shows that the covellite phase exists at room temperature as a discrete phase. It is the predominate stoichiometry for cupric sulfide. However, higher proportions of sulfur create more complex and varied stoichiometries in the djurleite, digenite and chalcocite phases.

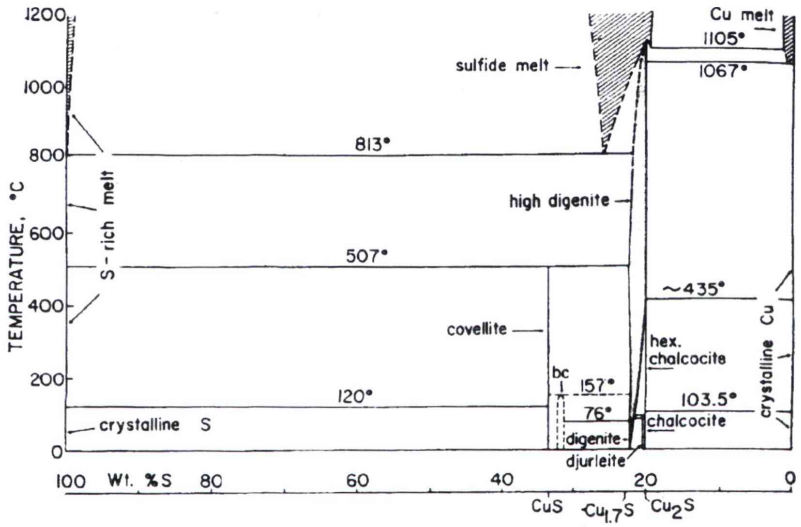

Figure 2.3: Phase diagram for the system Cu-S, from Roseboom-Jr (1966).

Chapter 3

Scanning Electron Microscopy: Instrumentation and Techniques

3.1 Scanning Electron Microscopy

Scanning electron microscopy (SEM) is a powerful tool for both visualising and obtaining elemental information about samples on a scale not achievable with optical microscopy. In this project scanning electron microscopy instrumentation and techniques are utilised in a number of ways to investigate the interaction between artistic pigments. The analyses available from SEMs have only relatively recently been applied to provide information about artistic and historic pieces. It is a technique that is frequently used in conjunction with other analytical methods to provide information on how a work of art or historic object was constructed and how it has been affected over time. X-ray microanalysis is a popular technique that has been used to examine ancient Greek and Roman pottery (Mirti 2000) and perform multi-element analysis in medieval glass samples (Kuisma-Kursula 2000). SEM instrumentation has been used in conjunction with other analyses to draw comparison between gilding techniques in post-Byzantine wall paintings (Katsibiri & Boon 2004). Doménech-Carbó *et al.* (2001) have used SEM x-ray microanalysis to examine an entire collection of paintings to help determine what, if any, undocumented repainting had been applied to the collection. Studies into deterioration of bone black pigment (van Loon & Boon 2004) and the discolouration of smalt pigment in 16th century paintings (Boon *et al.* 2001) have also utilised scanning electron microscopy. Electron microscopic analyses have also aided in confirming authenticity of Titan's 16th century *Portrait of Federico II Gonzaga, Duke of Mantua* (Tucker & DeGroft 2002).

In terms of cross-sectioned paint layer analysis, traditionally performed using optical microscopy, electron microscopy is a very useful tool. The determination of the chemical nature of a pigment by optical microscopy requires a great deal of skill and operator experience. When that pigment consists of tiny particles within a cross-sectioned paint layer containing other pigments it becomes even more difficult to

determine the nature of the pigment. In a scanning electron microscope, microscopic pigment particles can be analysed by their x-ray signal, produced during imaging, to determine the elemental composition of the pigment. This is less complex and a more conclusive technique for determining which pigments make up an individual paint layer. Dredge *et al.* (2003) used electron microscopy to examine paint layers taken from a Monet painting, *Port-Goulphar, Belle-Ile* 1887. Here, the scanning electron micrographs as well as energy dispersive x-ray spectrometry (EDS) and x-ray mapping (XRM) techniques were used to examine which pigments appeared in a fragment of the painting. These results complemented the optical microscopy observations and provided a greater understanding of the artist's painting techniques. Microanalysis performed with an SEM has also been used to confirm the presence of past restoration efforts in old Chinese paintings (Cam & Fan 2000) and to examine the use of blue pigments in Swiss church wall paintings (Cavallo 2006)

3.1.1 SEM instrumentation

In the investigations carried out in this project both conventional (high vacuum) and so called Environmental or low vacuum scanning electron microscopes were employed. The basic process by which a sample is imaged is common to both types of scanning electron microscopes. An electron beam is produced at the top of an evacuated column. As it is accelerated (to an energy between 1 and 40 keV) downwards towards the sample surface it is focussed to as small as possible diameter. The interaction of the electron beam with the sample surface produces an array of signal types from a volume below the surface of the sample which it affects. The size and shape of this interaction volume are determined by the material the sample is made of and the energy of the electron beam, with higher energy electron beams producing deeper interaction volumes. The types of signals emitted from the interaction volume include

secondary and back-scattered electrons and x-rays. These emissions are a result of the beam interacting with the atoms in the sample. Secondary electrons (SE) are loosely bound electrons from the chemical bonds in the sample and are produced from the inelastic scattering of the primary beam electrons. They are low energy electrons and only the secondary electrons produced within approximately ten nanometres of the surface are detected. Those produced below this depth are absorbed by the sample. Consequently, the SE signal carries information about the sample's surface topography. Back-scattered electrons (BSE) are also known as composition contrast electrons and are primary beam electrons that have exited the sample after undergoing elastic scattering. They can have energies up to that of the primary beam energy ($E_\circ$), and can escape the sample from micro-metre depths. The higher the average atomic number of the sample the more back-scattered electrons are produced. A measure of this is known as the back-scatter coefficient, η, which is the ratio of the number of BSE to the number of electrons incident on the specimen. This ratio can be determined by Monte-Carlo Electron-Trajectory simulation (Goldstein *et al.* 1992). The back-scatter coefficient is independent of $E_\circ$ above 1 keV, and compounds with higher average η values will appear brighter on back-scattered contrast images. X-rays are produced from the excitation and subsequent relaxation of inner core shell electrons of the atoms within the interaction volume. The intensity of these emission signals can be measured and are used to create images and to gain information about the sample. To create the image, the intensity of the selected emission signal (normally secondary or back-scattered electrons) is measured at successive points as the beam completes a raster across the sample. The magnification of the selected sample area is determined from the linear size of the raster compared to the linear size of the image on the viewing screen. Detailed descriptions of the components used to create and optimise scanning electron micrographs are available in Goldstein *et al.* (1992).

In this project, conventional scanning electron microscopy is used for x-ray microanalysis by energy dispersive x-ray spectrometry (EDS) and x-ray mapping (XRM) with subsequent scatter diagram analysis at high vacuum. A relatively new type of instrumentation, the Environmental (or low vacuum) scanning electron microscope is also utilised for its ability to tolerate low-vacuum conditions in the sample chamber. This capability was exploited to determine if this could be used to examine pigment discolouration *in situ*.

3.1.2 X-ray microanalysis

X-rays are produced by an inelastic scattering process. Here the incident primary beam electrons remove inner shell electrons from the sample atoms and x-rays are emitted as the atom's electrons rearrange to achieve its ground state. Each element in the periodic table has a characteristic x-ray emission energy spectrum resulting from the transition of electrons from other shells to replace the removed electrons. For K_α x-rays to be emitted from an atom the incident electrons from the beam need to have enough energy to remove a K shell electron, (E_c). This electron is then replaced with an electron from the L shell and a K_α x-ray is emitted as a result of that transition. Its energy is determined by the energy difference between the shell energies participating in the transition. If the electron is replaced by an electron from the M shell the emitted x-ray is a K_β x-ray. The transition of electrons from adjacent shells is more likely; therefore the K_α x-ray signal is always more intense than the K_β x-ray signal. In addition to the K-family x-rays, L-family and M-family x-rays are also produced. However, these x-rays can be produced at lower electron beam energies as the removal of electrons in the L and M shells requires less energy. The intensity of the x-ray signals produced increases with the accelerating voltage ($E_\circ$) of the electron beam to a point, then decreases due to (i) internal absorption as the x-ray escape depth increases,

and (ii) a reduction in the number of ionisation events as the overvoltage ($V=E_\circ/E_c$) moves away from its optimum value ($V \simeq 3.5$) (as discussed below). Ratios between the different K-L-M x-ray signal families will vary as accelerating voltage increases but the ratio between alpha, beta and gamma signals of each family will not in the absence of absorption effects. X-ray signal intensity is also affected by the depth of the interaction volume. X-ray signals emerging from within the interaction volume can be absorbed to a greater or lesser extent depending at what depth they were generated. In addition to the characteristic x-ray signals background or Bremsstralung radiation and secondary fluorescence occur. Background (Bremsstralung) radiation creates a continuum of x-ray signals due to the coulombic de-acceleration of the primary beam electrons, which monotonically increases towards the low energy end of the spectrum. The continuum is generally removed during analyses of the x-ray spectrum. Secondary fluorescence is the production on x-rays from the absorption of characteristic x-rays produced by the incident beam electrons. This occurs as the characteristic x-rays travel through the sample and are absorbed by the inner shell of another atom, which in turn produces an x-ray when returning to its ground state. The detection of x-rays can be accomplished using wavelength-dispersive or energy-dispersive x-ray spectrometers. In this work energy-dispersive x-ray spectrometry (EDS) has been used. Detection occurs by x-ray photons being converted to an electrical signal using a lithium-doped silicon crystal (Goldstein *et al.* 1992). The conversion of these electrical signals to voltages and finally to the production of the x-ray spectrum is covered in great detail by Goldstein *et al.* (1992). The EDS x-ray spectrum produced indentifies the elements present within the interaction volume by measuring x-ray peak intensities and correcting for matric effects. The concentration of each element can then be quantified by measuring the x-ray peak if appropriate standards are incorporated in the analyses.

3.1.3 X-ray mapping and scatter diagrams

An aspect of x-ray microanalysis is x-ray mapping (XRM), also known as compositional imaging. The x-ray signals for a particular element (from the area of the sample surface being imaged) are assembled into an image, or map, representing the locations of that element within that selected area. X-ray maps are produced by selecting a specific energy window, or region of interest (ROI), on the x-ray spectrum that corresponds to the characteristic x-ray peak of the element of interest. As the electron beam is slowly rastered over the selected surface area (with a dwell time per point or pixel generally between milliseconds to seconds) the number of x-rays with an energy within that region of interest are measured. For digital XRM the number of x-ray counts detected per pixel is recorded. The greater the number of x-rays detected in a pixel the greater is the concentration of that element. After all the x-ray counts are recorded for each pixel the relative number of counts is rescaled over a 0 to 255 grey-scale to maximise the dynamic range. Pixels with no x-ray counts are designated 0 on the grey-scale and represented as black. The largest number of x-ray counts for a pixel is designated 255 on the grey-scale and represented as a white pixel. X-ray counts per pixel, that are between no counts and the largest number of counts, are normalised from 0 to 255 across the grey-scale. These pixels are then combined to form an image which represents the spatial distribution and relative concentrations of that element in the selected mapping area. Provided the ROIs do not overlap, x-ray maps of a number of elements can be created at the one time. However, due to differences in x-ray signal intensities between selected ROIs, the relative intensity of the pixel brightness only gives an indication of variation in element concentration within a single element map and cannot be directly compared with maps of other elements. Region of interest mapping is one of a number of XRM methods which are detailed elsewhere (Goldstein *et al.* 1992, Wuhrer *et al.* 2006).

X-ray maps for different elements from the same area can be compared to indicate common distributions. An extension of this is scatter diagram analysis, or concentration histogram imaging. This analysis technique is used to determine phase associations between selected elements and visualise their distribution (Bright 1995). A frequency histogram, known as a scatter diagram, is created from the information contained in the x-ray maps for two elements. The grey-scale intensities (0 to 255) of the pixels in each x-ray map are normalised to a range of 0 to 100. This can be represented as an intensity histogram (Moran & Wuhrer 2006). A two-dimensional scatter diagram is produced by plotting the normalised pixel intensity of the same pixel from both x-ray maps against each other (Bright & Newbury 1991). The number of counts at each point can be represented on a thermal colour scale to show areas of greatest correlation (Bright & Newbury 1991).

If clusters of points, or nodes, form in the scatter diagram it is an indication that the two elements are chemically or physically associated with each other. There may be more than one cluster or node present in a scatter diagram. This indicates that more than one chemical phase containing both those elements is present. The position of a particular cluster or node relative to the axes of each element gives an indication of the relative concentration of each element within that phase (Moran & Wuhrer 2006). Hence, a node equidistant from the axes indicates a phase containing equal proportion of the two elements. Phases containing similar concentrations of the two elements may exist close together or as a single elongated node (Moran & Wuhrer 2006). If there is little or no phase association between the elements, clusters form along the individual element axes (Moran & Wuhrer 2006). Many of the software packages that are used to create x-ray maps and scatter diagrams also allow the visualisation of spatial distribution of a phase, identified by scatter diagram, to be superimposed on the original SE or BSE image of the sample area. This analysis method is useful for comparing two and three elements (in three-dimensional scatter diagrams).

3.2 Environmental Scanning Electron Microscopy

Its environmental capabilities allow the Environmental Scanning Electron Microscope (ESEM) to be used to produce and monitor physical and chemical changes in samples at a microscopic level. The particular instrument used is one of a range of electron microscopes with low vacuum or "environmental" capabilities, produced by different manufacturers, that are collectively known as variable pressure SEMs. An ESEM produced by the Philips/FEI company was used in this work. For ease, it will be referred to as the ESEM within this thesis.

3.2.1 ESEM instrumentation and features

The ESEM is different from the conventional SEMs used for x-ray microanalysis and x-ray mapping. Its design allows the presence of a higher pressure of gas in the chamber than is possible in conventional instruments. This means that uncoated and insulating samples can be analysed in their natural state and that experiments can be carried out within the microscope and the changes produced can be observed microscopically as they occur.

The higher pressures possible in the chamber of the ESEM are achieved by the placement of pressure limiting apertures between the chamber and the beam column. The vacuum system creates a pressure differential of 6 orders of magnitude across these apertures. Figure 3.1 (Morgan 2005) is a diagram of the vacuum system of an ESEM, showing the pressure limiting apertures separating the chamber from the beam column. The sample chamber, environmental chambers between the pressure limiting apertures and the beam column have separate pumping systems to produce a graduated vacuum from 50 Torr to 10^{-5} Torr in the beam column. The beam column is maintained at this high vacuum to ensure that the beam is not scattered before it reaches the pressure limiting apertures (PLAs). The pressure in the chamber is

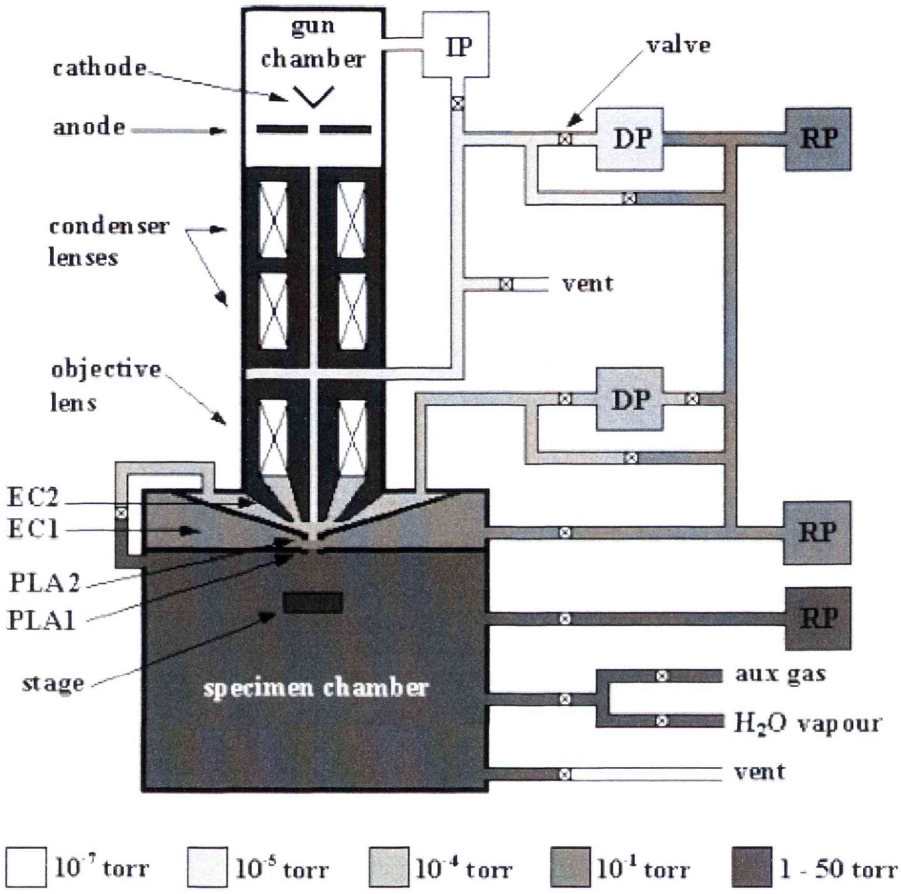

Figure 3.1: Schematic diagram showing the ESEM vacuum system. The vacuum system consists of five stages of increasing vacuum level. The stages are the specimen chamber, first environmental chamber (EC1), second environmental chamber (EC2), electron column and electron gun. The column and chamber regions are separated by two pressure limiting apertures (PLAs). The PLAs are placed close together to minimize primary electron scattering (adapted from Philips Electron Optics, 1996). IP=ion pump, DP=diffusion pump, RT=rotary pump. (Morgan 2005).

controlled by the flow of gas into and out of the chamber via the pressure limiting apertures and can be controlled to any pressure up to 50 Torr in most instruments.

As the pressure in the chamber of an ESEM is higher than in a conventional SEM there is some scattering of the electron beam after it leaves the lower PLA. The effect of this scattering is minimised by maintaining a short working distance between the final pressure limiting aperture and the sample. However, some scattering of the beam electrons does occur, and for a given gas, scattering increases with increasing chamber pressure and working distance, but this does not affect image resolution. The unscattered electrons still produce a high resolution spot on the surface of the same distribution as would occur in a vacuum (Danilatos 1997). The scattered electrons form a skirt of electrons around the spot and produce background noise (Danilatos 1997). The degree of scattering is also dependant on the energy of the electron beam, $E_\circ$. Although the scattering does not affect the image resolution it does affect the beam intensity ($E_\circ$), decreasing exponentially with increasing gas pressure and working distance, which leads to a large decrease in the intensity of the unscattered probe at low voltage and results in a loss of contrast (Danilatos 1997).

The ESEM detection systems were developed to cope with the gas atmosphere. The secondary electron signal is detected by a gaseous detection device. These devices use the gas within the sample chamber to amplify the signal. As a secondary electron leaves the sample it accelerates towards the positively biased detector. The electron collides with a gas molecule and causes the molecule to ionise, producing a gaseous or "environmental" electron and a positive ion. The effect is a cascade of electrons received by the detector that have amplified the original signal. The positive ions produced during the signal amplification are attracted to the build up of charge on the sample surface and suppress the charging artifacts on insulating samples. Generally the detection of back-scattered electrons in the ESEM is similar to conventional SEM. A scintillation detector detects the back-scattered electrons which pass easily through

the gas due to their high energy (Danilatos 1997). X-rays are detected using energy dispersive spectroscopy (EDS) detector. The amplification of the secondary electron signal is a complex process (Thiel *et al.* 1997, Thiel 1999) and can be affected by a number of variables. The ionisation efficiency of the gas used in the chamber, the distance required for the electron cascade to achieve steady state and the pressure in the chamber can be altered to optimise the signal to background ratio (Thiel 1999). Accurate detection of x-rays produced from the region of interest is marred by detection x-rays produced from the skirt electrons. This effect can be reduced by decreasing the radius of the electron skirt by either reducing the gas pressure to as low as practical or reducing the working distance if possible (Danilatos 1997). Also the use of an x-ray cone attachment that places the lower PLA closer to the specimen while maintaining the x-ray working distance and using the highest possible $E_{\circ}$ to conduct the analysis can minimise the effect.

With the need for high chamber vacuum removed, experiments can be performed in the ESEM by using different gas atmospheres and altering the gas pressure in the chamber as well as controlling a number of other parameters that can be introduced. These include heating or cooling of the sample using temperature controlled stages, devices for mechanical testing, and injectors for introducing reactants (Danilatos 1997). This capability has been used in a wide range of applications.

3.2.2 Hydration techniques

The hydration of samples within the ESEM is a common experiment. It can be used to monitor the effect of humidity and liquid water on a sample or to maintain the wet state of a sample. This capability is particularly significant for biological samples and much work has been done to develop techniques for maintaining the hydration of samples during the pump-down sequences. In this project the hydration capabilities

of the instrument were utilised both to hydrate dry samples and to maintain the hydration of already wetted samples.

The hydration of a dry sample is a simple procedure, and is achieved by using water vapour as the imaging gas. The sample is cooled to a set temperature using a Peltier cooling stage in the ESEM chamber and the chamber is evacuated to a selected pressure, below that of its saturated vapour pressure. The pressure in the chamber is raised to the saturated vapour pressure (for that temperature) and water vapour condenses on the sample. Alternatively, the sample can be placed in the Peltier stage and kept at room temperature during the pump-down sequence. The temperature is then reduced, at constant water vapour pressure, until the sample reaches the conditions for the condensation of water on the surface. The sample can then be dehydrated by decreasing the chamber pressure or increasing the sample temperature. This process can be done repeatedly to examine the effects of humidity cycling or hydration-dehydration on the microstructure of the sample. Figure 3.2 is a phase diagram for water and from it the pressure and temperature values to create the desired relative humidity can be selected.

For an already wet sample, maintaining the hydrated state throughout the pump-down sequences and imaging is more complicated. Ensuring a sample does not undergo any evaporation or condensation processes is not as simple as pumping the chamber to a pressure to provide one hundred percent relative humidity at the sample. The pumping sequence and subsequent flooding sequences must be optimised so that the sample is subjected to minimal dehydration and condensation before imaging commences (Cameron & Donald 1994). The method for minimising sample evaporation is dealt with in detail by Cameron & Donald (1994). This involves placing the sample at a low temperature (generally 3°C to 6°C using a Peltier cooling stage) and ensuring that the pressure in the chamber does not fall below the saturated vapour pressure of the sample during the initial pump-down sequence. The chamber

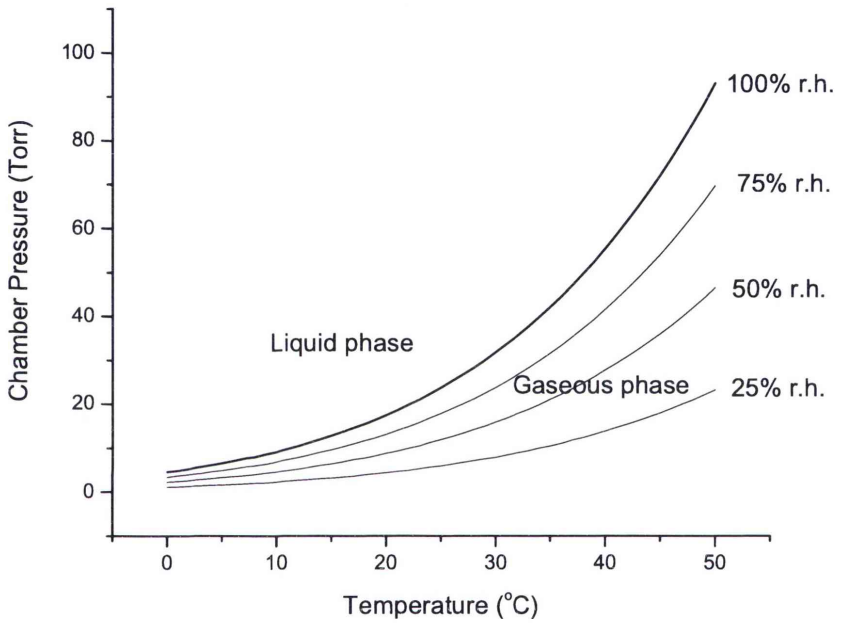

Figure 3.2: Vapour pressure diagram for maintaining relative desired humidity in the ESEM (adapted from Philips Electron Optics (1996)).

is then flooded with water vapour by raising the pressure in the chamber eight times to make sure the chamber gas is almost entirely water. Sacrificial ("free") water drops are placed on insulating parts of the Peltier stage near the sample to provide additional water vapour. There are, however, some practical difficulties with this procedure. Ideally, the sample temperature should be reduced simultaneously with chamber pressure during the initial pump-down sequence to ensure minimal condensation or evaporation occurs (Thiel & Donald 1999). This may not always be possible with samples that have poor thermal conductivity. The surface of these samples could undergo dehydration during the latter stages of the pump-down sequence if the final chamber pressure reaches its set pressure before the sample has completely cooled to the temperature required to ensure 100% relative humidity. The rate of cooling would vary from sample to sample and make this step impractical to achieve in most cases. It seems that poor thermally conductive hydrated samples would need to be chilled prior to the initial pump-down sequence and some condensation during the initial higher pressure stages of this sequence would need to be tolerated. In addition, the flooding of the chamber with water vapour by raising the pressure of the chamber repeatedly would cause condensation on the sample surface if its temperature is not raised in line with the saturated vapour pressure diagram (Figure 3.2). There is the potential for this condensation to cause disturbance of delicate samples during these procedures.

3.2.3 Use in conservation studies

As well as its advantages for biological samples the ESEM has found significant use in the field of historical object conservation. Samples taken for works of art or museum objects are generally small (so as not to disturb the appearance of the object), non-conductive, and often dirty or contaminated. This makes the use of the ESEM ideal

for such samples and has the added advantage that the sample does not need to be coated so it can then be subsequently analysed by other techniques. This is very important for historic oil paintings analysis as minimal sampling is performed.

The ESEM has also allowed dynamic studies of the degradation processes of museum objects undergo and refined their care and conservation (Doehne & Stulik 1990, Wallert 1996). Examples of the use of the ESEM as a experimental tool include studies on the cracking of albumen photographs on exposure to humidity and aqueous conservation treatments (Messier & Vitale 1993). The effect of humidity fluctuations on the salts present in the Dead Sea Scrolls has been examined dynamically by Wallert (1996), showing that the storage conditions of an object could greatly affect its stability. Humidity cycling effects have also been applied to adobe building materials to understand the behaviour of these materials and the effect of possible consolidants (Doehne & Stulik 1990). ESEM is also used to examine conservation samples that do not lend themselves to the sample preparation required by conventional SEM. Cotton swabs used to clean the Sistine Chapel have been analysed to determine if the cleaning process was removing any pigment from the ceiling (Doehne & Stulik 1990). Cross-sections of painting fragments can be examined for elemental composition and pigment position without the coating layer impeding further analyses (Bower *et al.* 1994).

Chapter 4

Experimental Techniques

4.1 Sample preparation

4.1.1 Pigment samples

The pigments examined in this project were obtained through an art supplier. All were received and used as fine dry powders. A list of pigments used and their manufacturers is included in Table 4.1. The size of pigment particles is dependent on their formation. Pigments ground from mineral samples are made up of larger particles whereas pigments produced by chemical precipitation are generally smaller, with their shape and size governed by their crystal structure. Cadmium yellow pigment was chosen as the representative pigment of the range of cadmium sulfide pigments, that range from yellow through orange to red, as it is the pigment used in the painting *Summer* (Figure 2.1). The yellow colour is achieved by a small amount of zinc sulfide in solid solution, the red by the addition of selenium sulfide and orange is the natural colour of pure cadmium sulfide. Malachite pigment was chosen as the representative green copper pigment. X-ray diffraction patterns were taken of all pigments used to characterise the pigment and ensure its expected formulation.

Table 4.1: Pigments used

Pigment name	Chemical formulation	Supplier
Cadmium Yellow	Cadmium zinc sulfide	Kremer Pigments (NY,USA)
Lead White	Basic Lead carbonate	Kremer Pigments (NY,USA)
Malachite	Basic copper carbonate	Kremer Pigments (NY,USA)
Vermillion	Mercury sulfide	Winsor and Newton (England)

Additional reagents, cadmium sulfide, copper sulfate, cadmium nitrate and sodium sulfide, were obtained through chemical suppliers (BDH and Sigma Aldrich) as general laboratory grade and used as received. Some orange coloured cadmium sulfide was produced in the laboratory from the mixture of cadmium nitrate and sodium sulfide solutions. The resulting product was rinsed extensively in deionised water to remove any remaining reagents. The product was then left to dry as a solid mass. This provided solid pieces of cadmium sulfide as an alternative sample to the finely divided cadmium yellow (a cadmium sulfide containing a small amount of zinc in solid solution).

4.1.2 Paint samples

Initially a number of potentially discolouring pigment combinations were tested by placing layers of suspected paints in contact with one another and examining their colour after a period of time. These combinations were of the lead containing pigment (lead white) or malachite (a copper-containing pigment) with sulfide-containing pigments (cadmium yellow and vermillion). The combinations used are listed in Table 4.2. All paint samples were prepared using windmill cold-pressed linseed oil supplied by Sthebeningen (Holland). The paints were prepared by blending the dry pigment with cold-pressed linseed oil on a ground glass plate using a muller (a circle of ground glass with a handle shown in Figure 4.1d) or a spatula. Paints were made up to an artistic paint consistency, according to the oil absorption values for the pigments (Section 2.2). The blending of pigment and linseed oil on a glass plate using a palette knife and a glass muller is a traditional method of paint making (Figure 4.1) and was used to prepare all the paint samples. The paints were spread onto glass microscope slides and allowed to dry in normal laboratory conditions. Layers of suspected discolouring combinations were produced by applying the paints both as wet paint onto

dry paint and as wet paint onto wet paint.

Table 4.2: Paint layers prepared

Pigment combination	Painting method
Lead White and Cadmium Yellow	Wet on wet paint
Lead White and Cadmium Yellow	Wet on dry paint
Lead White and Vermillion	Wet on wet paint
Lead White and Vermillion	Wet on dry paint
Lead White and Vermillion	Mixed paint
Cadmium Yellow and Malachite	Wet on wet paint
Cadmium Yellow and Malachite	Wet on dry paint

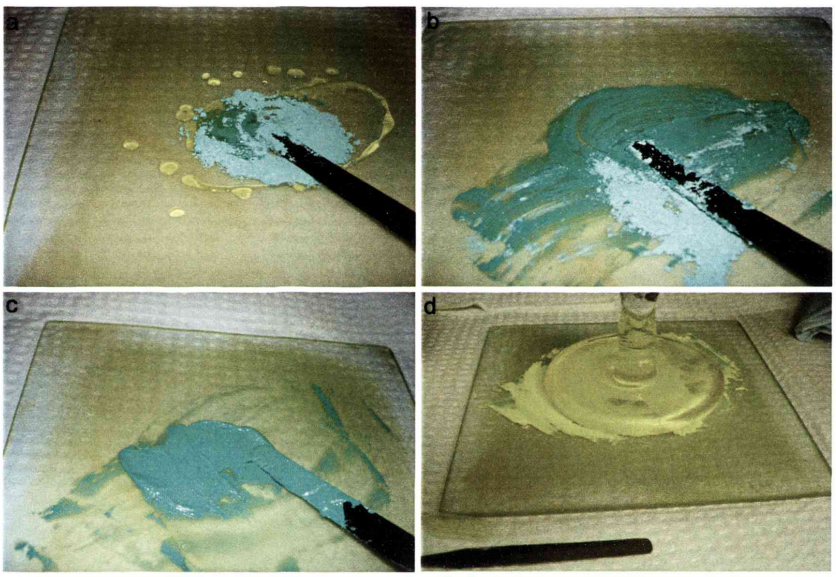

Figure 4.1: The preparation of oil paint in a traditional manner. Images (a), (b) and (c) show the preparation of malachite paint by blending cold pressed linseed oil with malachite pigment using a spatula. Image (d) shows the use of a muller to ensure even consistency of a cadmium yellow paint.

4.1.3 Interaction samples

As a result of the initial discolouration tests (Section 5.1), the combination of cadmium yellow and malalchite was selected for further study as it was the only combination that discoloured. Several types of samples were prepared to allow the observation and analysis of this discolouring interaction. Typical sampling methods for the identification of interaction products were performed by various methods.

The discolouration of this pigment combination occurs gradually in both water and linseed oil. As the reaction in water is faster and does not bind the pigment particles in oil during the discolouration, deionised water was used to produce the majority of the discoloured samples used for chemical analyses. A completely discoloured sample was prepared by mixing malachite and cadmium yellow pigments in equal proportion in deionised water. This sample was agitated periodically over several months until completely blackened, after passing through deepening olive green colours from the mixture's initial yellow-green. The products were characterised by x-ray diffraction, SEM and x-ray mapping, and used in ESEM experiments.

Partially discoloured samples were produced to examine the processes occuring during the discolouration. X-ray diffraction was used to analyse the changes occurring during the initial discolouration by taking a diffraction pattern of a sample of evenly mixed dry cadmium yellow and malachite pigments. The sample was then discoloured slightly in deionised water, then dried and another pattern taken. This step was repeated twice with the pigment mixture becoming more discoloured each time. Another partially discoloured sample was produced for x-ray mapping: a mixture of the pigments was allowed to discolour in deionised water for one hour before being dried.

In addition, cadmium yellow was reacted with other copper compounds, specifically the soluble copper salt copper sulfate. The discolouration of the cadmium yellow was almost instantaneous upon mixing with the copper salt solutions. Orange

cadmium sulfide was produced in the laboratory by chemical precipitation from cadmium nitrate and sodium sulfide solutions, allowing the washed precipitate to dry so that a sediment cake formed. These pieces were then reacted with both malachite and copper sulfate solutions to allow easier examination of the formation of a layer of discolouration product on the cadmium sulfide surface by back-scattered (or compositional) electron signal in the SEM. The use of a soluble copper solution makes the compositional contrast of the discolouration products easier to detect in the SEM images as it removes the presence of highly insoluble malachite particles as the source of copper ions.

The discolouration of the pigments in paint layers was also examined. Layered samples were prepared by applying one layer of paint over another, both when the first layer was freshly applied (wet on wet paint) and when it had had a few days of drying (wet on dry paint). Separately prepared malachite and cadmium yellow paints were also applied side by side to glass microscope slides and allowed to dry in the laboratory. Once dry the paint layers were cross-sectioned, mounted in Serafix epoxy resin and microtomed for observation by optical microscopy.

4.1.4 Solvent action on paints

An additional series of observations was made on samples of separately dried, and hence not discoloured, cadmium yellow and malachite paints. Chips of these paints were placed in a range of solvents (Table 4.3), commonly used by conservators for cleaning and restoration activities, to determine if the discolouring interaction could be activated in non-discoloured paints. The chips of the separate paints in the solvents were monitored over several days for any changes. Two alternative sources of copper ions were also tested, by adding cadmium yellow paint chips to a solution of copper sulfate and to deionised water with a piece of copper metal foil.

Table 4.3: Solvent action on paints

Paint combination	Solvent
Cadmium yellow and malachite	Deionised water
Cadmium yellow and malachite	Ethanol
Cadmium yellow and malachite	Turpentine
Cadmium yellow and malachite	Acetone
Cadmium yellow and malachite	Petroleum spirits
Cadmium yellow and copper foil	Deionised water
Cadmium yellow	Copper sulfate solution

4.2 Optical microscopy

Optical microscopy was used to observe the changes in the discoloured paints and pigments. Some small fragments of the paint samples were mounted in resin and microtomed to achieve a flat surface before observation and imaging. The instrument used was a reflected light Olympus BH-2 system research microscope with Optimas digital software.

4.2.1 Time resolved microscopy

In addition to imaging previously discoloured samples, optical microscopy was used to video the progression of the discolouration between cadmium yellow and copper-containing compounds. It was not possible to produce discolouration between wetted pastes of cadmium yellow and malachite pigments visible under the microscope as the samples dried out rapidly and they could not be re-wetted without significantly disturbing the interface. Due to the speed of the initial interaction between cadmium yellow and copper ions a method of immobilising the copper ions was developed. This involved the production of a film of polyethylene glycol containing copper sulfate on a microscope slide. When dry there is no reaction between the film and cadmium sulfide particles, but the film readily becomes a source of mobile copper ions when wetted. The cadmium yellow pigment particles were placed on the dried film of polyethylene glycol and copper sulfate. Under the optical microscope water was allowed to flow across the slide hydrating the polyethylene glycol and copper sulfate film and providing copper ions for reaction with the cadmium yellow pigment particles. The additional advantage is that the discolouration of the cadmium yellow particles by copper ions was viewed without the presence of opaque solid malachite particles. During the discolouration process the reflected light Olympus BH-2 system research microscope was used to acquire images at set time intervals using Optimas software.

4.3 Characterisation techniques

Chemical and structural characterisation is vital when examining pigment systems. Over the centuries sources of artistic pigments have evolved to standard formulations but there are still variations in formulation between suppliers. In this project, the reactant compounds and their products were characterised using several techniques. X-ray diffraction was used to identify the compounds present. SEM was used to examine particle size and shape along with x-ray microanalysis of the unreacted and reacted particles.

4.3.1 XRD

X-ray diffraction (XRD) analyses (Skoog & Leary 1992) were performed using Siemens D500 Diffractometer with a copper Kα1 tube with a post monochromator (to reduce background) in a theta-theta configuration.

Samples were prepared as bulk powder or as thin layers of powder on low background discs. The low background discs used were single crystal quartz with no atomic planes parallel to the surface so that no diffraction peaks are observed from the disc. Diffraction patterns of bulk, as received, malachite and cadmium yellow pigments were made. For the reacted samples a small amount of discoloured material was mixed with ethanol and spread onto a low background disc mounted in a sample holder and dried in air. This allowed a smaller amount of sample to be analysed. Diffraction patterns for all samples were taken between 2θ angles of 15° and 80° with a step size of 0.02°. Time per step varied from 2 to 90 seconds. All diffraction patterns identified by comparison with standard patterns in the Joint Committee for Diffraction on Powder Diffraction Standards (JCPDS 2005) system.

4.3.2 Thermal Analysis

Thermogravimetric analysis coupled with mass spectroscopy (TG-MS) for evolved gas analysis (Skoog & Leary 1992) was used to characterise the interaction between cadmium yellow and malachite pigments. Samples analysed were pure cadmium yellow, pure malachite and blends of malachite and cadmium yellow in the ratios 10:1, 1:1 and 1:10 by mass. Each blend was mixed with deionised water and the resulting suspension was left at room temperature for two months, agitated periodically, before the water was removed and the sediments dried for analysis. The TG-MS measurements were carried out using a Setaram Setsys 16/18 thermobalance coupled with a Balzers ThermoStar mass spectrometer for evolved gas analysis. All experiments were carried out in alumina (Al_2O_3) crucibles at a heating rate of 10°C/min from ambient temperature to 800°C under flowing (20mL/min) high purity argon gas. These analyses were performed to aid identification of the phases formed during the discolouration.

4.3.3 SEM EDS

Samples were analysed using a Zeiss 55VP Supra SEM. X-ray information was gathered with an Oxford Instruments energy dispersive x-ray spectrometer and analysed with Inca analysis software. The samples were mounted on aluminium sample holders with carbon sticky tabs and were carbon coated prior to analysis. Samples analysed were the as-received cadmium yellow and malachite pigments and some discoloured samples. These discoloured samples were: a cadmium yellow and malachite mixed sample partially discoloured for seven hours in deionised water; a discoloured interface between cadmium yellow and malachite, produced by placing wet pastes in contact; and samples of cadmium yellow pigment and a cadmium sulfide flake, briefly exposed to copper sulfate solutions to produce surface discolouration.

For the x-ray mapping experiments, samples of unreacted, partially discoloured and fully discoloured cadmium yellow and malachite pigment mixtures were analysed as particles spread on a holder and as pressed pellets. These analyses were performed using a Jeol 35CF SEM using Kevex energy dispersive x-ray spectrometer. Moran Scientific x-ray mapping software was used for data processing.

4.4 X-ray Mapping

All x-ray mapping was performed using a Jeol 35CF scanning electron microscope with an Oxford Pentafet Si(Li) energy dispersive x-ray spectrometer. X-ray maps and scatter diagrams were produced using Moran Scientific software. Mapping was performed on unreacted cadmium yellow and malachite pigment mixture, a mixture which had been discoloured for one hour in deionised water, and the completely discoloured sample of the mixed pigments. The background and overlap corrected region of interest (ROI) x-ray maps were produced by mapping for K or L x-ray peaks for the elements sulfur, cadmium, copper and zinc using ZAF matrix corrected standardless analysis (Goldstein *et al.* 1992). X-ray maps are produced by scanning the selected sample surface and collecting the x-ray signal intensity for the selected elements at each pixel point (generally 512 by 512 pixels for these maps). For each element the range of x-ray signal intensities are normalised to the greyscale (0 for no signal to 255 for the greatest signal) and presented as an image for that region which is known as an x-ray map. Hence the intensity of elements cannot be compared between individual x-ray maps as only the x-ray signal intensities for that element are normalised. The software was used to produce scatter diagrams for the mapped regions. This is carried out by normalising the pixel grey-scale intensities of an individual elements x-ray map to a range of 0 to 100. A two-dimensional scatter diagram is produced by plotting the normalised pixel intensity of the same pixel in both the copper and sulfur x-ray maps against each other. The resulting scatter diagram shows concentrations, or nodes, of the plotted points that represent phase associations between the two elements within that region of the sample.

4.5 ESEM

4.5.1 ESEM instrumentation

The Philips/FEI XL30 ESEM was used for all hydration experiments. Samples were placed in specialised aluminium holders in a Peltier-cooling stage in the microscope chamber. The temperature of the samples was regulated using a temperature controller. Sacrificial water drops were placed on insulating parts of the Peltier-cooling stage. The back-scattered electron detector (BSED) was attached to the high pressure bullet in the pole piece using an adaptor. The sample height was adjusted visually to approximately one centimetre below the detector. Sample temperatures and chamber pressures were selected in line with the relative humidity isobars (see Figure 3.2) for the instrument to maintain hydration, to condense water on the sample or to dehydrate the sample.

4.5.2 ESEM techniques

Hydration method for wet samples

Samples of malachite and cadmium yellow pigments were mixed separately with deionised water to a wet paste consistency. The samples were then placed in a refrigerator for more than 30 minutes along with the recessed aluminium sample holder to allow cooling to around 4°C. The sample pastes were then placed in contact as flat as possible interface in the holder and immediately placed in the already cooled Peltier stage. This was done to minimise the time the pigments have to react before imaging could take place. The chamber pressure was then set to a pressure that would not dehydrate or hydrate the sample further. However during the pump-down sequences the hydrated samples often "boiled" and dried out slightly despite careful set up. The "boiling", observed via the chamber window, occurred mainly in the malachite slurry

during the roughing pump period of the pump-down sequence. This caused disturbance of the pigment interface, occasionally to an extent that the experiment could not be continued. Methods for minimising sample evaporation suggested by Cameron & Donald (1994) were attempted along with other approaches. Extra sacrificial water drops did not improve the situation. Nor did degassing the water by boiling prior to mixing with pigment. Setting a higher pressure than required for 100% humidity at the sample did not solve the problem as the "boiling" was occurring within the initial stages of the pump-down sequence, and often resulted in excess water being condensed on the sample.

There are two possibilities for "boiling" to occur. Firstly, the water in the sample evaporates by "boiling" due to the temperature of the sample and the humidity of the chamber being such that the relative humidity at the sample is less than 100%. Secondly, that dissolved gas in the water is evolving during the pump-down sequence. The first option can be remedied by thorough cooling of the sample, the use of sacrificial water drops and setting the pressure to an appropriate value to ensure 100% relative humidity. Despite all these steps being carried out the "boiling" still occurred. The short length of time over which the "boiling" occurs suggests that it is caused by the evolution of dissolved gas. Several steps were taken to minimise the effect of this disturbance. Thinner layers of the pigment pastes were used on a flat stub in the cold stage. This method only resulted in the samples drying out almost completely during the pump-down sequence. The water used to make the pigment pastes was degassed by boiling but this did not significantly reduce the "boiling" of the sample. Another potential cause for "boiling" of the sample may be due to the position of the vapour pressure sensor within the chamber. The pressure at the sample may be different to that at the sensor as the pressure within the chamber can only be assumed to be uniform if no temperature gradients exist (Danilatos 1997).

Automatic or custom purge sequences were not selected in these experiments as

it was found that these condensed water onto the sample and provided significant disturbance of the interface prepared by the flow of this water over the interface.

Hydration method for dry samples

Preparation of dry interface samples was relatively simple compared to the wet pigment interfaces. Malachite and cadmium yellow pigments were pressed side by side into recessed aluminium sample holders to create an interface. The holder was then placed in the Peltier-cooling stage set to a low temperature, usually 5°C. The chamber was then pumped to a pressure, usually 3 Torr, in order to keep the sample dry before imaging. The samples were imaged before the chamber pressure was increased to allow water to be condensed on the sample. Again care had to be taken to prevent the over-hydration of the sample and water on the surface disturbing the interface. This hydration of the sample was maintained for a time before dehydration (by decreasing the chamber pressure) of the sample and further imaging. This hydration and dehydration process was repeated to monitor the progress of the discolouration. This method often resulted in cracking and movement of the interface samples during repeated hydrations and dehydration. In some cases the experiment had to be abandoned due to severe cracking or movement of the specimen.

Back-scattered contrast coefficients

Images were produced using the back-scattered electron signal. This allows for compositional contrast imaging of samples containing varying atomic mass components. The back-scattered contrast coefficient for a material at a particular accelerating voltage can be obtained by modeling the sample using Monte-Carlo Electron-Trajectory simulation (Goldstein *et al.* 1992). For malachite, cadmium yellow and their discolouration products the back-scattered contrast coefficients were determined by modeling using

a Monte-Carlo simulation computer program (Kanda & Joy 1996) for an accelerating voltage of 25 kV and ten thousand trajectories. The back-scattered compositional contrast coefficients (Table 4.4) of the discolouration products are between the coefficients of the malachite and cadmium yellow pigments. Therefore they will have a compositional contrast in back-scattered electron imaging between the darkest malachite and brightest cadmium yellow.

Table 4.4: Back-scattered contrast coefficients at 25 kV

Cadmium sulfide	0.3528
Malachite	0.1209
Copper sulfide	0.2756
Cadmium carbonate	0.1980
Cadmium sulfate monohydrate	0.1484

The visible differences in contrast (C) between each of the reactants and products can be calculated from the back-scattered contrast coefficient (η) values in Table 4.4 using the following relationships (Goldstein *et al.* 1992) and are listed in Table 4.5.:

$$C = (\eta_2 - \eta_1)/\eta_2$$

The minimum beam current, i_b, required to observe a certain contrast C, as a frame time, t_f, can be determined using the Rose Criterion (that the change in signal must exceed the noise by a factor of 5, $\Delta S > 5N$) (Goldstein *et al.* 1992):

$$i_b > 4 \times 10^{-3}/(\varepsilon C^2 t_f) nA$$

where ε is the detector collector efficiency. Using this expression and the smallest contrast value from Table 4.5, it was determined that a current of > 0.4 nA is sufficient to observe all phases in BSE mode using TV rate ($t_f = 0.1$ seconds) imaging.

Table 4.5: Contrast visible between interaction products

Contrast	CdS	$CuCO_3.Cu(OH_2)$	CuS	$CdCO_3$	$CdSO_4.H_2O$
CdS	0	0.657	0.219	0.439	0.579
$CuCO_3.Cu(OH_2$	0.657	0	0.561	0.389	0.185
CuS	0.219	0.561	0	0.282	0.462
$CdCO_3$	0.439	0.389	0.282	0	0.251
$CdSO_4.H_2O$	0.579	0.185	0.462	0.251	0

Chapter 5

Observation of pigment interaction

5.1 Interactions between paint layers

A number of pigment combinations that could potentially cause paint discolouration (Table 5.1) were tested to determine which pigments interacted in oil paint media. The widely reported discolouring interaction between lead white and vermillion paints did not occur initially or over a three year period (Figure 5.1). Paint layers produced from the mixed lead white and vermillion pigments also did not discolour (Figure 5.2). The interaction of lead white with cadmium yellow (Figure 5.3) did not occur in samples prepared. However the combination of cadmium yellow and malachite paints did exhibit noticeable discolouration effects. Figure 5.4 shows the discolouration after four months; the darkening of the layers is more obvious in the underside view of the paints through the glass microscope slide substrate. As a result of these tests the combination of cadmium yellow and malachite pigments was selected as the discolouring interaction for this project.

Table 5.1: Paint layer discolourations

Pigment combination	Painting method	Evidence of discolouration
Lead White and Cadmium Yellow	Wet-on-wet paint	None
Lead White and Cadmium Yellow	Wet-on-dry paint	None
Lead White and Vermillion	Wet-on-wet paint	None
Lead White and Vermillion	Wet-on-dry paint	None
Lead White and Vermillion	Mixed paint	None
Cadmium Yellow and Malachite	Wet-on-wet paint	Darkening of paints
Cadmium Yellow and Malachite	Wet-on-dry paint	Darkening of paints

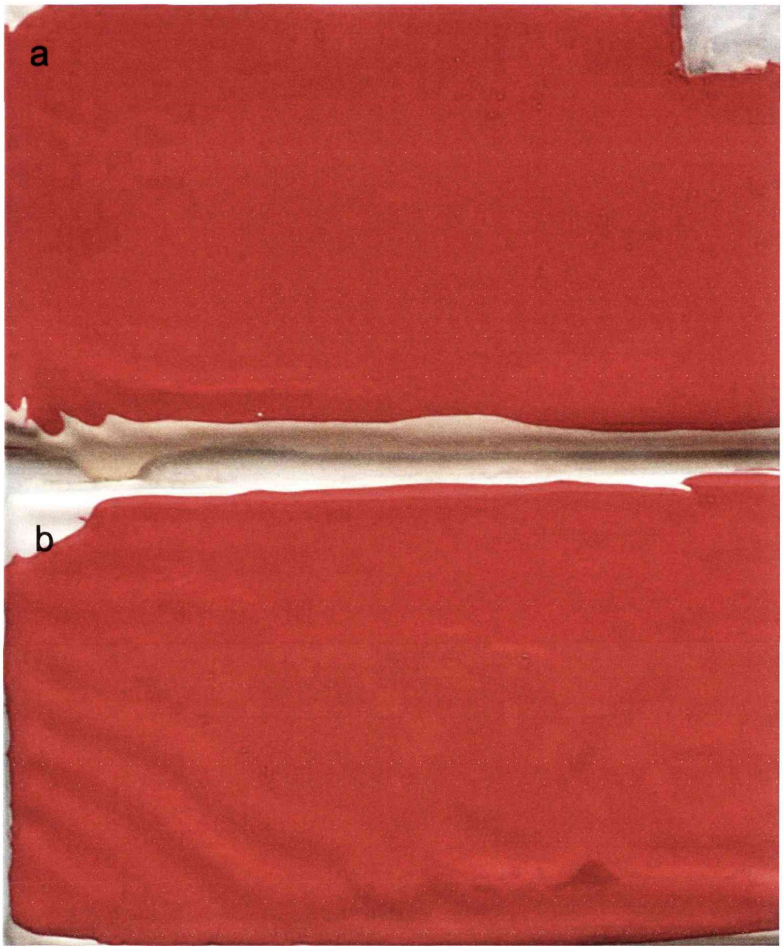

Figure 5.1: Three year old paint layers of lead white and vermillion pigments placed in contact (a) wet-on-wet paint and (b) wet-on-dry paint, showing no visual colour difference compared to fresh layers (WOF = 5cm).

Figure 5.2: Three year old mixed paint layer of lead white and vermillion pigments, showing no dark discolouration (WOF = 5cm).

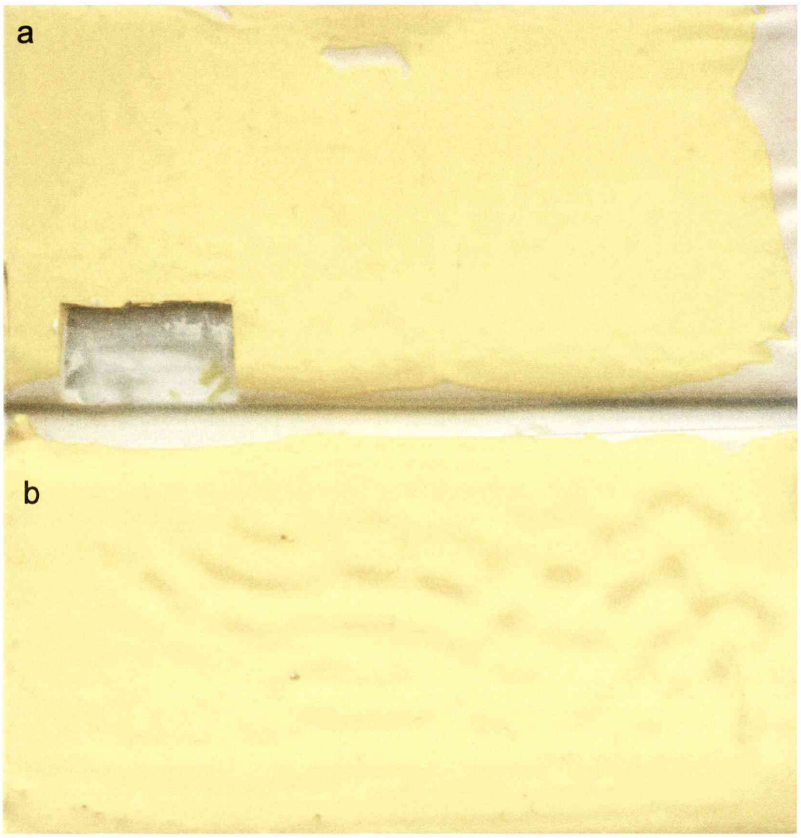

Figure 5.3: Three year old paint layers of lead white and cadmium yellow pigments placed in contact (a) wet-on-wet paint and (b) wet-on-dry paint, showing no visual colour difference compared to fresh layers (WOF = 5cm).

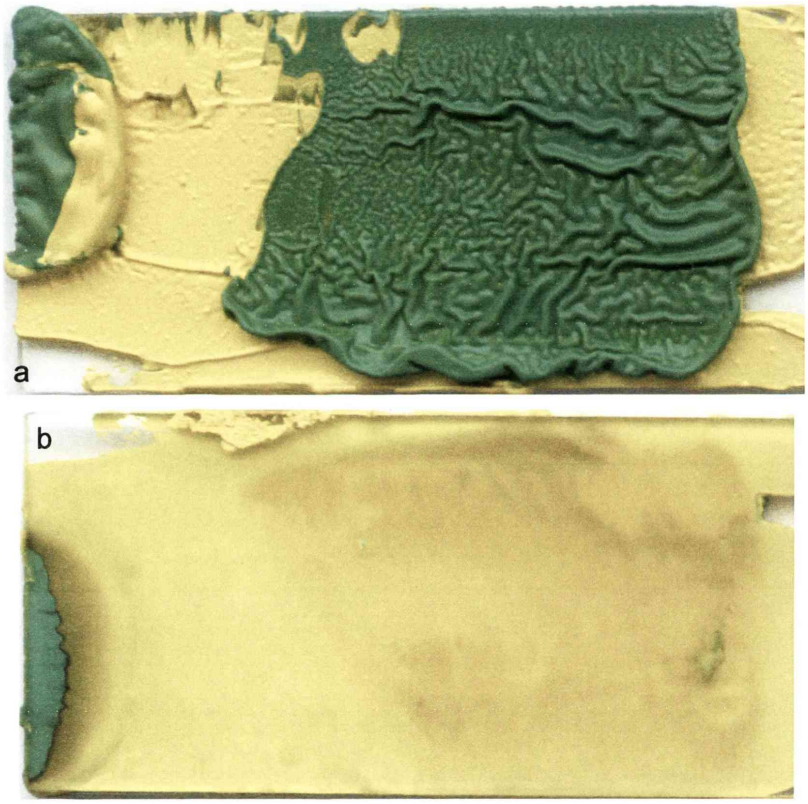

Figure 5.4: Malalchite paint over cadmium yellow paint layer. This visible discolouration occurred over a four month period. A view of the (a) topside and (b) underside of the paint layer, showing the dark discolouration spreading into the cadmium yellow paint layer from the interface with the malachite paint (WOF = 5cm).

5.2 Cadmium yellow and malachite interaction

5.2.1 Aqueous media interaction

A mixture of cadmium yellow and malachite pigments in water gradually darkens over time. Initially it produces an olive green colour that becomes darker after a period of several weeks. Figure 5.5 shows the initial darkening of the pigment mixture mixed with deionised water. The bright colours of the individual dry pigments (Figures 5.5(a) and 5.5(b)) are initially muted by mixture with deionised water (Figure 5.5(c)). Over two hours the mixture becomes significantly discoloured (Figures 5.5(d), (e), (f) and (g)).

If the wetted pigments are placed in contact with each other an interface of dark discolouration will form between them (Figure 5.6). The drying of the pigment pastes in air halts the progress of the discolouration interface. This interface of discolouration is also observed in samples that have been hydrated in the ESEM (Figures 5.7 and 5.8).

In order to observe this layer of dark discolouration product more clearly, pieces of cadmium sulfide were discoloured in water with malachite. A layer of dark discolouration product formed over the surface of the cadmium sulfide pieces (Figure 5.9). This same sample was also imaged using the ESEM (Figure 5.10). The back-scattered electron signal was used to image the sample and the dark coating on the cadmium sulfide piece (seen in Figure 5.9) has low contrast compared to the particle. This is consistent with the layer consisting of a copper sulfide as its back-scattered contrast coefficient is lower than that of cadmium sulfide (Section 4.5.2).

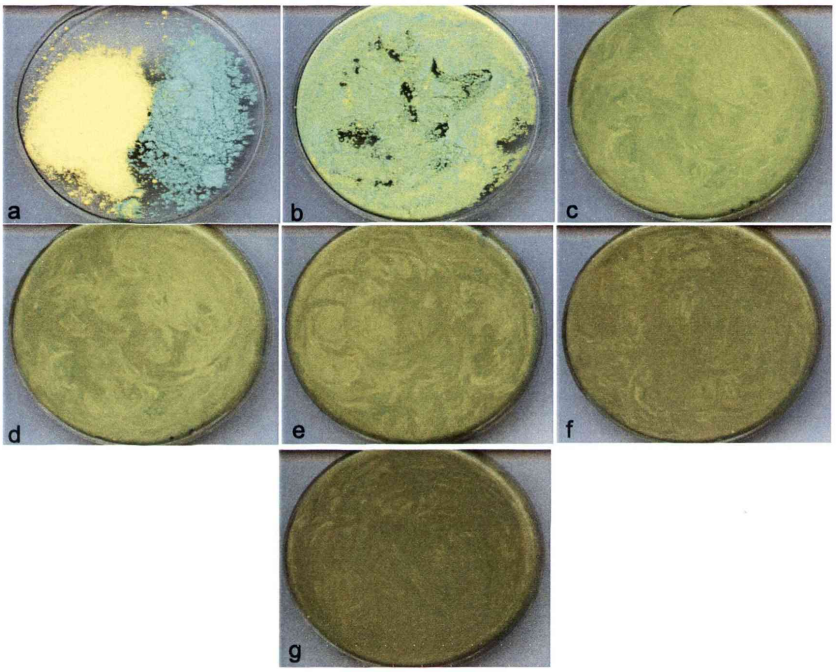

Figure 5.5: Mixtures of cadmium yellow and malachite pigments as (a) separate dry pigments and (b) mixed dry pigments. Increasing discolouration is visible after mixing with deionised water at (c) 0 minutes, (d) 7 minutes, (e) 26 minutes, (f) 47 minutes and (g) 122 minutes (WOF = 7cm).

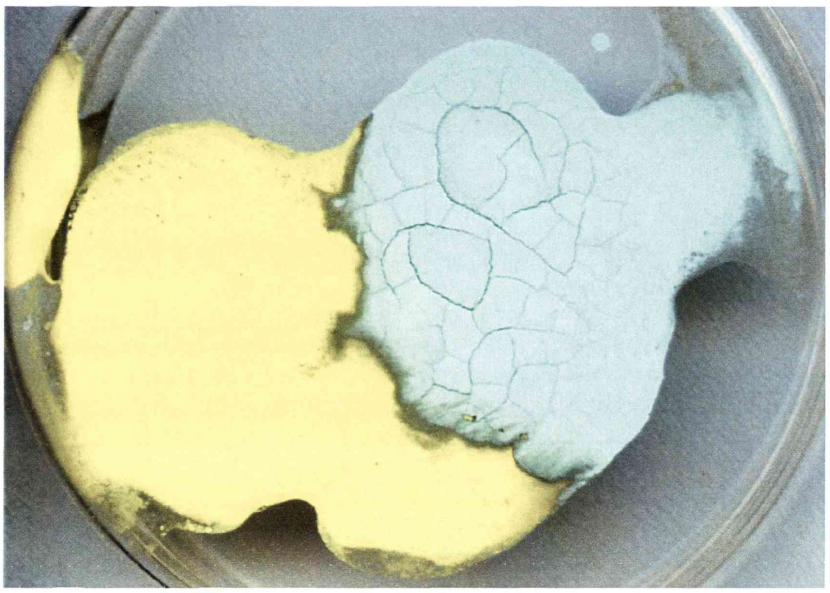

Figure 5.6: A dark coloured interaction product forms at the interface between cadmium yellow and malachite pigment pastes (WOF = 6cm).

Figure 5.7: An optical micrograph of the darkening of cadmium yellow particles on a malachite pigment substrate resulting from a brief hydration in the ESEM (WOF = 0.25mm).

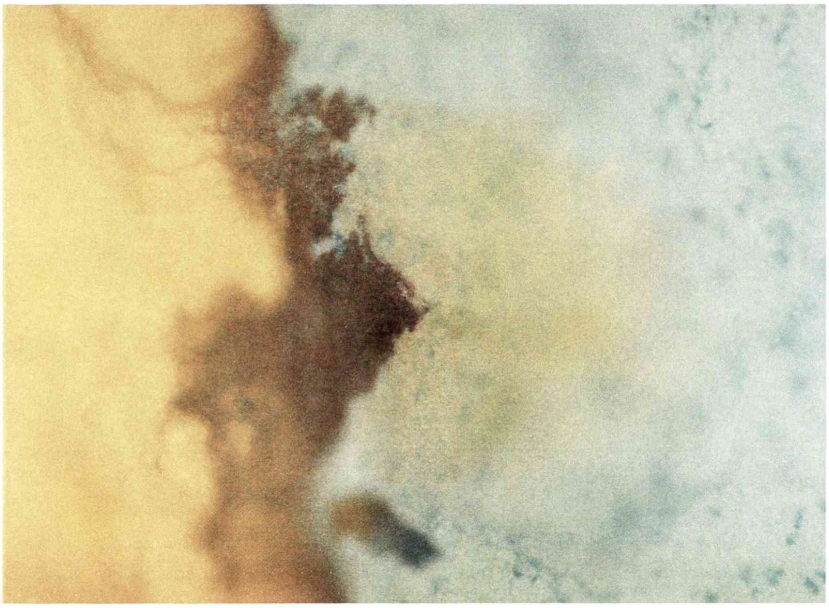

Figure 5.8: An optical micrograph showing the discoloured interface formed between cadmium yellow and malachite pigment pastes during hydration in the ESEM (WOF = 1mm).

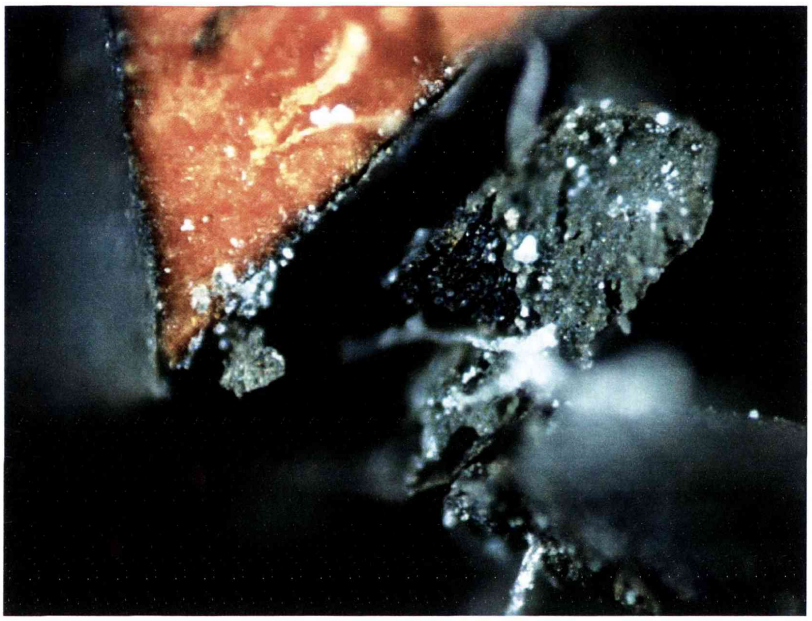

Figure 5.9: Optical micrograph of the dark discolouration layer that has formed on a bright orange cadmium sulfide pigment particle after contact with malachite and water (WOF = 0.5mm).

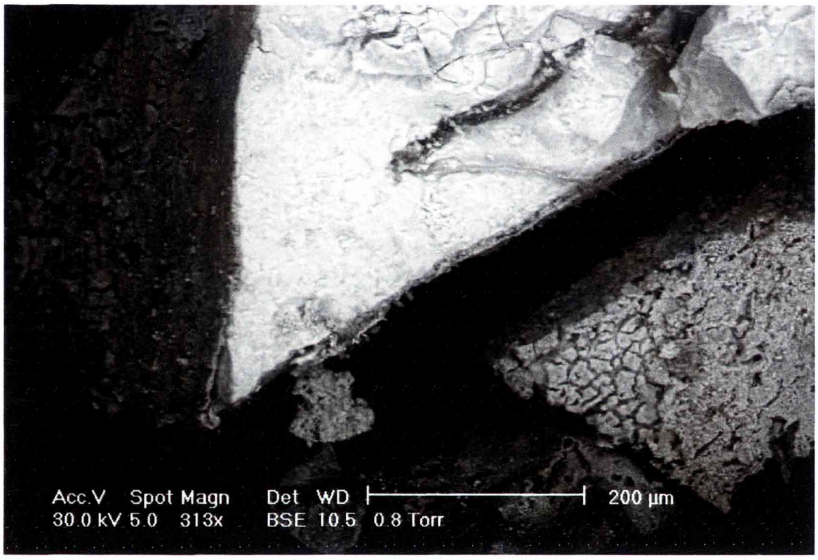

Figure 5.10: ESEM micrograph of the dark discolouration layer on cadmium sulfide pigment particle, showing the bright cadmium sulfide particle covered with the lower contrast discoloured layer.

5.2.2 Oil paint interaction

The darkening interaction between cadmium yellow and malachite pigments also occurs in oil paint media. The discolouration occurs more slowly than in aqueous media, generally taking several weeks to appear. In Figure 5.11 the discolouration can be seen between the cadmium yellow and malachite paints. The interface of discolouration is wider almost two years later and the malachite paint has darkened considerably.

Fragments of discoloured cadmium yellow and malachite paint interfaces were resin mounted and microtomed for optical microscopy. Figure 5.12 shows the darkened interface on the cadmium yellow paint where it is in contact with the malachite paint.

Over the time that the discolouring interaction occurs, the entire malachite paint layer also darkens. This is not caused by the presence of cadmium sulfide but is a result of uptake of copper ions into the oil medium. This causes a darkening of the oil resulting in the paint layer taking on an olive colour (Church 1892, Gunn *et al.* 2002). An example of this is shown in Figure 5.13, where the difference between fresh and aged malachite paint layers is visible. This change in colouration only occurs in the surface layers where more oil is present than pigment particles due to settling during the drying process. Inside the paint layer there is more pigment in the oil and the colour is lighter and closer to that of the fresh paint (Figure 5.14).

Cadmium yellow pigment does not significantly change colour in oil paint. A slight yellowing can be noted between fresh and aged paint (Figure 5.15). This is due to the yellow colour of the ageing linseed oil, which intensifies as the oil film dries.

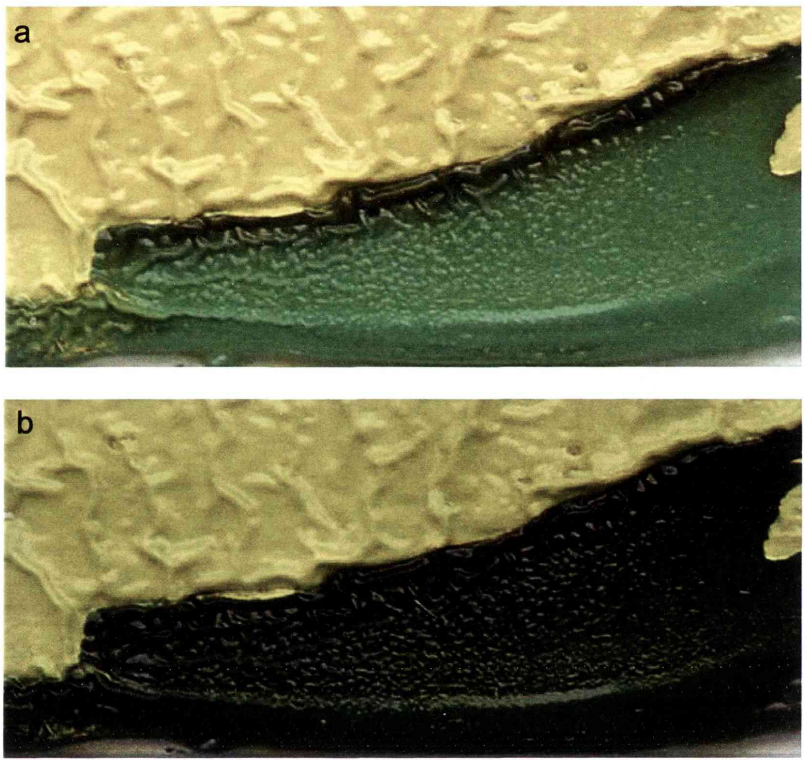

Figure 5.11: A dark coloured interface between cadmium yellow (upper layer) and malachite (lower layer) oil paints. Image (a) was acquired at three and a half months and image (b) was taken two years after the paints were made and placed in contact (WOF = 4cm).

Figure 5.12: A dark coloured interface region in a microtomed cross-section of cadmium yellow (left) paint in contact with malachite (right) paint (WOF = 3mm).

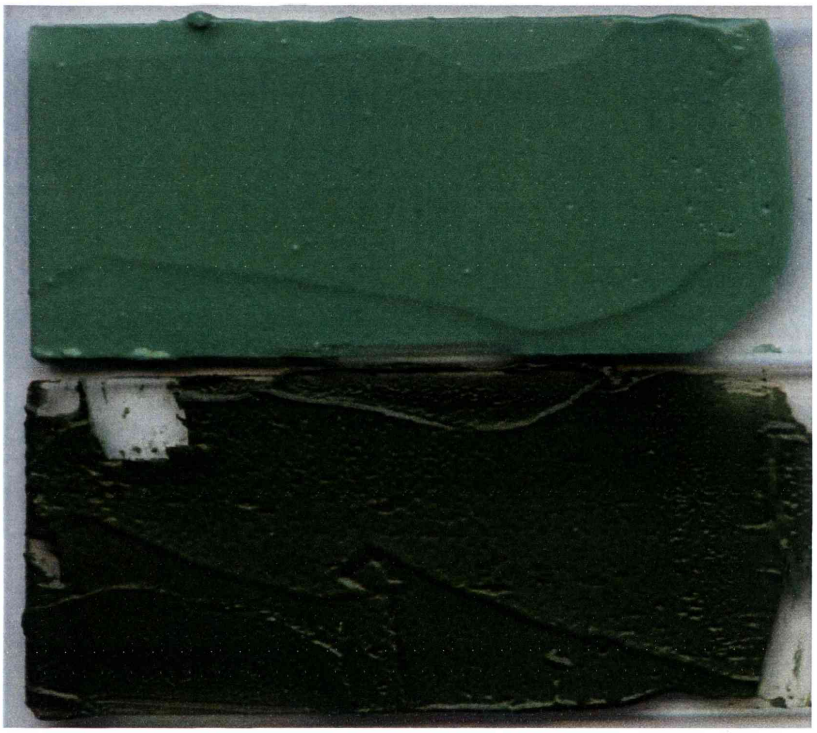

Figure 5.13: Colour change in malachite oil paint over two years. Fresh malachite paint (top) and malachite paint aged naturally for two years in the laboratory (bottom). The darkening occurs on the surface and without the influence of other pigments (WOF = 5cm).

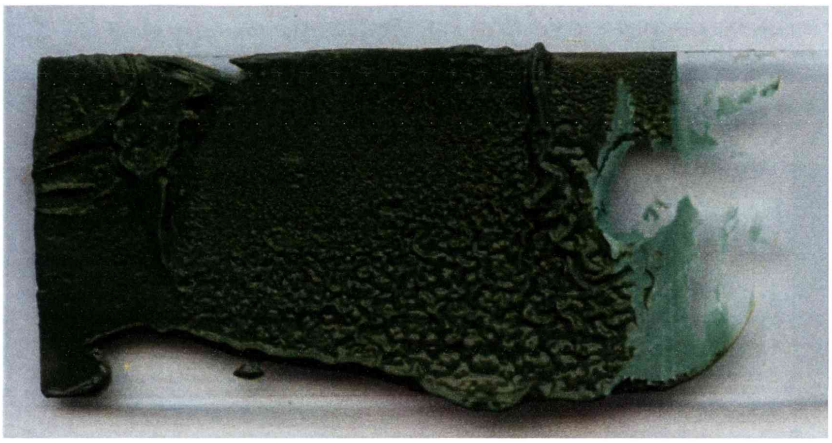

Figure 5.14: An aged malachite paint layer cut to show the true colour of the paint layer beneath the olive coloured surface layer. The darker surface is caused by the uptake of copper ions into the oil medium (WOF = 6cm).

Figure 5.15: Fresh (top) and two year old (bottom) cadmium yellow oil paints, showing slight yellowing due to the aging of the linseed oil medium (WOF = 5cm).

5.2.3 Solvent activation of interaction

Cadmium yellow and malachite paint chips were together exposed to different solvents to determine if discolouration of the cadmium yellow paint could occur. Table 5.2 shows that the cadmium yellow paint chips were only discoloured in the presence of malachite paint in deionised water and acetone. It seems that copper ions are extracted from the malachite paint layer by the solvent and are transported through it to the cadmium yellow paint. Ethanol, turpentine and petroleum spirits did not result in discolouration even after several days. Turpentine had the effect of disintegrating the paint layers as a result of its action on the linseed oil binding medium. Discolouration also occurred on the cadmium yellow paint placed in water with copper foil and in copper sulfate solution. In the latter example there was an immediate darkening of the paint layer to an olive green colour that blackens over time, even after the solution evaporates.

Table 5.2: Solvent action on paints

Paint combination	Solvent	Observations
Cadmium yellow and malachite	Deionised water	Discolouration
Cadmium yellow and malachite	Ethanol	No discolouration
Cadmium yellow and malachite	Turpentine	No discolouration
Cadmium yellow and malachite	Acetone	Discolouration
Cadmium yellow and malachite	Petroleum spirits	No discolouration
Cadmium yellow and copper foil	Deionised water	Discolouration
Cadmium yellow	Copper sulfate solution	Immediate discolouration

5.3 Interaction of cadmium yellow with other copper compounds

The discolouration of cadmium yellow pigment was observed to occur in contact with aqueous copper sulfate. The darkening of cadmium yellow particles was observed to happen instantaneously on contact with copper sulfate (Figure 5.16).

5.3.1 Time resolved interactions

The interaction between cadmium yellow pigment and other sources of copper was observed using time-lapse optical microscopy. Figure 5.17 is a series of images taken during a time-lapse experiment. In this experiment a film of polyethylene glycol and copper sulfate was allowed to dry on a microscope slide. Particles of cadmium yellow pigment were placed on the surface and water was allowed to flow over the sample. The result is a series of images showing the water moving across the sample hydrating the polyethylene glycol and copper sulfate film. As the water reaches the cadmium yellow particles the copper ions dissolved in the water react with the particles causing a brown discolouration.

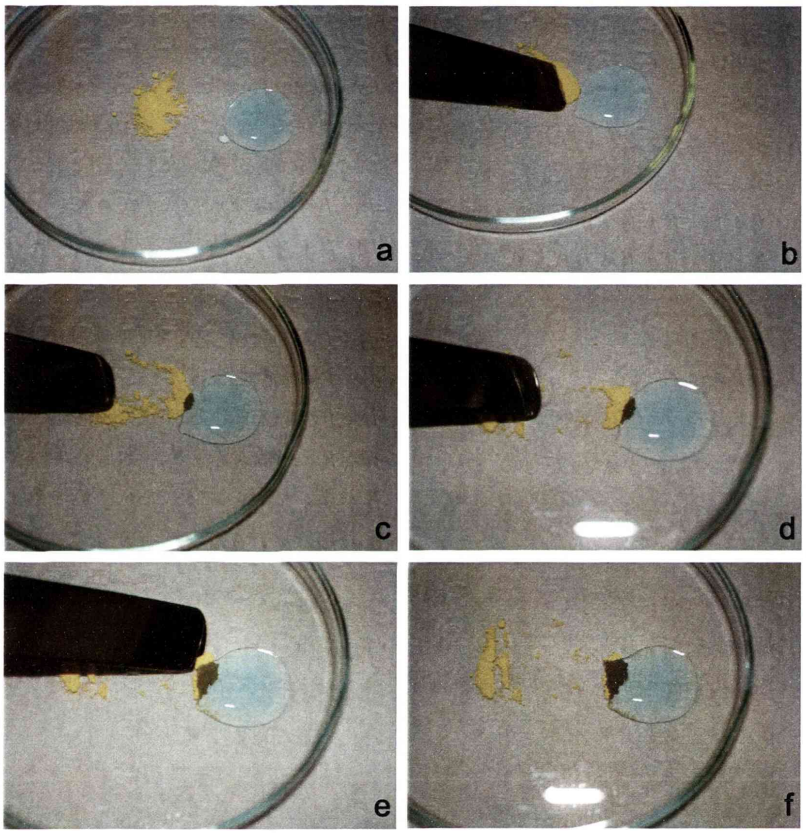

Figure 5.16: Discolouration of cadmium yellow pigment on contact with copper sulfate solution. The series of images was taken over one minute (WOF = 8cm).

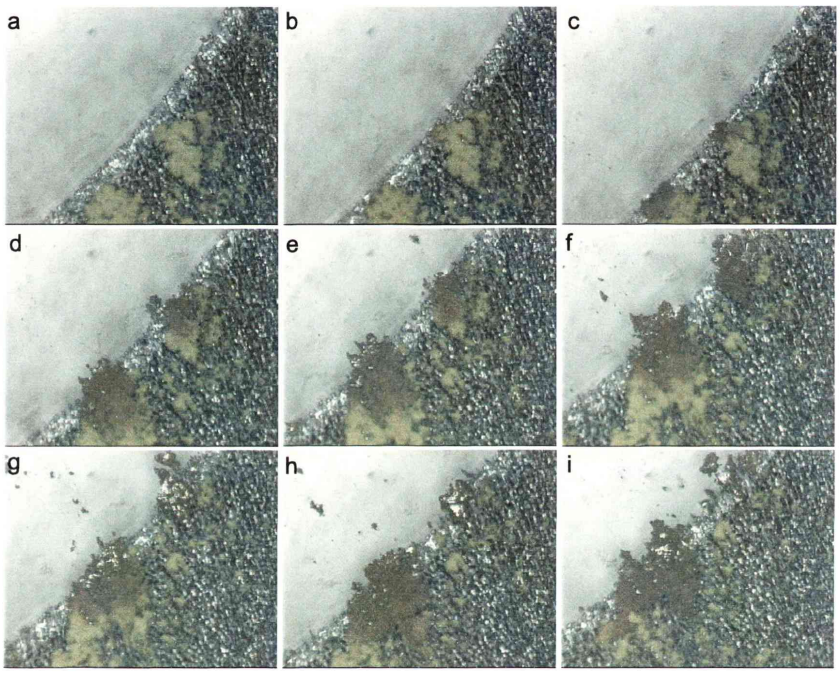

Figure 5.17: Time-lapse images of cadmium yellow particles being discoloured by the flow of water across the polyethylene glycol - copper sulfate substrate. The water dissolves the copper ions allowing them to discolour the cadmium yellow pigment. This series of images was taken over 45 seconds (WOF = 5mm).

5.4 Summation

A dark discolouration occurs between cadmium yellow pigments and malachite (copper-containing) pigment, and other copper compounds, in the presence of both aqueous and oil mediums. The rate at which the discolouration occurs is increased by decreasing viscosity of the medium being used and by the increasing solubility of copper compound. Hence, cadmium yellow will react to form a dark product immediately on contact with an aqueous copper sulfate solution, whereas a malachite paint layer in contact with a cadmium yellow paint layer will take several months to produce a noticeable dark interface.

Chapter 6

Characterisation of cadmium yellow and malachite interaction

6.1 XRD

X-ray diffraction (XRD) was used to characterise the raw pigments and the discolouration products produced. All x-ray diffraction patterns were collected using a Siemens D5000 Diffractometer. Samples were prepared in bulk, or on low background disks for small amounts of samples.

6.1.1 Pigment characterisation

Cadmium Yellow pigment

Cadmium yellow is a cadmium sulfide pigment. This group of pigments ranges in colour from yellow through orange to red (Fiedler & Bayard 1986). The basic composition is orange cadmium sulfide (CdS). The red colour is created by the presence of selenium in solid solution and the yellow by the presence of zinc in solid solution. The presence of zinc is noted in the diffraction pattern of the pigment. The pattern matches closely with two structures: greenockite (CdS, JCPDS 41-1049) and a cadmium zinc sulfide ($(Cd_{8.05}Zn_{1.95}S_{10})$, JCPDS 40-0835). As can be seen in Figure 6.1 the pattern of the cadmium zinc sulfide structure closely matches the height ratio of the three peaks between the two-theta values of 25° and 29°. The greenockite structure peaks are slightly offset from the pigment pattern, indicating that the pigment structure is similar. This result agrees with the amount of zinc in the pigment being small as determined by SEM-EDS (Section 6.3.1).

Another sample of cadmium yellow pigment was prepared by allowing a mixture of cadmium yellow pigment and deionised water to dry in a layer on a piece of microscope slide. A diffraction pattern (Figure 6.2) was then made of this sample and it was found that, as well as the cadmium zinc sulfide of the pigment, there was cadmium sulfate and hydrated cadmium sulfate present. This indicates that the cadmium sulfate

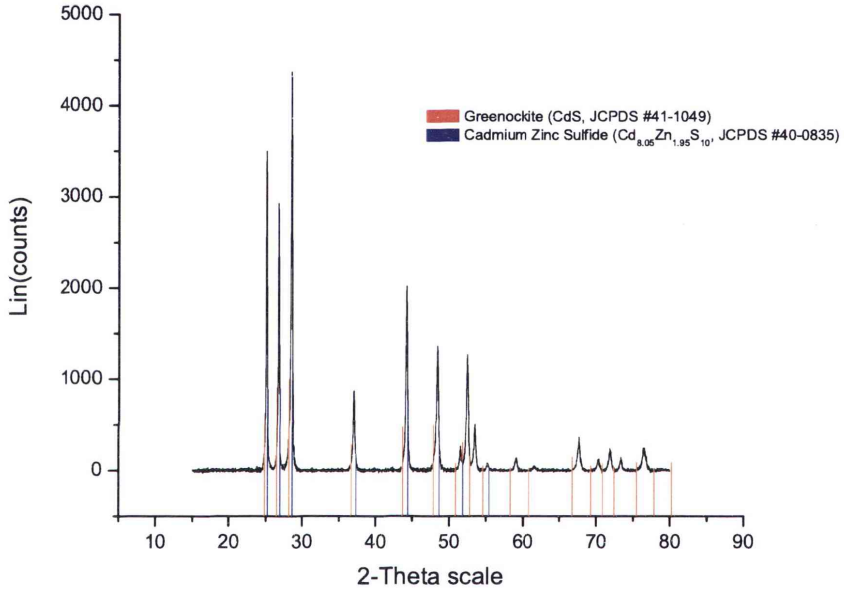

Figure 6.1: X-ray diffraction pattern for cadmium yellow pigment, showing Greenockite and cadmium zinc sulfide peaks.

monohydrate present as a discolouration product (Section 6.3.2) is most likely due to the oxidation of the pigment in water rather than the interaction between cadmium yellow and malachite. This means that this product is probably not present in the discoloured oil paints containing these two pigments.

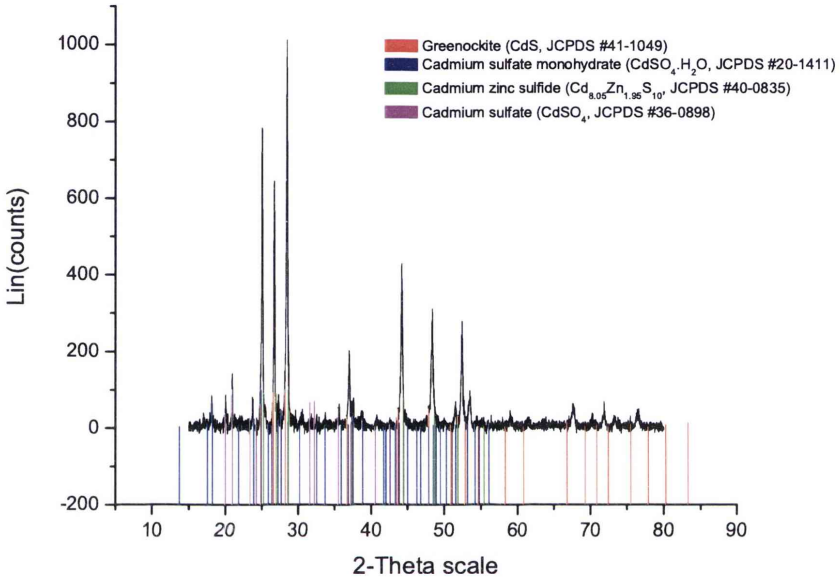

Figure 6.2: X-ray diffraction pattern for cadmium yellow pigment after exposure to deionised water, showing the presence of cadmium sulfate and hydrated cadmium sulfate.

Malachite pigment

Malachite is a copper carbonate hydroxide ($CuCO_3.Cu(OH)_2$). The x-ray diffraction pattern identified the pigment as pure malachite (JCPDS 41-1390) (Figure 6.3).

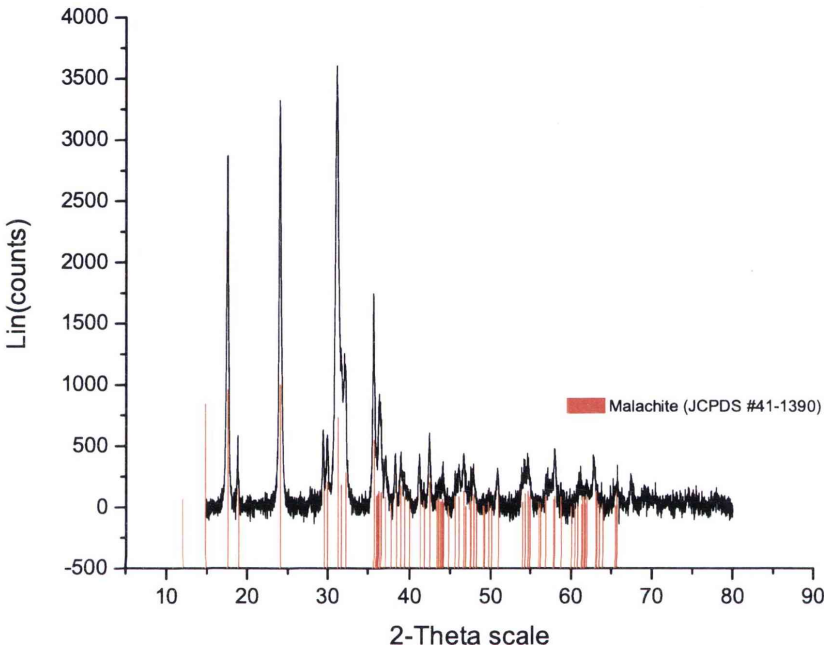

Figure 6.3: X-ray diffraction pattern for malachite pigment, showing malachite peaks.

6.1.2 Characterisation of interaction products by XRD

A mixture of cadmium yellow and malachite pigments, reacted in water until completely discoloured, was placed on a low background disk and an x-ray diffraction pattern was obtained (Figure 6.4). The structures identified were hydrated cadmium sulfate ($CdSO_4.H_2O$, JCPDS 20-1411), otavite (cadmium carbonate, $CdCO_3$, JCPDS 08-0456) and covellite (copper sulfide, CuS, JCPDS 06-0464). Hydrated cadmium sulfate and otavite are both white coloured compounds and could not be contributing to the dark colour produced in the discolouration. The copper sulfide is a black compound and the cause of the dark colour observed on the interaction of the two pigments. The presence of hydrated cadmium sulfate in the discolouration product is a result of the oxidation of cadmium sulfide in water (Section 6.1.1).

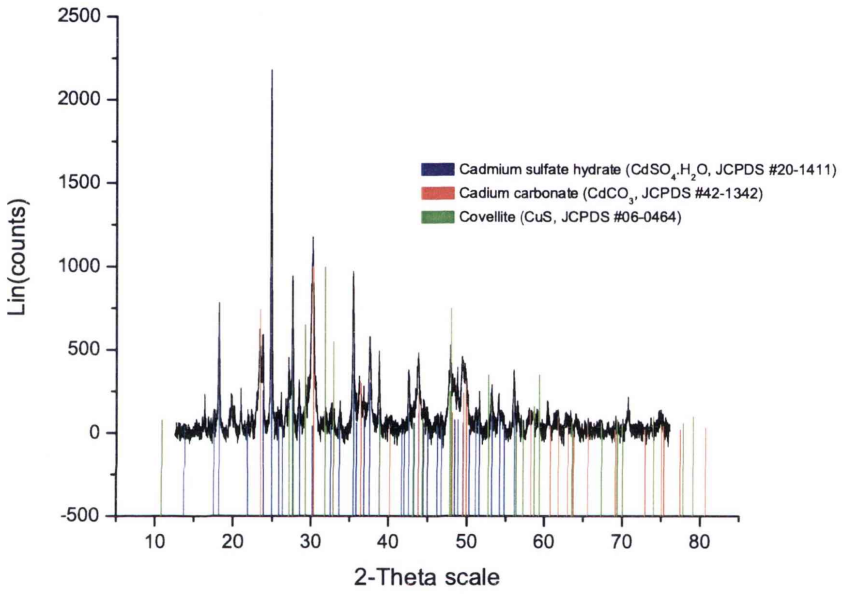

Figure 6.4: X-ray diffraction pattern for completely discoloured cadmium yellow and malachite mixture. Peaks shown are the discolouration products covellite (CuS), otavite ($CdCO_3$) and cadmium sulfate hydrate ($CdSO_4.H_2O$).

6.1.3 Effect of progressive discolouration

A series of progressively discoloured cadmium yellow and malachite pigment mixtures was analysed by x-ray diffraction to show the changes occurring in the early stages of the interaction. Initially a diffraction pattern for a mix of the dry unreacted pigments was made. The sample was then reacted in water until slightly discoloured, then dried and another diffraction pattern made. After further discolouration with water two more diffraction patterns were taken. The series of diffraction patterns (Figure 6.5) shows that the unreacted pigment mix contains only cadmium yellow and malachite. As the discolouration increases in the sample, the malachite peaks are reduced (at two-theta values of 17.50°, 24.25°, and 31.00°) and a new peak is formed at two-theta value 23.5°. This peak matches the pattern for otavite (cadmium carbonate) shows the discolouration products beginning to form with the loss of the malachite.

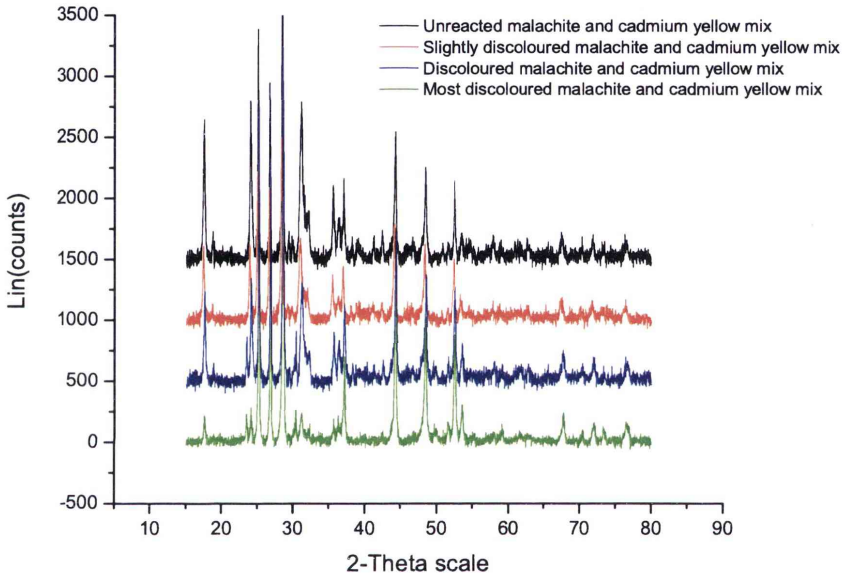

Figure 6.5: Series of progressively discoloured cadmium yellow and malachite pigment mixes. The top pattern is unreacted pigment mix, with patterns for increasing discolourations in order downwards.

Another form of progressive discolouration was characterised with x-ray diffraction. Three samples of cadmium yellow and malachite pigment mixtures were prepared in ratios of one-to-one, ten-to-one and one-to-ten (ratio of cadmium yellow to malachite by weight). These mixtures were combined with deionised water and agitated periodically over two months. Visually, there are obvious differences between the mixtures. The one-to-one ratio mixture has become black whereas the ten-to-one and one-to-ten samples retain some of the colour from one pigment (cadmium yellow and malachite respectively). This colour difference can be seen in Figure 6.6. The x-ray diffraction patterns of these three mixtures reflect the colour difference. The one to one ratio combination contains both the cadmium yellow pigment - a cadmium zinc sulfide ($Cd_{8.05}Zn_{1.95}S_{10}$), JCPDS 40-0835) and malachite pigment ($CuCO_3.Cu(OH)_2$, JCPDS 41-1390) along with cadmium carbonate ($CdCO_3$, JCPDS 08-0456) and covellite (CuS, JCPDS 06-0464) (Figure 6.7).

In the pattern for the mixture containing ten times as much cadmium yellow as malachite pigment it can be observed that malachite is no longer present after discolouration. The mixture contains cadmium yellow pigment ($Cd_{8.05}Zn_{1.95}S_{10}$), JCPDS 40-0835), cadmium carbonate ($CdCO_3$, JCPDS 08-0456) and covellite (CuS, JCPDS 06-0464) (Figure 6.8). Figure 6.9 shows the pattern for the mixture of one part cadmium yellow to ten parts of malachite pigment. In this case there is none of the original cadmium yellow pigment remaining in the discoloured sample. Malachite ($CuCO_3.Cu(OH)_2$, JCPDS 41-1390), cadmium carbonate ($CdCO_3$, JCPDS 08-0456) and covellite (CuS, JCPDS 06-0464) were all identified. This experiment indicates that each of the reactant pigments, cadmium yellow and malachite, will react completely to form discolouration products when in contact in aqueous solution.

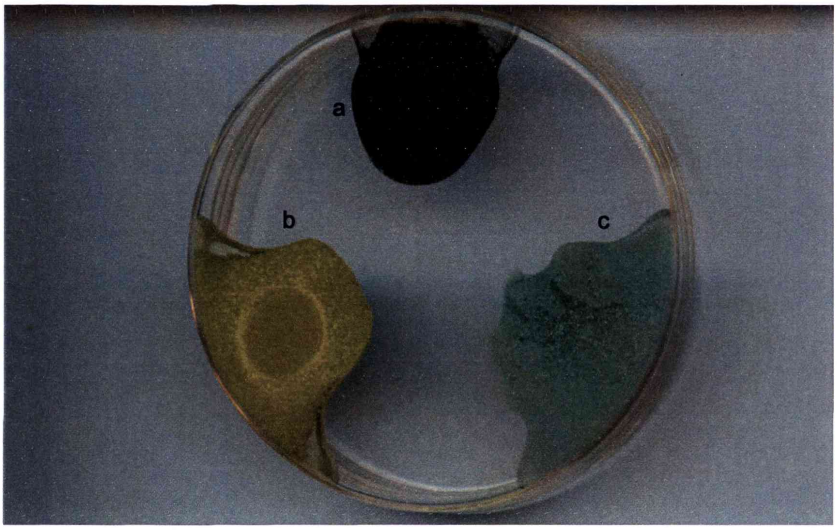

Figure 6.6: Discoloured cadmium yellow and malachite mixtures in (a) one-to-one, (b) ten-to-one and (c) one-to-ten weight ratios (cadmium yellow to malachite) (WOF = 10cm).

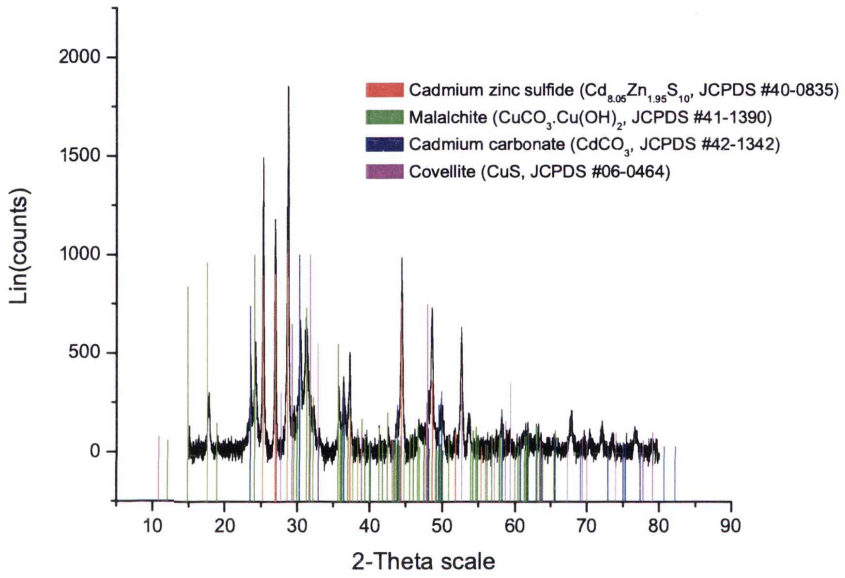

Figure 6.7: The diffraction pattern of discoloured cadmium yellow and malachite in a one-to-one weight mixture, showing the presence of the reactant pigments with cadmium carbonate and copper sulfide.

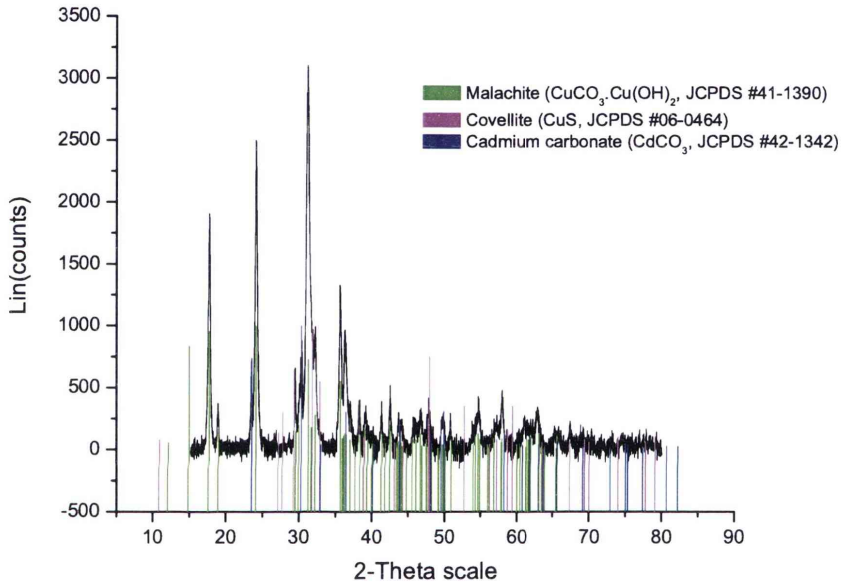

Figure 6.8: The diffraction pattern of discoloured cadmium yellow and malachite in a one-to-ten weight mixture, showing the discolouration products cadmium carbonate and copper sulfide with malachite only.

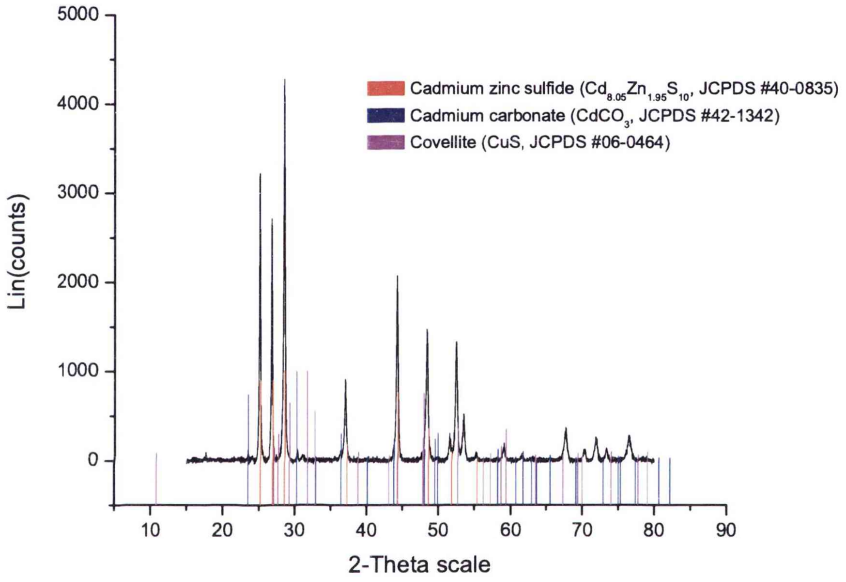

Figure 6.9: The diffraction pattern of discoloured cadmium yellow and malachite in a ten-to-one weight mixture, showing the discolouration products cadmium carbonate and copper sulfide with cadmium yellow only.

6.2 Thermal Analyses

Thermogravimetric analysis coupled with mass spectroscopy (TG-MS) for evolved gas analysis was used to analyse the phases formed during the discolouration of cadmium yellow and malachite pigment mixtures in the ratios of 1:1, 1:10 and 10:1 by comparison with the pure pigments. A limit of 800°C was used as cadmium sulfide is known to sublime at 980°C. The thermogravimetric analysis (TG) and differential thermogravimetric analysis (DTG) curves are shown in Figures 6.10 and 6.11. Figures 6.12, 6.13 and 6.14 show the mass spectroscopy curves for 18 (attributed to H_2O), 44 (CO_2) and 64 (SO_2 ions) atomic mass units (amu). The 64 amu curves were chosen for analysis rather than 32 and 34 amu curves as some of the sulphur evolved in the furnace would be oxidised by the small amount of oxygen (<10ppm) present in the purge gas.

The cadmium yellow was observed to be fairly stable to up to 800°C. However some mass loss was observed with approximately 3.2% mass loss observed at 800°C. This mass loss may be attributed to dehydration (around 1.0%) and to sulfide removal (around 2.2%). The x-ray diffraction results (Figure 6.2) showed the presence of cadmium sulfate hydrate ($CdSO_4.H_2O$) after conditioning the cadmium yellow in water and drying. This suggests that the cadmium sulfide has been oxidised by atmospheric oxygen dissolved in the deionised water. Peaks in the 18 amu curve (Figure 6.12) suggest that water is lost up to 550°C and is consistent with the dehydration of cadmium sulphate hydrates reported in the literature (Olszak-Humienik & Mzejko 2003). Sulfates formed at heterogenous interfaces are known to decompose at temperatures lower than the bulk crystalline phase (Thomas *et al.* 2003). The peaks at 556°C and 782°C, observed in both the DTG and the 64 amu curves (Figures 6.11 and 6.14), may, therefore, be attributed to sulfate decomposition.

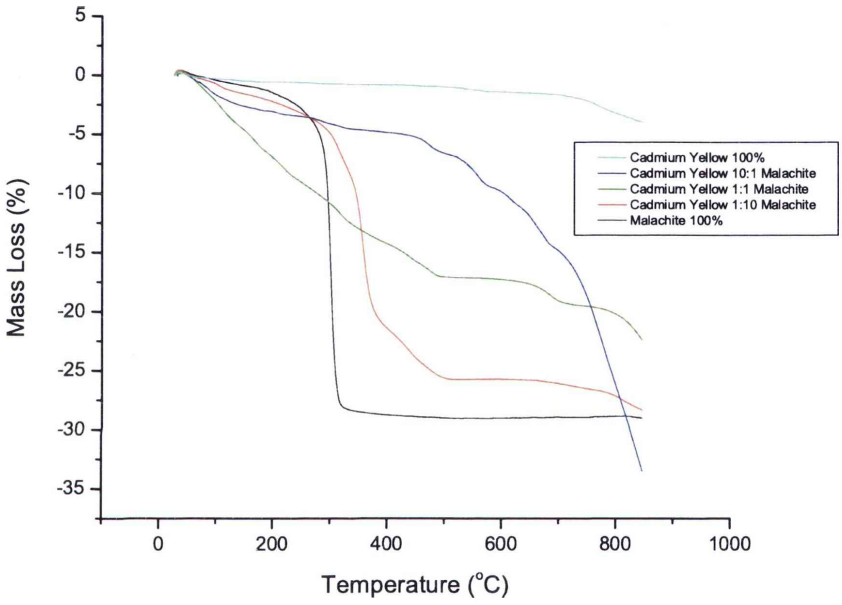

Figure 6.10: TG curves of the five systems studied: cadmium yellow, malachite and reaction blends of 10:1, 1:1 and 1:10 by mass.

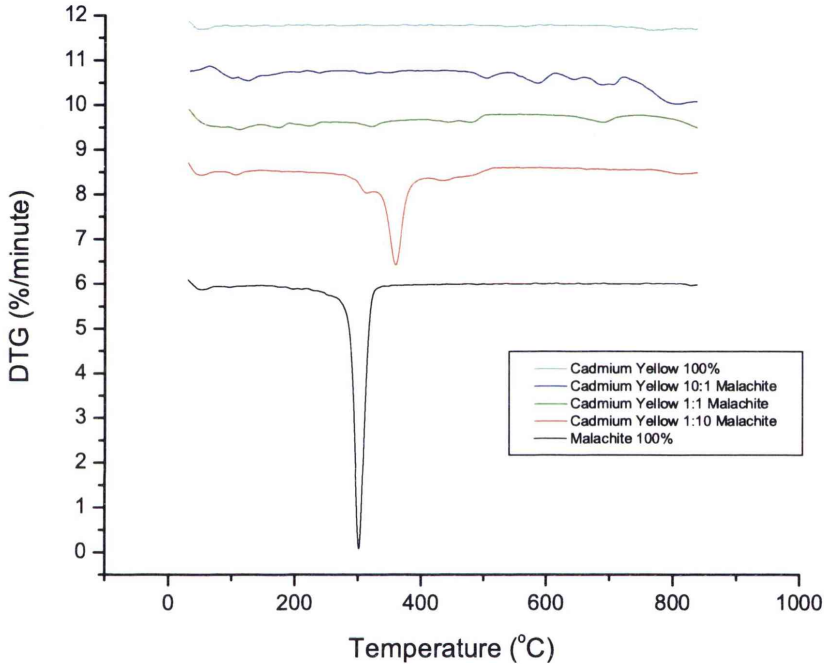

Figure 6.11: DTG curves of the five systems studied: cadmium yellow, malachite and reaction blends of 10:1, 1:1 and 1:10 by mass.

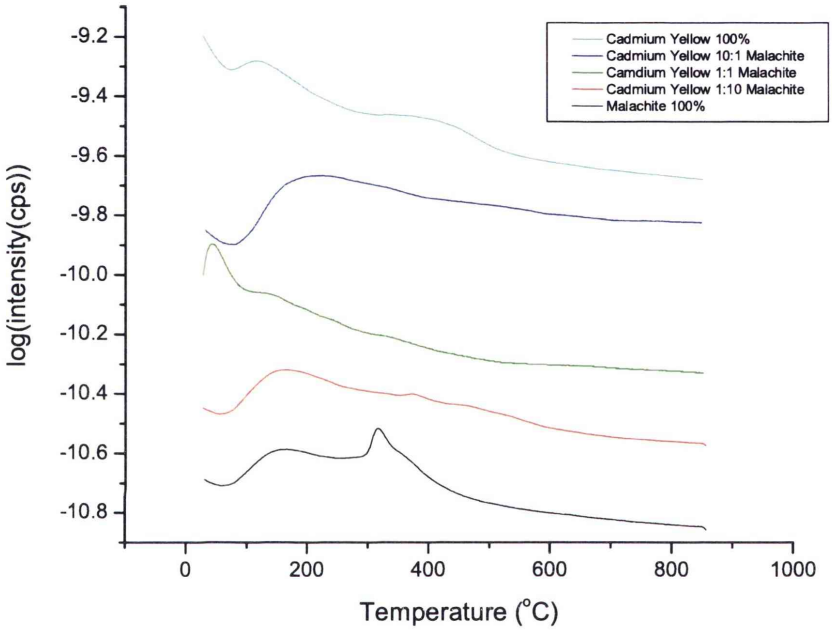

Figure 6.12: Mass spectra response curves (in arbitrary units as intensity is non-quantitative) for 18 amu for the five systems studied: cadmium yellow, malachite and reaction blends of 10:1, 1:1 and 1:10 by mass.

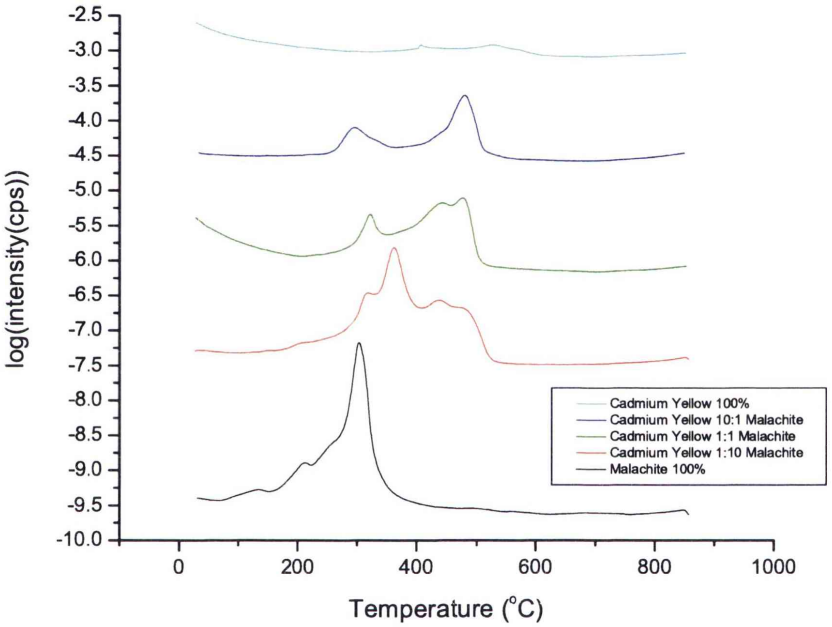

Figure 6.13: Mass spectra response curves (in arbitrary units as intensity is non-quantitative) for 44 amu for the five systems studied: cadmium yellow, malachite and reaction blends of 10:1, 1:1 and 1:10 by mass.

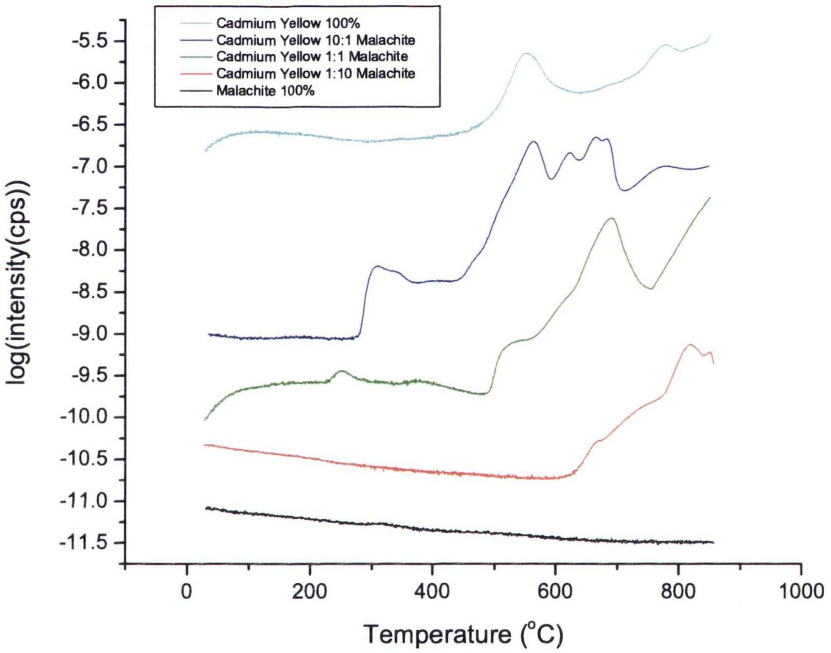

Figure 6.14: Mass spectra response curves (in arbitrary units as intensity is non-quantitative) for 64 amu for the five systems studied: cadmium yellow, malachite and reaction blends of 10:1, 1:1 and 1:10 by mass.

The malachite was observed to decompose through a single step with a peak in the DTG curve at 302°C, as has been reported in the literature (Wieczoreck-Ciurowa *et al.* 2000, Koga & Tanaka 2005). This single sharp peak is accompanied by a complex series of peaks in the 44 amu (CO_2) curve at 137°C, 214°C, 261°C and 306°C (Figure 6.13). The 18 amu curve (Figure 6.12) also showed a wide temperature range for decomposition attributable to adsorbed water with a broad peak at 170°C and a sharp dehydroxylation peak at 320°C with a shoulder at 370°C. The mass spectroscopy curves suggest a more complex decomposition process than the TG/DTG curves show, as has been reported elsewhere (Frost *et al.* 2002). The mass loss for the thermal decomposition of malachite was 29.0% which is a little lower than the expected 30.8% theoretical loss based on a stoichiometric reaction of the following equation in thermal decomposition (Wieczoreck-Ciurowa *et al.* 2000, Frost *et al.* 2002, Koga & Tanaka 2005):

$$CuCO_3.Cu(OH)_2 \longrightarrow 2CuO + CO_2 + H_2O$$

The decomposition of each pigment blend is observed to be quite complex passing through a number of steps in each case, suggesting significant change in composition in each sample. From the x-ray diffraction results (Section 6.1.3), the major species present were the reactants, malachite and cadmium yellow, CuS and $CdCO_3$. In the temperature range studied, CdS is expected to be stable, malachite is reported to decompose according to the previous equation, and CuS is expected to decompose at 507°C (Roseboom-Jr 1966):

$$2CuS \longrightarrow Cu_2S + S$$

Cadmium carbonate ($CdCO_3$) is expected to decompose with a peak in the DTG curve at 445°C (Biernacki & Pokrzywnicki 1996):

$$CdCO_3 \longrightarrow CdO + CO_2$$

The specimen with ratio cadmium yellow 1:10 malachite was observed to contain $CdCO_3$, malachite and CuS as the phases present after the reaction. Four peaks are observed at 315°C, 360°C, 439°C and 481°C in the DTG curve (Figure 6.11). These peaks correspond well with the peaks in the 44 amu curve CO_2 at 320°C, 362°C, 438°C and 482°C (Figure 6.13). This suggests a complex series of carbonate phases present which includes both the basic copper carbonate and the cadmium carbonate. It is likely that basic zinc carbonate is also present, although basic zinc carbonate has been observed to decompose with a peak rate at 250°C (Koga & Tanaka 2005), a temperature lower than the CO_2 evolution observed here. For the cadmium yellow 1:10 malachite ratio specimen SO_2 is not observed until 630°C, a much higher temperature than expected for the decomposition of CuS to Cu_2S (expected at 507°C) despite the fact that the x-ray diffraction results indicated the presence of covellite and the complete consumption of the cadmium yellow in the reaction (Section 6.1.3).

The cadmium yellow 1:1 malachite ratio sample loses mass throughout the temperature range studied. A series of small peaks is observed in the DTG at 116°C, 177°C, 226°C, 324°C, 446°C, 483°C and 694°C (Figure 6.11). It is likely that the lower temperature steps are associated with the removal of water of hydration. CO_2 is evolved from approximately 220°C with peaks in the 44 amu curve at 324°C, 444°C and 479°C (Figure 6.13) suggesting the presence of malachite, cadmium carbonate and possibly other phases such as zinc carbonate. The 64 amu curve (Figure 6.14), indicating sulphur evolution, has an onset of 495°C and is fairly close to the decomposition temperature of the CuS in accordance with the previous equation. Further loss of sulphur is likely to be associated with the decomposition of the cadmium yellow remaining.

The cadmium yellow 10:1 malachite ratio sample contained approximately 5% water which was removed at 200°C. Further mass loss is associated with the decomposition of the reaction species present. The 44 amu curve (Figure 6.13) has peaks

at 298°C and 482°C. Neither of these carbonate species are likely to be malachite as no malachite was observed in the x-ray diffraction pattern (Section 6.1.3). Identification is again difficult: however these peaks are likely to be associated with zinc and cadmium carbonates. For this specimen, the onset of the 64 amu evolution is at 282°C (Figure 6.14), the lowest of all the systems studied. Additionally, the peaks in both the 44 and the 64 amu curves in the low temperature region (<450°C) coincide indicating that it is the decomposition of partially reacted cadmium yellow that is occurring. Higher temperature peaks in the DTG curve are observed at 507°C, 590°C, 645°C, 690°C and 708°C with the onset of a larger mass loss process above 730°C (Figure 6.11). All of these peaks coincide well with the peaks in the 64 amu curve indicating sulfur loss from the specimen. The total mass loss for this blend ratio is greater than occurs in its counterparts suggesting significant disruption to the cadmium yellow phase.

Examination of the phases produced by reacting malachite with cadmium yellow in an aqueous medium by x-ray diffraction indicated that the reaction produced reaction products based on an ion exchange mechanism where copper (II) sulfide and cadmium carbonate were the products. The TG-MS data suggests that the phases present in the reaction products are much more complex with a variety of products being produced with a range of thermal stabilities. The Cadmium Yellow 10:1 Malachite ratio specimen, in particular, demonstrated the extent of the effect that copper ions have on sulphide pigments. These results demonstrate the complexity of the reaction and that a greater range of reaction products was produced than those identified by x-ray diffraction.

6.3 SEM EDS

Conventional scanning electron microscopy was used to examine the cadmium yellow and malachite pigments and the products of interaction. This was carried out on carbon coated samples using a Zeiss 55VP Supra SEM.

6.3.1 Pigment characterisation

Cadmium Yellow

Cadmium yellow pigment is made up of nano-particles. Figure 6.15 shows the fine particle size of the pigment. Most particles are around 75 to 100 nanometres in diametre and tend to agglomerate into larger masses of material. Figure 6.16 is an EDS x-ray spectrum of cadmium yellow pigment. The presence of zinc is detected which is consistent with the colour of cadmium yellow being due to zinc in solid solution (Section 6.1.1). The amount of zinc is considerably lower than cadmium. This supports the conclusion that x-ray diffraction identification of the pigment has a cadmium zinc sulfide structure ($Cd_{8.05}Zn_{1.95}S_{10}$).

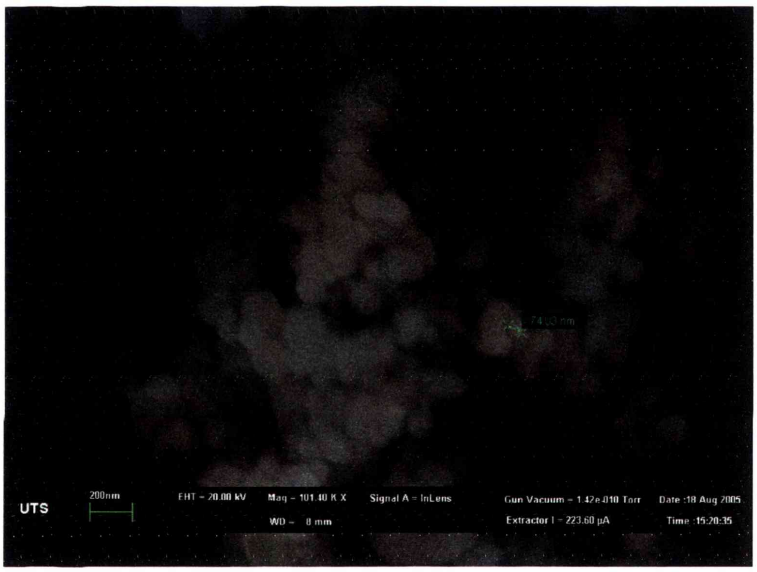

Figure 6.15: Cadmium yellow pigment particles, indicating average particle diameter of 75nm.

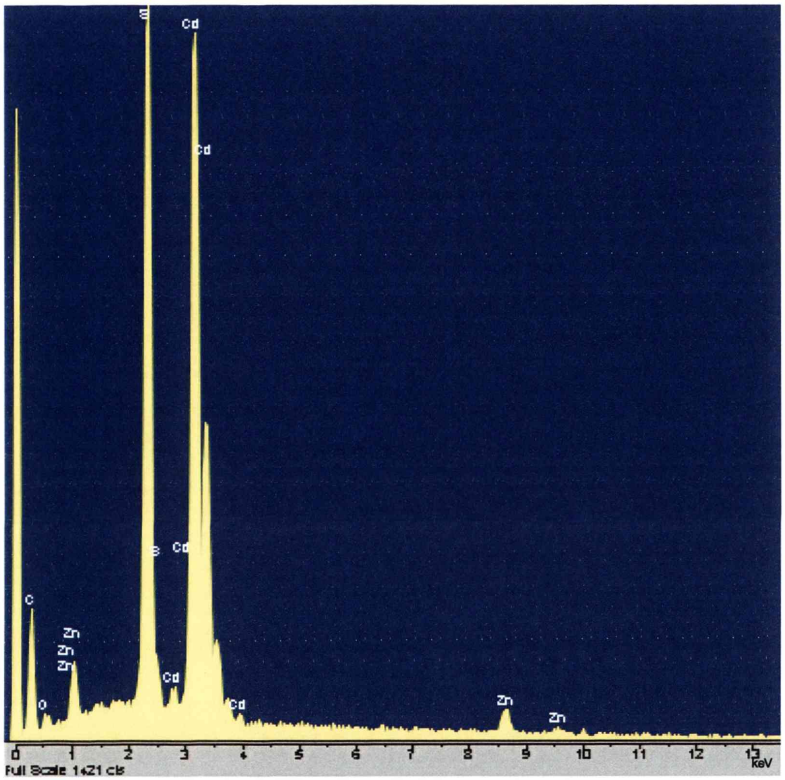

Figure 6.16: EDS x-ray spectrum of cadmium yellow pigment particles, showing the presence of zinc with the cadmium and sulfur.

Malachite

Malachite pigment shows a greater range of particle size (from 1μm to 5μm) than cadmium yellow, as can be seen in Figure 6.17. It also agglomerates readily. The x-ray spectrum of this sample shows the presence of only copper, carbon and oxygen as expected (Figure 6.18).

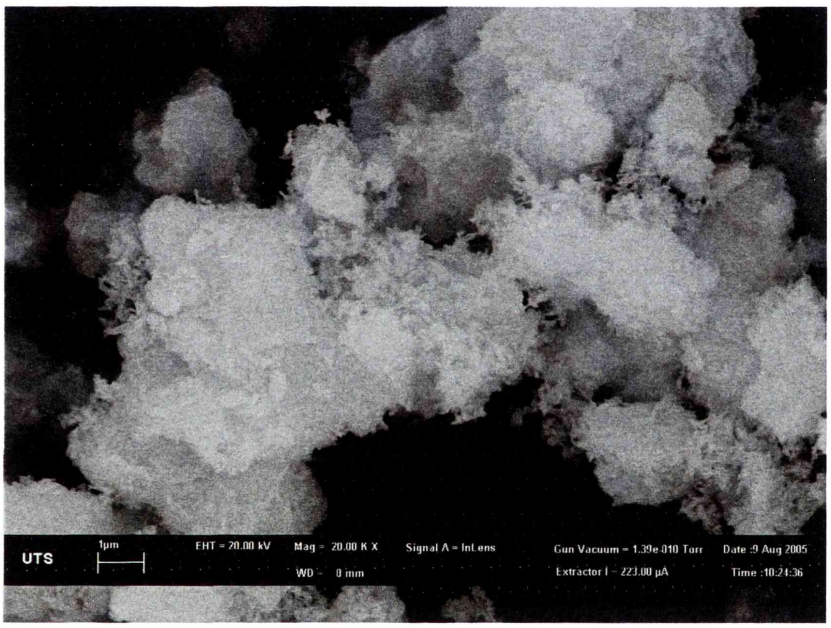

Figure 6.17: A micrograph of malachite pigment particles, showing particle sizes of 1μm to 5μm.

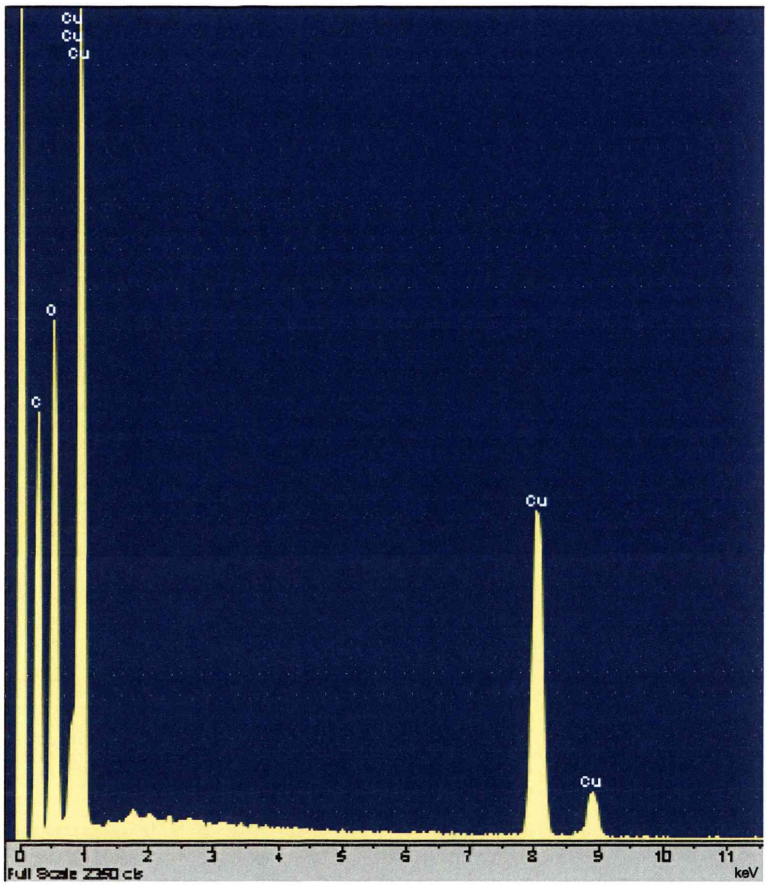

Figure 6.18: EDS x-ray spectrum for malachite pigment particles.

6.3.2 Characterisation of interaction products

In this work both malachite and other copper compounds were reacted with cadmium yellow. The following are conventional scanning electron microscope images of cadmium yellow reacted with various sources of copper ions.

Interactions with malachite

Cadmium yellow and malachite are both sparingly soluble pigments. Hence, complete discolouration in deionised water takes several weeks. Figure 6.19 is an image of a sample of the mixed pigments that has been allowed to discolour in deionised water for seven hours. In this back-scattered image, the dark large particles of malachite can be seen surrounded by small particles of a range of BSE signal intensities. These are the cadmium yellow particles that have reacted to a range of extents to form copper sulfides.

The interaction between these pigments can also be examined as a discolouration between the two pigments placed side by side. Figure 6.20 is a back-scattered electron image of the discoloured interface between cadmium yellow and malachite (as seen as a magnified image in Figure 5.6). In this image, and the following two figures, the range of particle morphologies created by the interaction is visible. In Figure 6.21 the plate-like hydrated cadmium sulfate crystals can be seen in the right of the image and in Figure 6.22 there are needle-like protrusions from the reacted malachite particles. These micron sized needles were no identifiable by XRD or SEM-EDS.

Figure 6.19: BSE image of cadmium yellow and malachite pigments after reaction in water for seven hours.

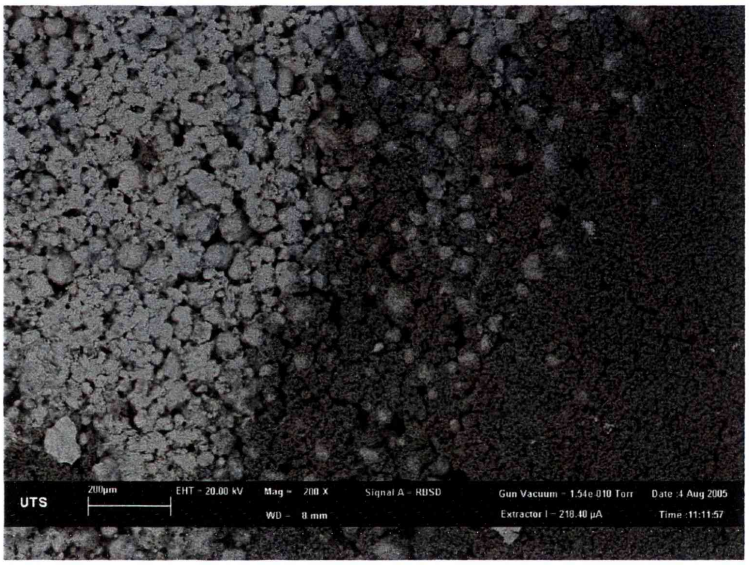

Figure 6.20: A BSE micrograph of a discoloured cadmium yellow (left) and malachite (right) interface.

Figure 6.21: A micrograph of the interface region from Figure 6.20, cadmium yellow (left) and malachite (right), showing plate-like cadmium sulfate crystals on the surface of the malachite region.

Figure 6.22: A micrograph of the malachite region near the interface from Figure 5.15, showing micron length needle-like protrusions from the malachite particles.

Interactions with other copper sources

Cadmium yellow was also reacted with a copper sulfate solution to examine the production of copper sulfides on the surface without the presence of an additional pigment during imaging. In Figure 6.23 the cadmium yellow pigment was briefly discoloured with a copper sulfate solution. The result of this is partial conversion of the exterior of the cadmium yellow particles to a copper sulfide. This is visible in the back-scattered electron image in Figure 6.23 as a darker edge around the individual particles. The darker region is not visible in the central part of the particles as the back-scattered electron signal from the cadmium yellow core of the particles dominates.

The effect of a darker copper sulfide layer on a cadmium sulfide substrate can be more clearly seen in Figure 6.24. This sample is a large cadmium sulfide particle, produced in the laboratory by synthesising cadmium sulfide in aqueous solution and allowing the product to dry as a solid mass. A piece of this cadmium sulfide was then briefly exposed to a copper sulfide solution which produced a dark layer all over the surface. The piece was then broken to reveal the surface layer and cadmium sulfide substrate for imaging. Figure 6.24 is a back-scattered electron micrograph of the cadmium sulfide substrate partially covered by a darker copper sulfide layer. The upper region of the image is completely covered in a cracked layer of copper sulfide. The lower area is the cadmium sulfide substrate, with a small amount of residual copper sulfide on the surface. The EDS spectra were taken of the copper sulfide (Figure 6.25) and cadmium sulfide (Figure 6.26) regions at 20 kV. As expected, there is very little cadmium present in the spectrum for the copper sulfide layer compared to the cadmium sulfide region. This small amount of cadmium present is likely to be due to the interaction volume of the beam penetrating through the copper sulfide layer into the cadmium sulfide substrate or some residual cadmium remaining in the dark layer. The relative proportions of copper and sulfur in this spectrum (Figure

6.25) indicate that a copper sulfide phase is present. Figure 6.26 shows that there is some copper present in the cadmium sulfide substrate spectrum but this is likely to be due to small areas of copper sulfide layer being present on that part of the surface.

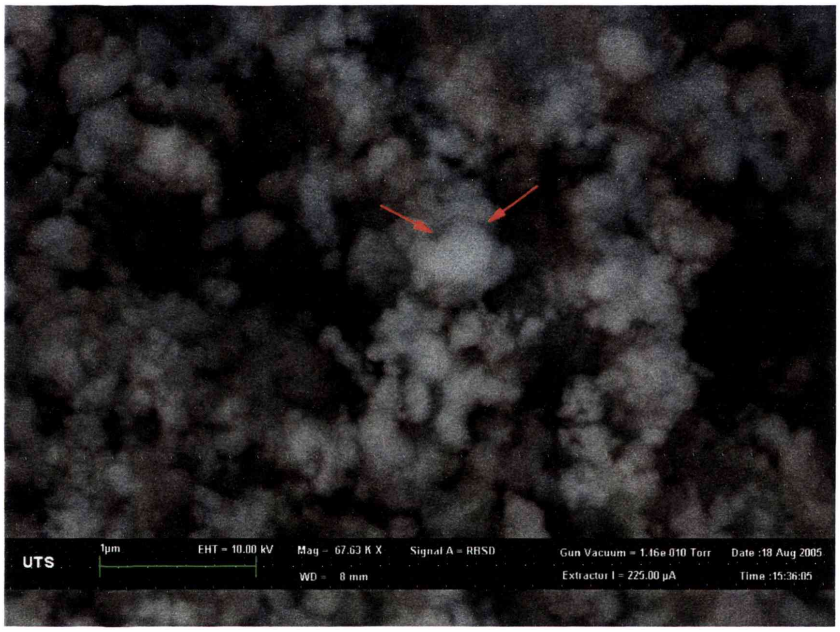

Figure 6.23: Cadmium yellow particles partially discoloured with copper sulfate solution, showing darker regions at the particle edges.

Figure 6.24: Cadmium sulfide substrate (lower bright area) with copper sulfide coating (upper darker area).

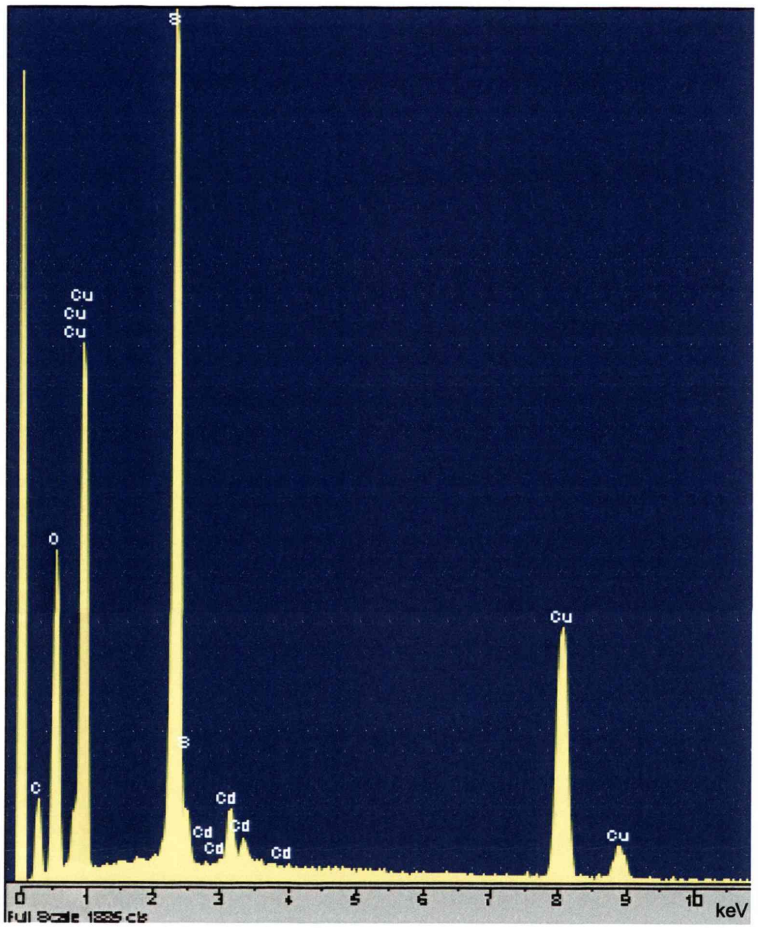

Figure 6.25: EDS spectrum at 20 kV of copper sulfide layer from Figure 6.24. Copper and sulfur are detected with a small amount of cadmium from the substrate.

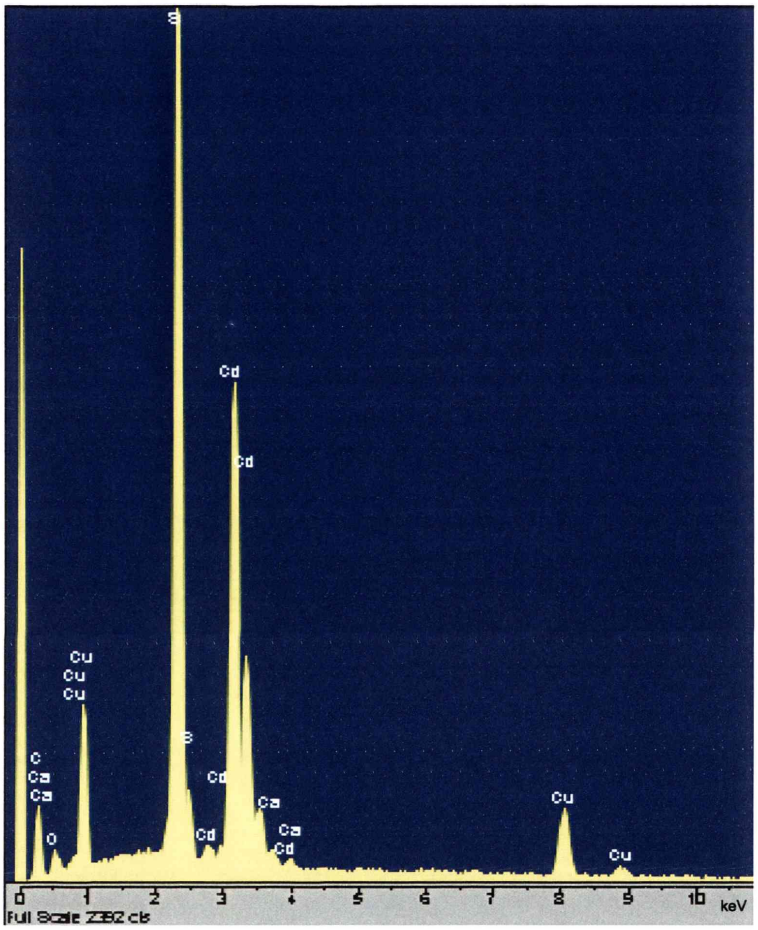

Figure 6.26: EDS spectrum at 20 kV of cadmium sulfide substrate from Figure 6.24. Cadmium and sulfur are detected with a small amount of copper from some residual copper sulfide layer as visible in the micrograph (Figure 6.24).

6.4 Summation

The structure and behaviour of cadmium yellow and malachite pigments and the products of their discolouring interaction have been characterised by a number of techniques. X-ray diffraction has confirmed the structure of the raw pigments and the products of their interaction as covellite (a divalent copper sulfide), hydrated cadmium sulfate and cadmium carbonate. This technique has also shown that as the interaction progresses, malachite is lost as the discolouration increases, and the reaction products begin to appear as this loss continues. Both the cadmium yellow and malachite pigments can be consumed completely in this interaction. The presence of cadmium sulfate hydrate has been shown to be due to oxidation of the cadmium yellow pigment in water. Covellite is to be expected as the product of reaction between divalent copper ions and cadmium yellow. The phase diagram for the Cu-S system (Roseboom-Jr 1966) (Figure 2.3) indicates that only this composition exists at room temperature for divalent copper. However, the thermal analyses indicate that the phases produced during the discolouration are more complex than indicated by the x-ray diffraction patterns. This may be due to the particle sizes of these phases being too small for adequate detection by XRD. The appearance of the reactant pigments and the discolouration products has been examined by SEM-EDS and the discolouration products have been visualised as lower contrast features on cadmium sulfide particles.

Chapter 7

X-ray Mapping

7.1 X-ray maps and scatter diagram analyses

X-ray maps of constituent elements were collected from specimens of unreacted pigment mixtures and pigment mixtures that were discoloured in water. From these x-ray maps, scatter diagrams were prepared for the elements of interest - copper, cadmium and sulfur. This was carried out in order to determine any phase associations between these elements in the sample and the changes in these associations due to discolouration processes. During these experiments, some artifacts due to the sample roughness were noted.

7.1.1 Unreacted pigment mixtures

Scatter diagrams for the combinations of copper, cadmium and sulfur were produced from x-ray maps of an unreacted cadmium yellow and malachite pigment mixture. The x-ray maps in Figure 7.1 are produced from clusters of particles and clearly show the cadmium yellow particles containing cadmium and sulfur and the malachite particles in the regions of high copper x-ray intensities. The dark regions that are common on all the maps show the regions where there are voids between particles, which are also visible on the secondary electron image (Figure 7.1(a)).

The scatter diagram for copper and sulfur, produced from the x-ray maps in Figures 7.1(c) and 7.1(d), shows two main lobes running along the copper and sulfur axes (Figure 7.2). This indicates that the copper and sulfur are not associated in the same phase. Some of the cross-over of the lobes on and immediately around the origin of the axes is due to voids in the mapped area of the sample that do not produce x-rays. The same applies for scatter points lying on the axes. The region between the lobes on the axes where there is some apparent overlap of the separate copper and sulfur nodes is due to x-ray signals from overlapped pigment particles giving intensities at the same pixel points and sample roughness affecting x-ray absorption. These points

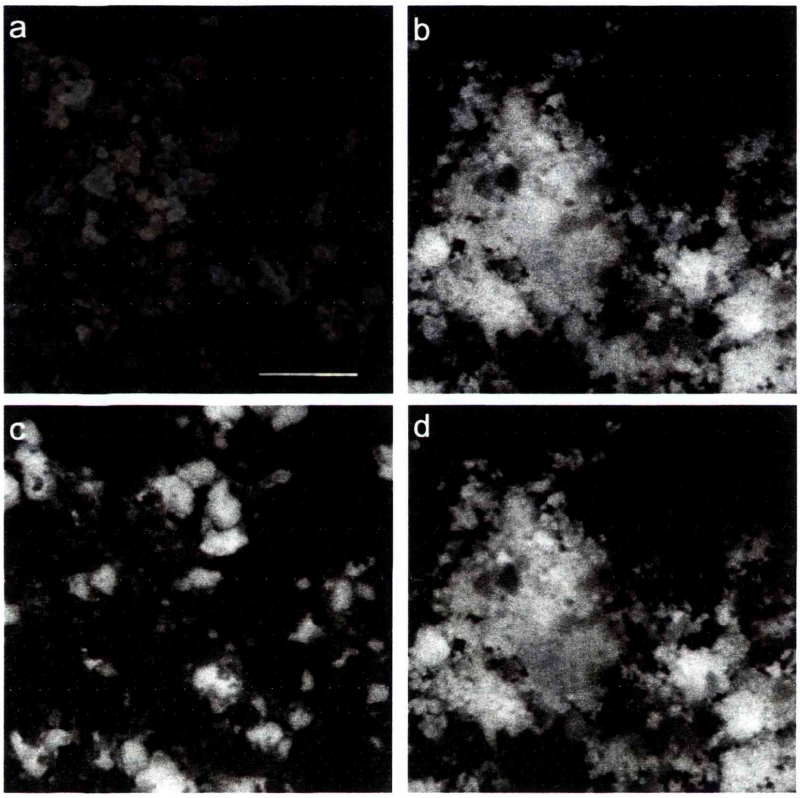

Figure 7.1: X-ray maps for an unreacted cadmium yellow and malachite pigment mix. Image (a) secondary electron image, and x-ray maps for (b) cadmium, (c) copper and (d) sulfur (20 kV, WOF = 43μm).

will be discussed further in Section 7.2. The scatter diagram for cadmium and sulfur (Figure 7.2), produced from the x-ray maps in Figures 7.1(b) and 7.1(d), clearly shows one phase association between the two elements, which is due to the cadmium yellow particles. The cluster is elongated and equidistant from both axes indicating the one to one ratio between the cadmium and sulfur components. Again the congregation of points around the origin is due to voids in the mapped sample area.

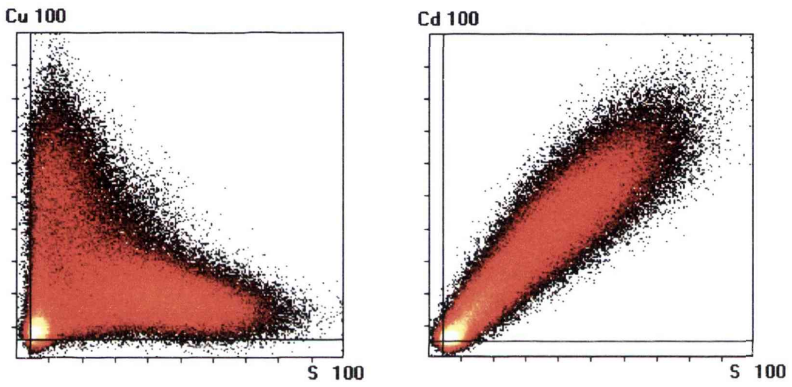

Figure 7.2: Scatter diagrams for copper and sulfur (left) and for cadmium and sulfur (right) from unreacted cadmium yellow and malachite pigment mixture x-ray maps (Figure 7.1).

The effects of the artifacts can be reduced by using a sample of both the unreacted and completely discoloured pigment mixtures that have been pressed into solid pellets prior to carbon coating. Figure 7.3 shows the secondary electron image and the x-ray maps for cadmium, copper and sulfur for a pressed sample of unreacted pigment. The accelerating voltage used was 15 kV, and the width of field 47μm. It is clear from these maps that this region of sample contains a greater amount of cadmium yellow pigment to malachite pigment. This is also apparent in the scatter diagrams (Figure 7.4) with the node along the sulfur axis of the copper-sulfur scatter plot being larger than the node on the copper axis. The collection of points around the origin seen in the scatter plots of the non-pressed sample (Figure 7.2) has disappeared in these scatter plots. This is due to voids no longer being present. The bridging between the theoretically discrete copper and sulfur nodes on the copper-sulfur scatter plot is still visible. Figure 7.5 shows that this area is between the malachite and cadmium yellow pigment areas. As this pigment sample was not discoloured, this bridging region between the nodes is most likely due to the overlap of copper-containing particles and cadmium containing particles within the interaction volume (Section 7.2).

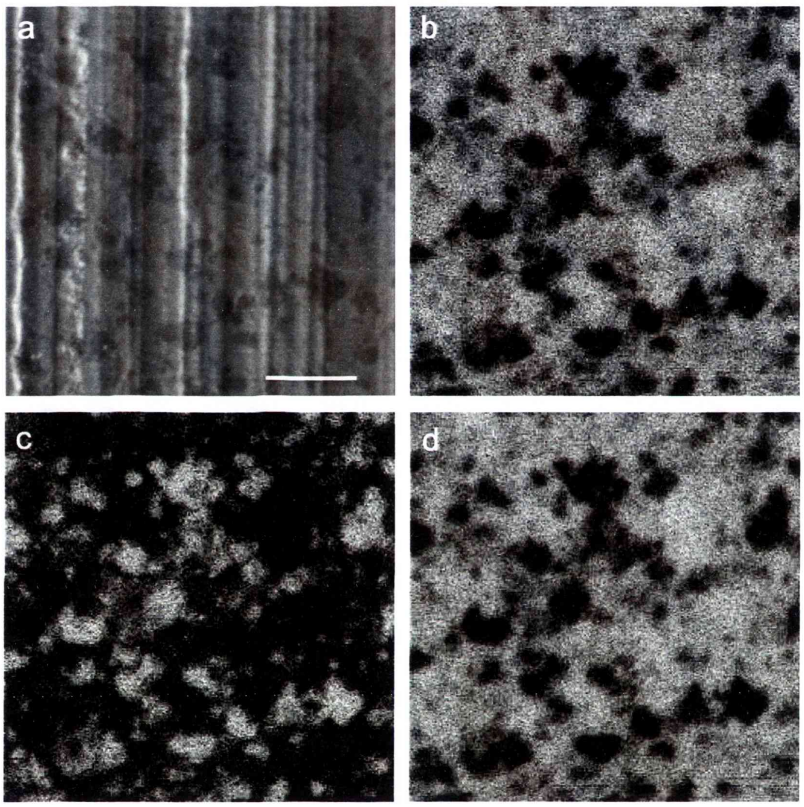

Figure 7.3: X-ray maps at 15 kV for a pressed pellet of unreacted cadmium yellow and malachite pigment mix. Image (a) secondary electron image, and x-ray maps for (b) cadmium, (c) copper and (d) sulfur (15 kV, WOF = 47μm).

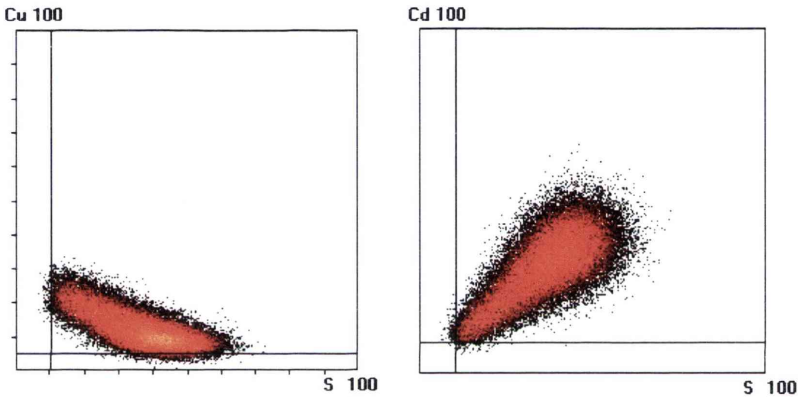

Figure 7.4: Scatter diagrams for copper and sulfur (left) and for cadmium and sulfur (right) from the pressed unreacted cadmium yellow and malachite pigment mixture x-ray maps (Figure 7.3).

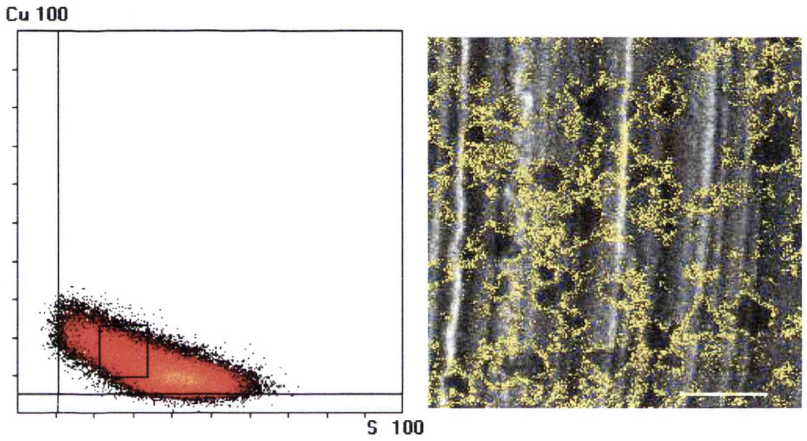

Figure 7.5: Scatter diagram for copper and sulfur (left) showing the mid region between the copper and sulfur nodes. The visual representation of that region on the secondary electron image (right) (15 kV, WOF = 47μm).

The selection of the individual copper and sulfur nodes on the scatter plot can be used to visually represent the malachite (copper-containing) and cadmium yellow (cadmium- and sulfur-containing) regions of the area mapped, as shown in figures 7.6 and 7.7 respectively. The program software can use the information from the individual element x-ray maps to pseudo-colourise the secondary electron image to give a visual representation of the distribution of the elements in the sample area. The x-ray maps for cadmium, copper and sulfur, are each designated a colour, in this case red, blue and green respectively. If a pixel contains just cadmium it will show as red, if just copper as blue, and if just sulfur it will appear green. If there is an association between two phases it will show as a colour represented between the two designated colours in the panel below the image - in this case yellow is positioned between the red of cadmium and green of sulfur on the colour scale at the bottom of the image. This means that the yellow areas of the colourised image are the common cadmium- and sulfur-containing phase, cadmium yellow pigment. Figure 7.8 shows that the regions of malachite (copper-containing) and cadmium yellow (cadmium- and sulfur-containing) pigments are separate.

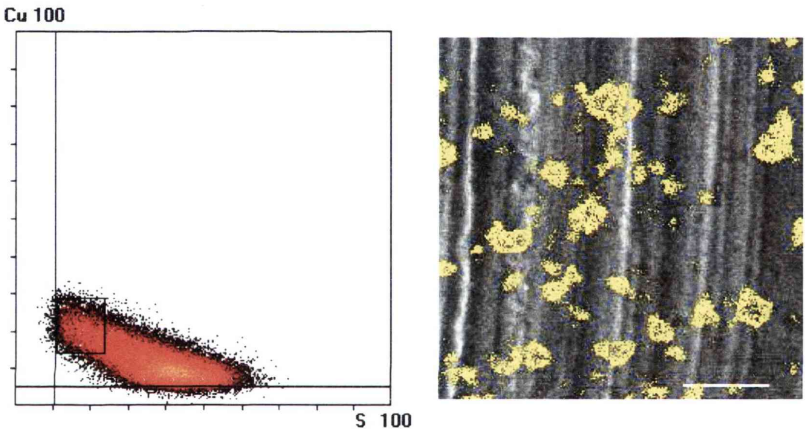

Figure 7.6: Scatter diagram for copper and sulfur (left) showing the copper node. The visual representation of the copper region on the secondary electron image (right) (15 kV, WOF = 47μm).

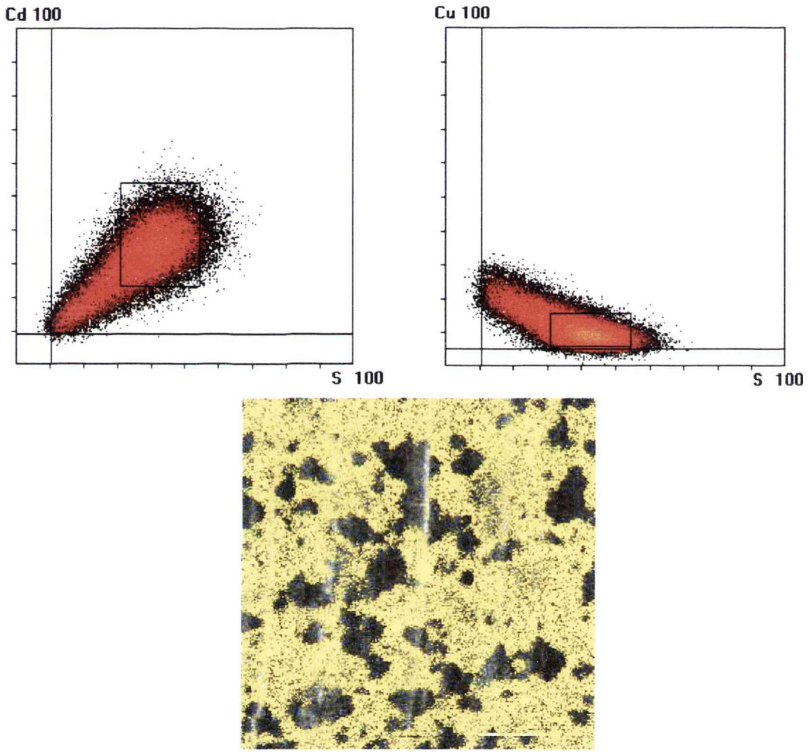

Figure 7.7: Scatter diagrams for cadmium-sulfur and copper-sulfur (top) showing the selection of the sulfur node. The visual representation of the cadmium sulfide region on the secondary electron image (bottom) (15 kV, WOF = 47μm).

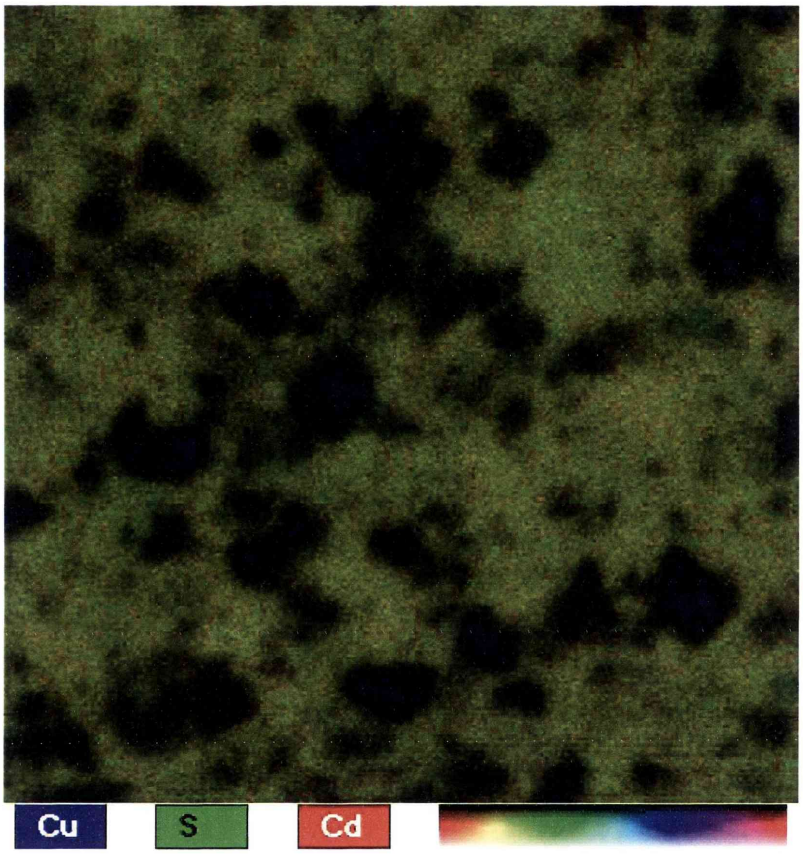

Figure 7.8: Pseudo-coloured image of the pressed unreacted pigment mixture. The blue colour indicates the copper-containing regions; the yellow shows the cadmium sulfide phase; and the lack of a light blue colour indicates no common copper-sulfur phase. (15 kV, WOF = 47μm).

7.1.2 Pigment mixtures reacted in water

Partially discoloured samples

Another series of x-ray maps was taken of a cadmium yellow and malachite pigment mixture that had been reacted for an hour in deionised water (Figure 7.9). The scatter diagram for copper and sulfur (Figure 7.10) is significantly different from that of the unreacted pigment mixture. Here we see a common copper and sulfur phase forming between the axes. The cadmium and sulfur scatter diagram (Figure 7.10) again shows the one phase for the cadmium yellow particles that have not yet reacted and are still present.

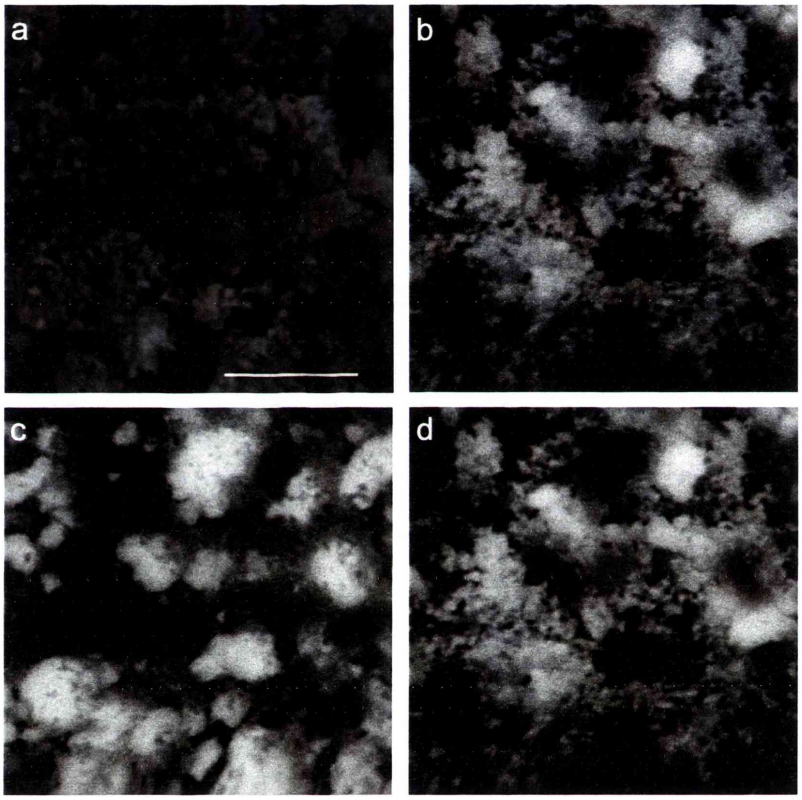

Figure 7.9: X-ray maps for a cadmium yellow and malachite pigment mix reacted in water for one hour. Image (a) secondary electron image, and x-ray maps for (b) cadmium, (c) copper and (d) sulfur (WOF = 31.5μm).

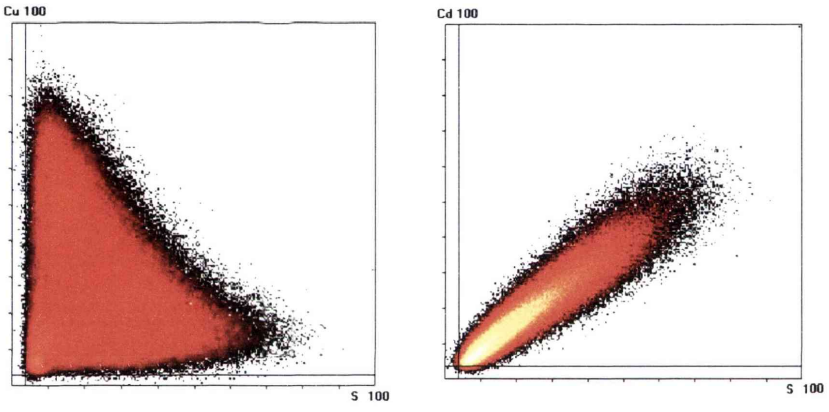

Figure 7.10: Scatter diagrams for copper and sulfur (left) and for cadmium and sulfur (right) from x-ray maps of a cadmium yellow and malachite pigment mixture reacted for one hour (Figure 7.9).

Discoloured samples

The x-ray maps from completely discoloured cadmium yellow and malachite pigment mixture on a glass substrate and carbon-coated are shown in Figure 7.11. The scatter diagram for copper and sulfur (Figure 7.12) from these maps shows a number of nodes of phase association between these elements in the sample. This indicates that a number of forms of copper sulfide exist throughout the sample. The copper sulfide phases represented by these nodes indicate differing chemical stoichiometries. The node positioned along a line at a forty five degree angle to the axes through the origin would represent copper and sulfur in a one-to-one ratio in that phase, suggesting a cuprous sulfide. The remaining nodes could be of varying stoichiometry and possibly be present as non-stoichiometric phases.

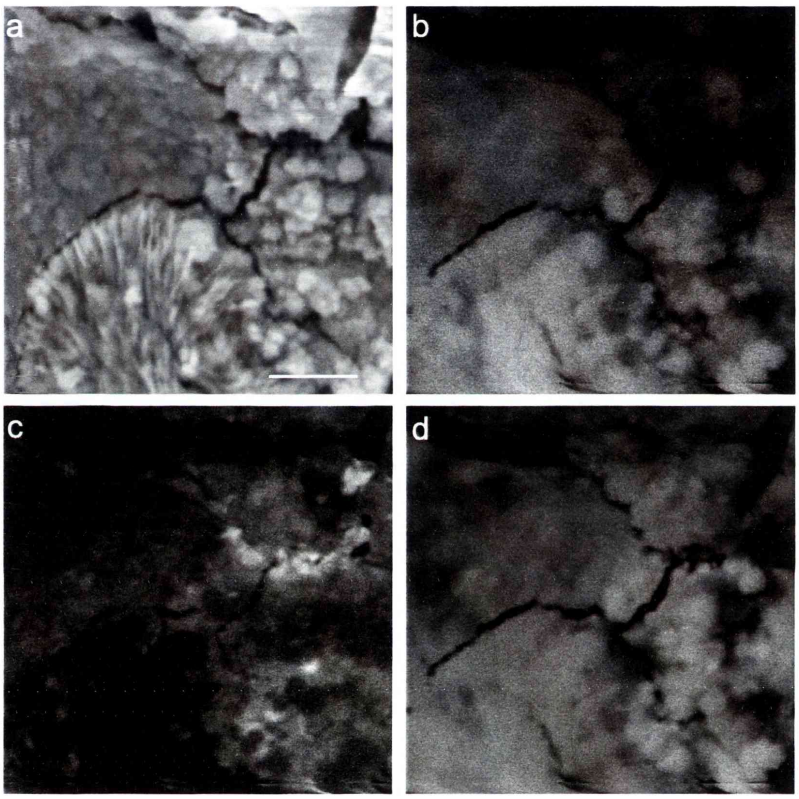

Figure 7.11: X-ray maps for a completely discoloured cadmium yellow and malachite pigment mix. Image (a) secondary electron image, and x-ray maps for (b) cadmium, (c) copper and (d) sulfur (20 kV, WOF = 47μm).

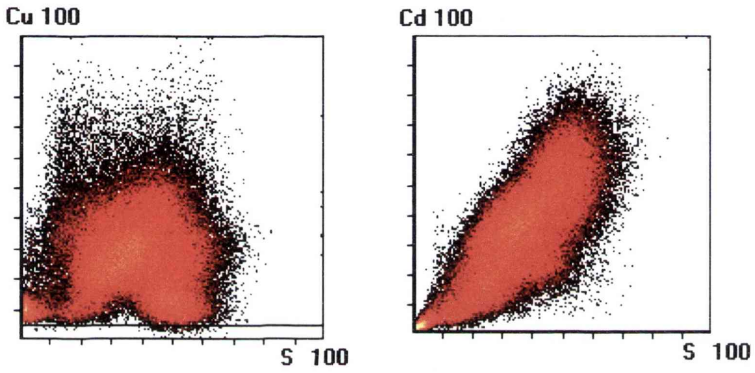

Figure 7.12: Scatter diagrams for copper and sulfur (left) and for cadmium and sulfur (right) from x-ray maps of a completely discoloured cadmium yellow and malachite pigment mixture (Figure 7.11).

In comparison, Figure 7.13 has the x-ray maps from a sample of completely discoloured cadmium yellow and malachite pigment mixture which has been pressed into a solid pellet.

The scatter plots created for these maps are markedly different from those of the particles that were mapped in Figure 7.12. Figure 7.14 does not show the concentration of scatter points on the axes or at the origin that indicate voids in the mapped area. There are apparently fewer nodes within the plot but there is still a strong phase association between copper and sulfur.

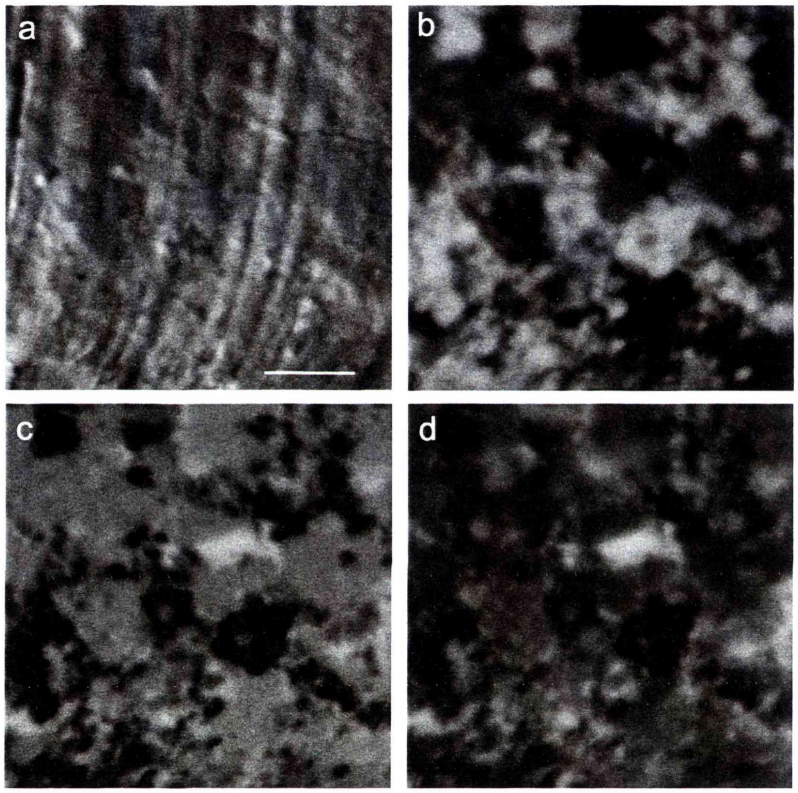

Figure 7.13: X-ray maps for a pressed sample of completely discoloured cadmium yellow and malachite pigment mix. Image (a) secondary electron image, and x-ray maps for (b) cadmium, (c) copper and (d) sulfur (15 kV, WOF = 47μm).

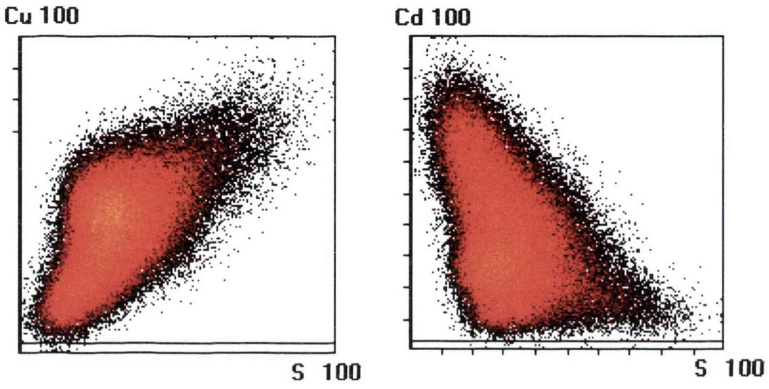

Figure 7.14: Scatter diagrams for copper and sulfur (left) and for cadmium and sulfur (right) from x-ray maps of a completely discoloured and pressed cadmium yellow and malachite pigment mixture (Figure 7.13).

There are three main phase nodes present in the scatter diagrams. These are shown in Figure 7.15. The monovalent copper sulfide phase region (CuS) occurs equidistant from the axes of the copper-sulfur scatter diagram and appears diffuse. This is due to the small size of the formed particles. Only the high copper and sulfur pixels are seen as copper sulfide has a small volume fraction of the map. The monovalent copper and sulfur phase can be selected on the scatter diagram, see Figure 7.16. This is visualised directly on the secondary electron image that is collected while the x-ray maps are collected. The image represents the regions of a common monovalent copper and sulfur phase. The region shown as yellow on the secondary electron image is common with the location of high copper and sulfur areas in the x-ray maps (Figure 7.13 (c) and (d)).

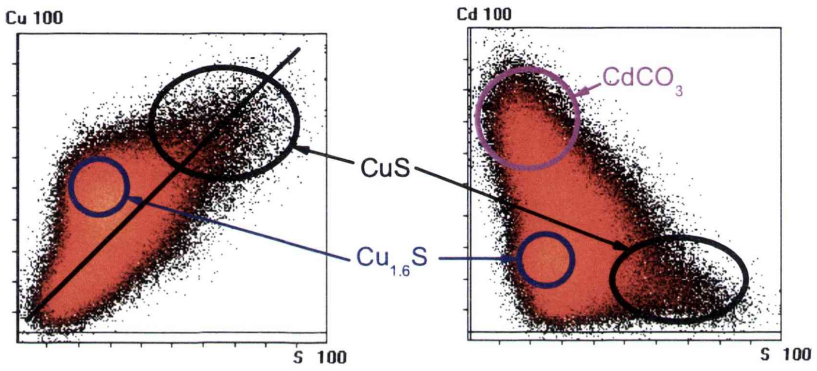

Figure 7.15: Scatter diagrams for copper and sulfur (left) and for cadmium and sulfur (right) with copper sulfide, cadmium carbonate and a previously unidentified high-copper copper sulfide phase nodes indicated.

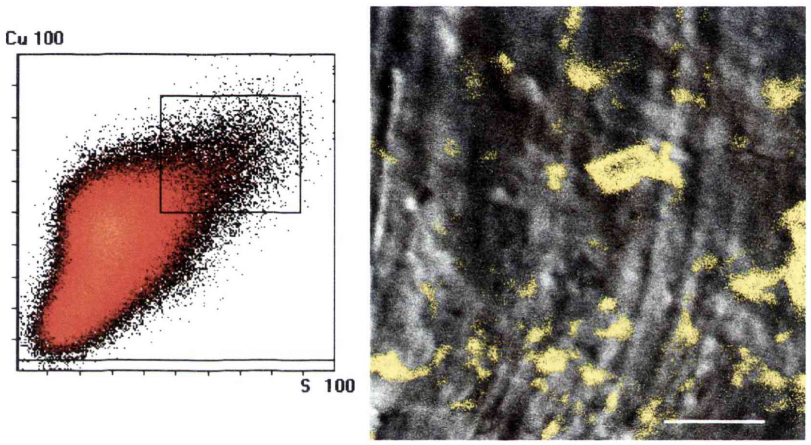

Figure 7.16: Copper-sulfur scatter diagrams of the pressed completely reacted pigment mixture (left) with the selected area visualised on the secondary electron image (right) (15 kV, WOF = 47μm).

The phase node that is offset from the CuS phase axis is due to another copper- and sulfur- containing phase. From its position in the copper-sulfure scatter diagram (Figure 7.15) it appears to contain more copper than the monovalent CuS, with an elemental ratio of approximately $Cu_{1.6}S$. Figure 7.17 shows the scatter diagram with this phase selected. This high-copper copper sulfide species was not identified by x-ray diffraction. This could be due to the small size of that phase's particles being x-ray amorphous or that it is a non-stoichiometric phase and therefore not identifiable using the JCPDS database (JCPDS 2005).

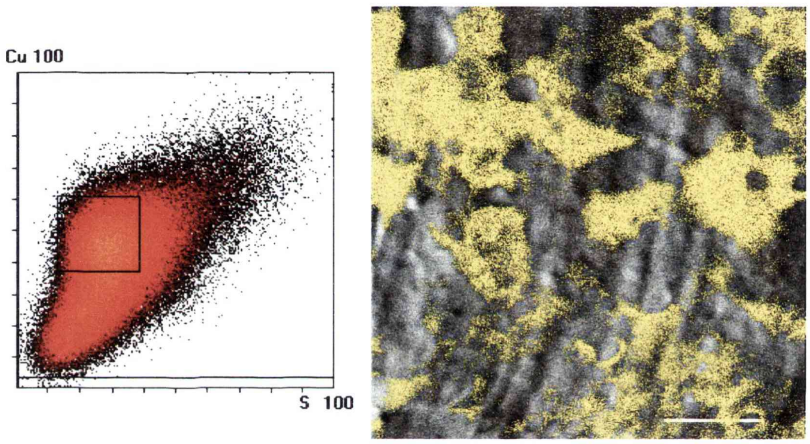

Figure 7.17: Scatter diagrams for copper and sulfur with the copper region selected and overlaid on the SE image. This area is high-copper copper sulfide species not identified by XRD (15 kV, WOF = 47μm).

Similarly, the cadmium-containing phase is visualised in Figure 7.18 by selection of an area on the scatter plots that is associated with high cadmium. The area selected is close to the cadmium axes on the cadmium-sulfur scatter plot, indicating a phase that is not associated with sulfur in a one-to-one ratio (as for CdS). The cadmium represented in this phase node would be in the form of cadmium carbonate and cadmium sulfate monohydrate.

The overlap of particles within the x-ray generation or interaction volumes contributes to a bridging between the phase nodes on the scatter plots. Figure 7.19 shows the selection and visualisation of an area of the scatter plots between the phase nodes. The visualisation indicates that this region of the scatter plots is due to x-rays from the interface regions being collected at the same point.

The distribution of the various phases can be visualised using a pseudo-coloured combination of the x-ray maps (Figure 7.20). The x-ray maps for cadmium, copper and sulfur, are designated colours, green, blue and red respectively. The green areas contain just cadmium. There are regions containing copper that are indicated in blue. If there is an association between two phases it will show as a colour between the two designated colours - in this case purple is positioned between the blue of copper and red of sulfur on the colour scale at the bottom of the image. This means that the purple areas of the colourised image are the common copper- and sulfur-containing phase. No yellow area (the mid colour between cadmium and sulfur on the colour scale) is present, indicating that there is no common cadmium- and sulfur-containing phase. It confirms the x-ray diffraction results that no cadmium sulfide is present in the completely discoloured pigment mixture.

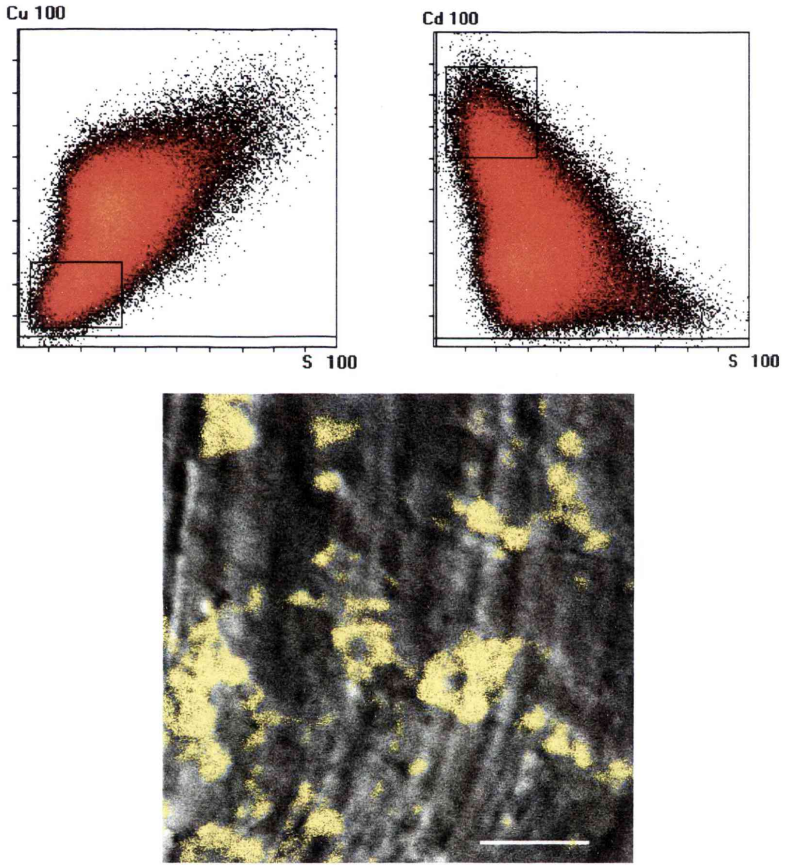

Figure 7.18: Scatter diagrams (copper-sulfur on the left and cadmium-sulfur on the right) of the pressed completely reacted pigment mixture with the cadmium containing phase selected and visualised on the SE image (15 kV, WOF = 47μm).

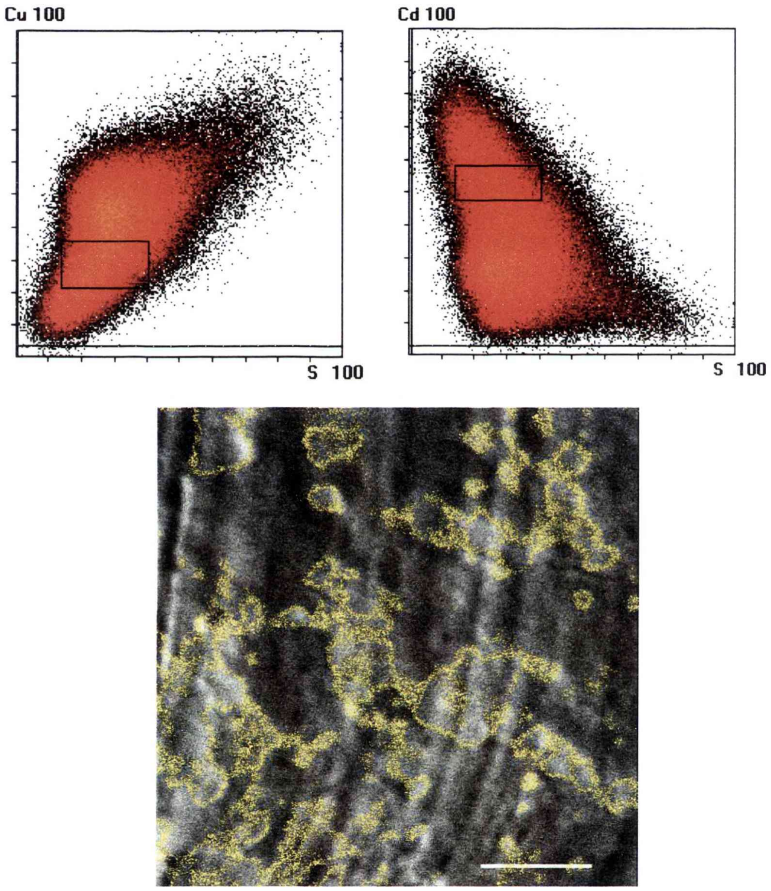

Figure 7.19: Scatter diagrams (copper-sulfur on the left and cadmium-sulfur on the right) of the pressed completely reacted pigment mixture with the area between the phase nodes selected and visualised on the SE image (15 kV, WOF = 47μm).

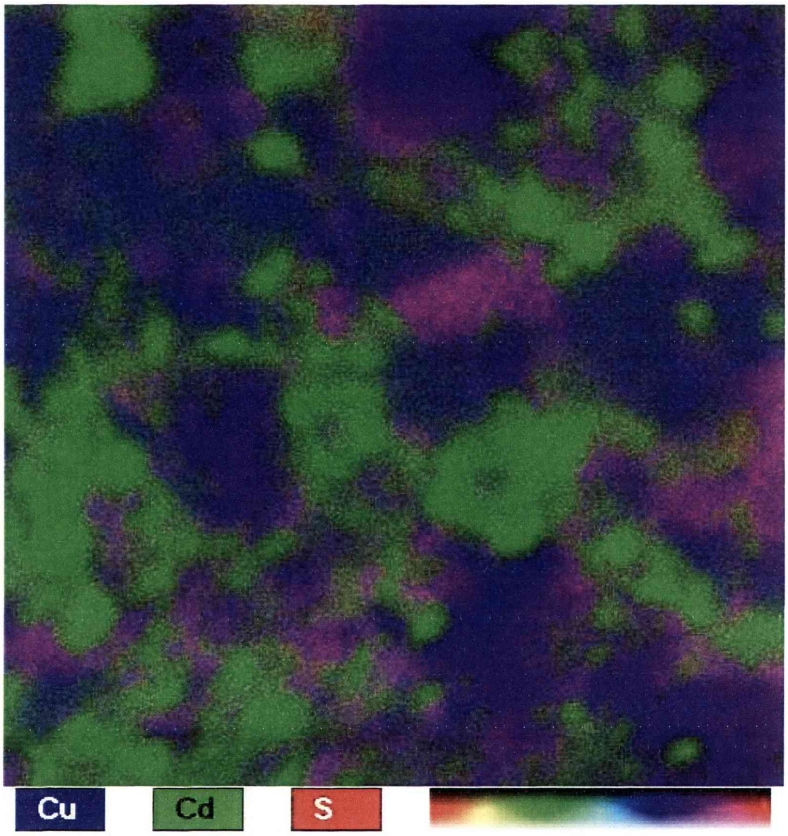

Figure 7.20: A pseudo-coloured image of the pressed completely reacted pigment mixture. Purple represents the copper- and sulfur-containing phase; blue the copper regions; green the cadmium-containing phase. The absence of yellow region indicates there is no cadmium sulfide phase present (15 kV, WOF = 47μm).

Comparing the copper and sulfur scatter plots from the unreacted, partially and completely discoloured pigment mixes shows the changes in phase association between the two elements (Figure 7.21). As discolouration progresses, there is a transition from no phase association between copper and sulfur in the unreacted mixture, through the partially discoloured sample showing a common region of phase association along with the separate copper and sulfur phases, to the number of copper- and sulfur-containing phases present in the completely discoloured pigment mixture.

These scatter plots (Figure 7.21) are of unpressed or uneven samples. Despite the effect of artifacts due to the uneven surfaces, they show that the phase association between copper and sulfur increases with the extent of discolouration. A comparison may be more easily made between the scatter plots generated from the x-ray maps of the pressed samples. Figures 7.22 and 7.23 show the comparison between copper-sulfur and cadmium-sulfur scatter plots of the unreacted pigment mixture and the completely reacted pigment mixture. In Figure 7.22, the phase nodes have changed from separate nodes on the axes (with a bridging phase due to artifacts of the imaging process) to a main phase node situated nearly equidistant from each axis, suggesting a one-to-one ratio of the elements present in the phase. This is a clear indication that the discolouration is due to the creation of a copper sulfide phase. During discolouration the cadmium sulfide phase association clearly present in the unreacted sample (Figures 7.7 and 7.8) has broken down into separated nodes in the completely discoloured sample (Figure 7.23).

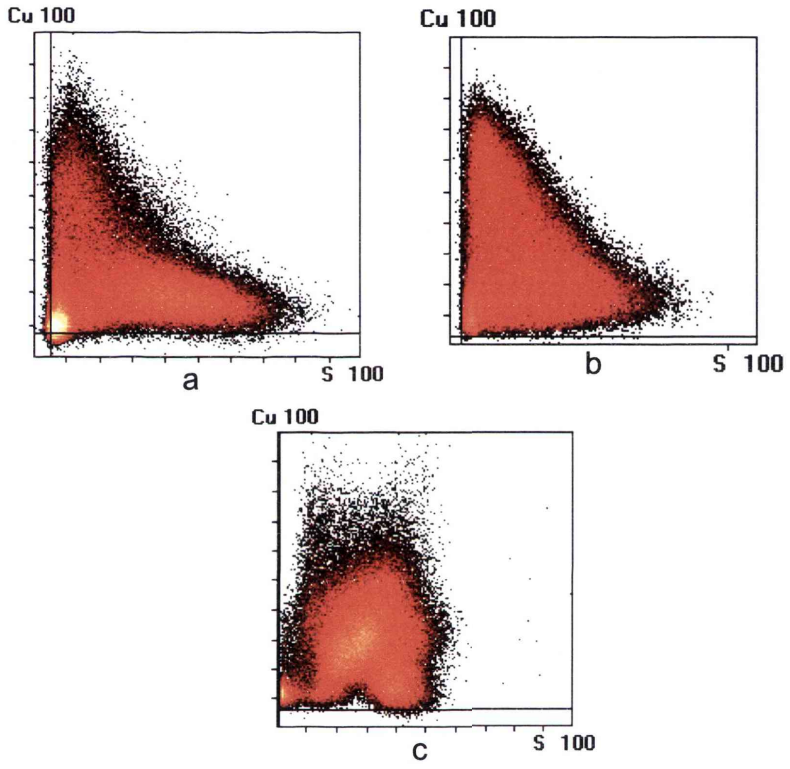

Figure 7.21: Scatter diagrams for copper and sulfur for unpressed samples of (a) unreacted pigment mix, (b) pigment mix reacted for one hour and (c) completely discoloured pigment mixture. These show that the association between copper and sulfur increases with the extent of reaction.

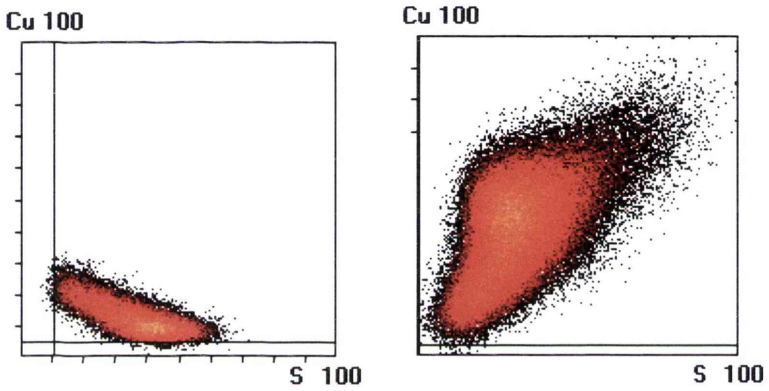

Figure 7.22: Copper-sulfur scatter diagrams for unreacted pigment mix (left) and the completely discoloured pigment mixture (right), showing the increase of copper-sulfur phase association after discolouration.

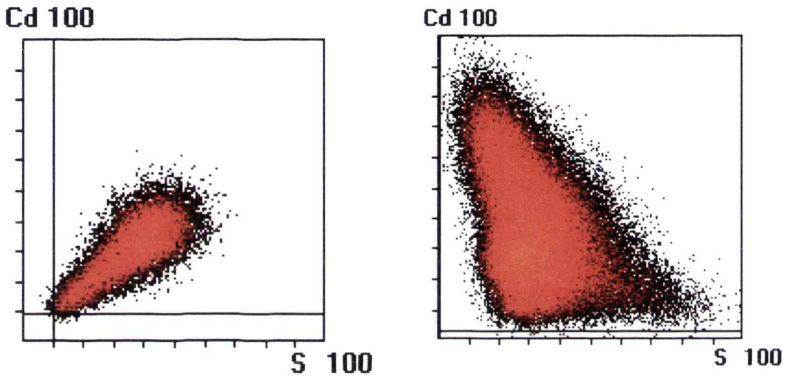

Figure 7.23: Cadmium-sulfur scatter diagrams for unreacted pigment mix (left) and the completely discoloured pigment mixture (right), showing the breakdown of the common cadmium-sulfur phase after discolouration.

7.2 Artifacts

Normally x-ray mapping and scatter diagram analyses are performed on flat polished samples to establish a well-defined relationship between the x-ray detector, the specimen and the electron beam. The pigment samples used in these experiments are made up of particles of varying compositions that are not arranged in a flat surface. This leads to overlapping particles of different compositions and pores or voids between agglomerates of particles. The uneven surface produces differences in the relative x-ray intensities which results in spreading of the phase nodes in the scatter plots. The phase nodes in the scatter diagram of the completely discoloured pigment sample (Figure 7.12) are indistinct when compared to the main node present in a pressed sample (Figure 7.16). Such samples make analyses of phase associations difficult. This effect can be seen in the scatter diagram for cadmium and sulfur of a pure cadmium yellow sample (Figure 7.24). The phase node is large and diffuse despite only one phase being present. Normally, with a known x-ray take-off angle, matrix effects, in particular x-ray absorption and fluorescence, can be corrected for using the appropriate mathematical algorithms by creating well-defined x-ray escape path lengths. The uneven surface of pigment samples creates variation in x-ray take off angles and path lengths.

In addition, incorrect phase associations can be formed in the x-ray maps and the scatter diagrams due to the overlapping of differently composed pigment particles within the x-ray generation volume of the sample. All of the mapping was done at accelerating voltages of 15 kV and 20 kV. This is a sufficient beam energy to produce an interaction volume below the surface of the sample that could penetrate through some pigment particles and into particles of different chemical composition below them. As the accelerating voltage increases the interaction volume becomes larger, potentially resulting in more overlap into neighbouring particles. This results

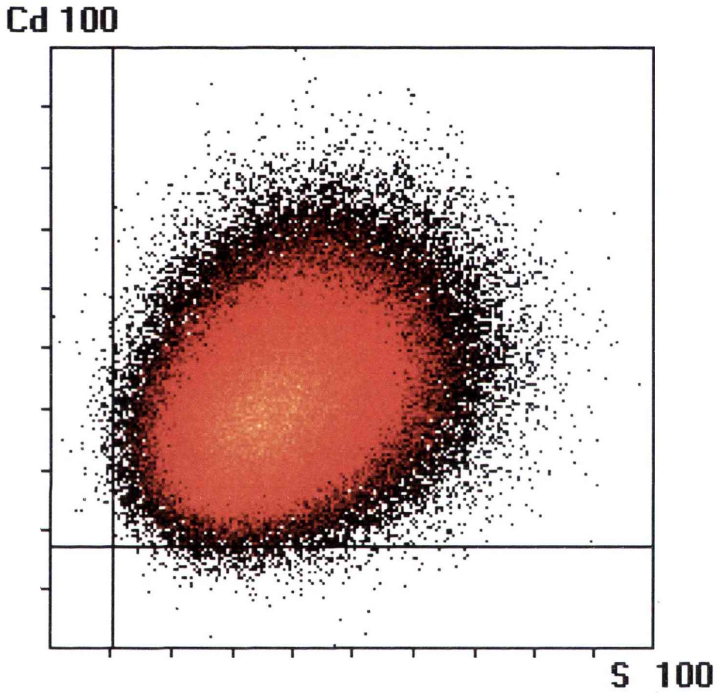

Figure 7.24: Scatter diagram of cadmium and sulfur for pure cadmium yellow pigment.

in the appearance of common intensities in the x-ray maps and therefore as a phase association in the scatter diagrams. This effect is noted in both particulate and pressed samples of the unreacted pigment mixture. Theoretically there should be separate copper and sulfur phase nodes. However, in Figure 7.5 there is a bridging between these nodes produced by both malachite and cadmium yellow particles being present in the interaction volume, from which the x-rays are produced, at the same time. This particle overlap would differ between samples and the extent of its effect on the interpretation of scatter diagrams would vary from sample to sample and map to map. X-ray spatial resolution would be improved using low voltage analyses. However, the decrease in x-ray intensity of the Cu Lα, S Kα and Cd Lα x-ray lines must be balanced by increasing the current in the probe which in turn increases the diameter of the probe decreasing the lateral x-ray spatial resolution. In this study, 15 kV and 20 kV were selected to ensure x-ray emission for characterisation and to minimise the effect of this artifact whilst still having sufficient energy to excite the necessary x-ray signals. If the beam energy is reduced to 5 kV, the scatter diagrams produced from the x-ray maps show a large diffuse node due to the decrease in x-ray spatial resolution. Figure 7.25 shows the comparison between scatter plots produced from x-ray maps of the same sample at 5 kV and 15 kV. The phase nodes visible at 15 kV are not discernible at 5 kV. This is due to the larger probe diameter required for low beam current to improve x-ray counting statistics.

Voids in the x-ray mapping area also have significant effect on the appearance of the scatter diagrams. These voids show up as the darkest areas on the x-ray maps and these pixels contribute to the scatter diagrams. They congregate around the origin and along the axes of the scatter diagram, often dipping below zero concentration.

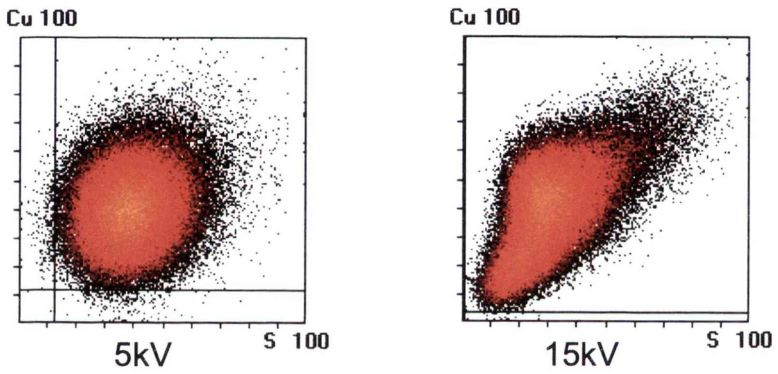

Figure 7.25: Scatter diagram of copper and sulfur at 5 kV and 15 kV, showing the lack of resolution at 5 kV.

7.3 Summation

X-ray mapping of the unreacted cadmium yellow and malachite pigment mixes and discoloured samples shows the appearance of two copper and sulfur phase associations as the discolouration increases. The production of the monovalent copper-sulfur phase (Figure 7.16) is consistent with the results obtained with x-ray diffraction analyses (Section 6.1.2). The other copper sulfide phase, a high-copper phase identified in Figure 7.17, was not detected by x-ray diffraction. However, both the thermal analysis (Section 6.2) and x-ray mapping results suggest that the discolouration products are more complex than the single CuS phase indicated by x-ray diffraction.

This technique allowed the visualisation of the changing phases within the samples. The effect of artifacts, due to sample roughness and particle overlap combined with a relatively high beam energy, on the analyses has been noted.

Chapter 8

Dynamic ESEM studies of pigment interaction

8.1 Hydration experiment procedures

One of the aims of this work was to determine if a technique for examining the chemical interaction between oil paint pigments dynamically in the ESEM could be developed. As interaction between cadmium yellow and malachite pigments occurs too slowly in linseed oil medium for effective in-situ visualisation using the ESEM, deionised water was used as the medium for the interaction. This medium is suitable for exploiting the hydration capabilities of the ESEM and allows two methods of producing the interaction to be performed. Firstly, an interface between the pigments can be made and the sample can be hydrated in the ESEM. Secondly, the pigments can be made up as pastes with deionised water and placed together as an interface and their hydration maintained in the ESEM as the interaction progresses, as detailed in Chapter 4.

8.1.1 Hydration of dry samples

Two types of hydration experiments were performed with the dry cadmium yellow and malachite pigments. The first involved a mixture of the two pigments and the second an interface between the two pigments created by pressing them into a holder side by side. In both cases the sample was maintained at a low temperature (between 3°C and 5°C in the Peltier stage while the pressure in the chamber was altered to hydrate water on to the sample and subsequently dehydrate the sample (according to Figure 3.2). The hydration of these samples was repeated several times to attempt to visualise physical structure or back-scattered contrast coefficient changes.

The experiments involving the hydration of the pigment mixture did not produce clear physical or contrast evidence of the discolouration. Figure 8.1 shows a sample of the dry mixed cadmium yellow and malachite pigments being hydrated in the ESEM at a temperature of 5°C. On comparison with Figure 8.2, it can be seen that the

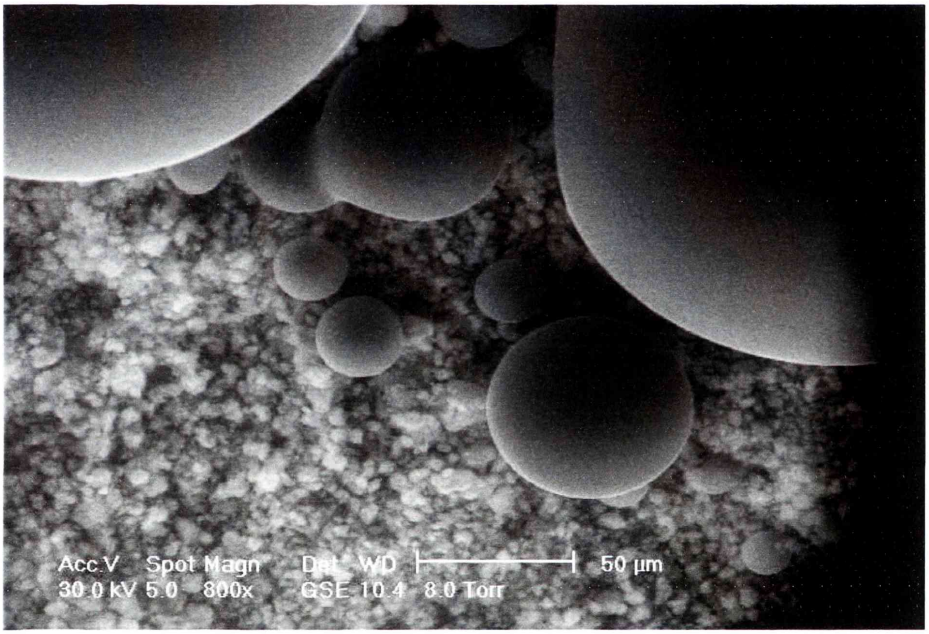

Figure 8.1: Gaseous secondary electron image of water droplets forming on a mixed cadmium yellow and malachite pigment sample during hydration in the ESEM

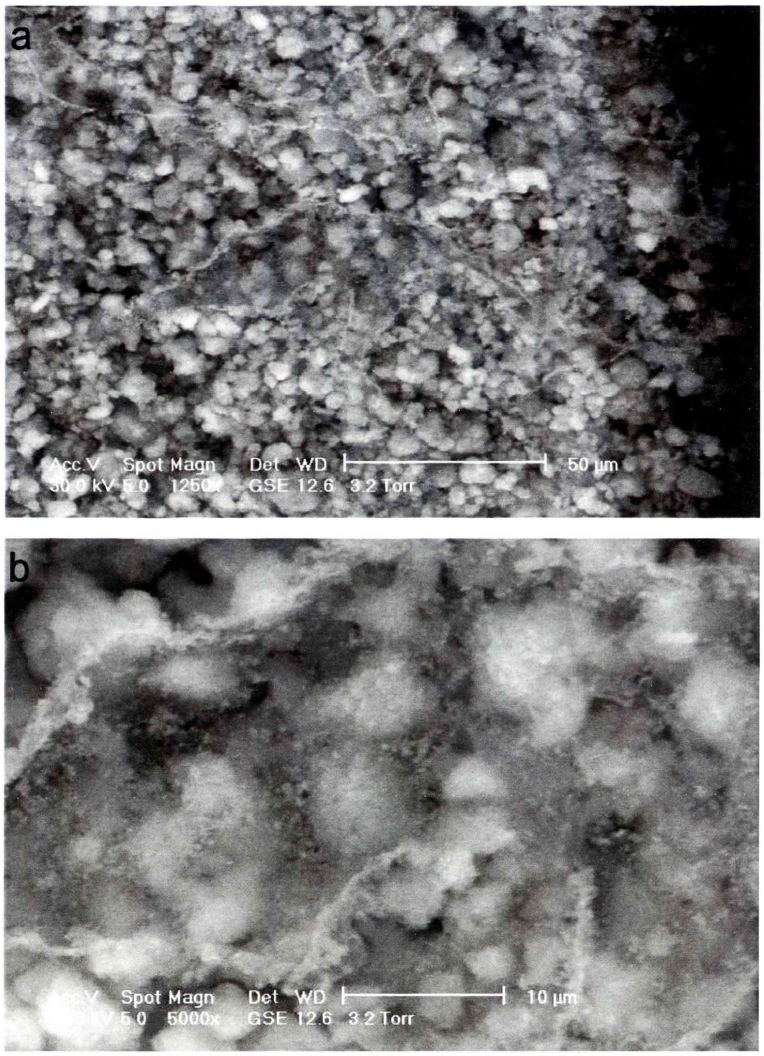

Figure 8.2: ESEM images, (a) and (b), showing the surface crust of reaction products of a cadmium yellow and malachite pigment mixture after hydration in the ESEM for four hours.

mixed pigment particles do not appear to be physically different before and after the hydration depicted in Figure 8.1. In Figure 8.2 there is a crust of nano-particles over the surface of the sample, the result of the hydration. This sort of physical change is not visible in all hydrated mixed pigment samples as these small crystals do not always form on the surface of the pigment particles in layers. This formation was the result of a sample that was hydrated for four hours, which allowed for extensive reaction of the pigments and the formation of the crystals on dehydration. These crystals are likely to be the cadmium sulfate and cadmium carbonate products of the interaction. Shorter hydration times would result in lower concentrations of these products in the water on the sample and less chance of crusts of crystals forming on dehydration.

The hydration of cadmium yellow and malachite pigment interfaces allows back-scattered contrast to be used to view the formation of the dark discolouration between the pigments over successive hydrations. In Figure 8.3(a), the contrast difference between the malachite and cadmium yellow pigments is distinct in the central highlighted region of the back-scattered electron images of the interface before hydration. Figure 8.3 (b) is the same area after one hour of hydration showing little change. However in the same region after the second hour of hydration (Figure 8.3(c)) there is significant contrast change in the cadmium yellow contrast region. This area darkens over the three images and indicates the presence of the discolouration products. The micrographs in Figure 8.3 were acquired at different chamber pressures. As chamber pressure effects the contrast, brightness and contrast gain was adjusted to give the same dynamic range for each image. The same applies for other series of images acquired during the hydration experiments.

This method of visualisation of the discolouration reaction can have limitations. As water is formed on the sample it often flows across the surface. This can cause disturbance of the pigment particles either side of the interface allowing them to be

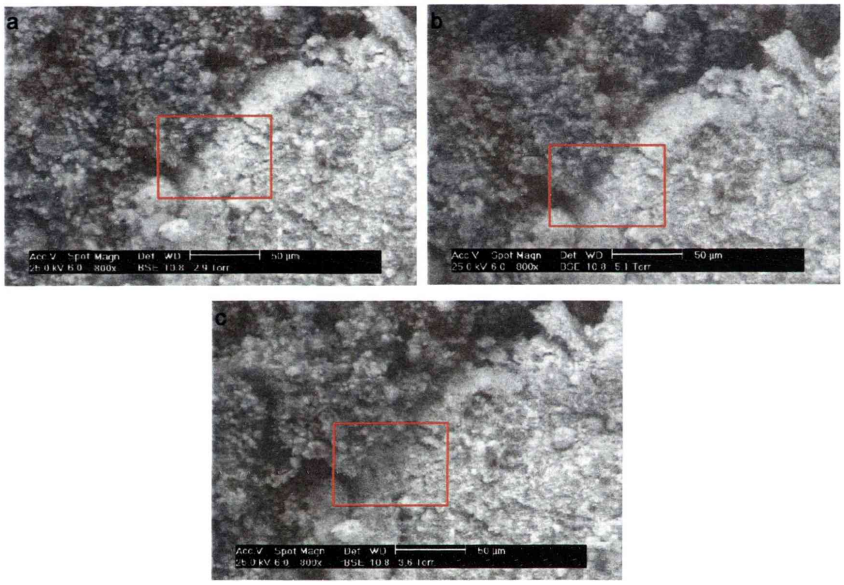

Figure 8.3: Back-scattered electron images of (a) a dry malachite (left) and cadmium yellow (right) pigment interface, (b) the interface after 1 hour of hydration and (c) after 2 hours of hydration, showing the darkening in the boxed region.

pushed across the interface. This potentially creates an area of different contrast that may be mistaken for the formation of discolouration products. In Figure 8.4, the water hydrated onto the sample can be seen to push the cadmium yellow pigment over the malachite pigment resulting in an area of mid-brightness between the two pigments. Figure 8.5, shows a nearby area at a range of accelerating voltages. The contrast of the mid region increases as the accelerating voltage decreases suggesting that a significant amount of cadmium sulfide is still present in the area. This could be as unreacted pigment particles that have been shifted, or as partially discoloured particles where the surface discolouration products are being penetrated by the beam so that some of the signal contrast is due to the interior cadmium yellow.

As the interaction occurs at the surface of the cadmium yellow particles and takes a long time to convert the entire particle to the new copper sulfide (up to several weeks (Section 5.2.1)), it is difficult to detect the creation of a new area of copper- and sulfur- containing particles using the back-scattered electron or x-ray signal. The back-scattered contrast or the presence of cadmium in the x-ray signal will not be greatly affected until discolouration is advanced. This is not achieved in the four- to eight-hour time frames of these experiments.

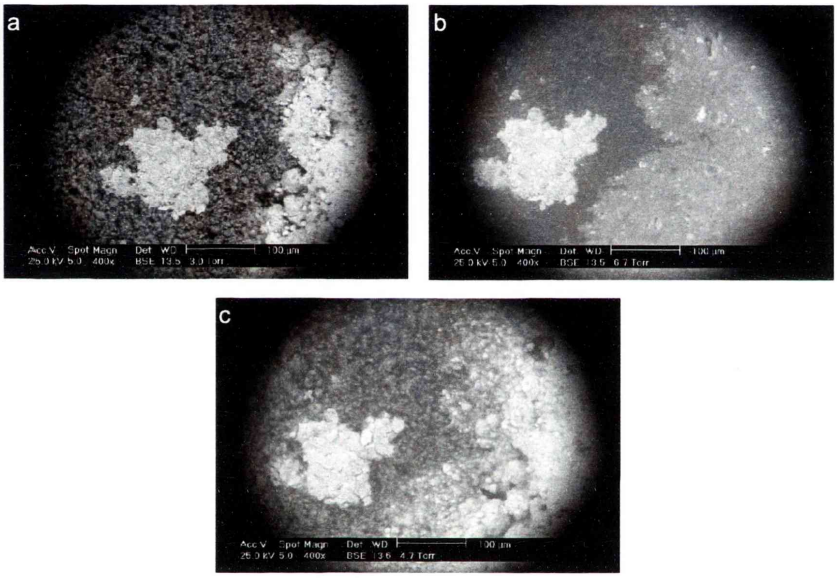

Figure 8.4: Series of back-scattered electron images showing cadmium yellow (bright regions) and malachite pigment interface. Image (a) is before hydration, (b) the interface during hydration and (c) the interface after dehydration, showing the development of a mid-brightness region.

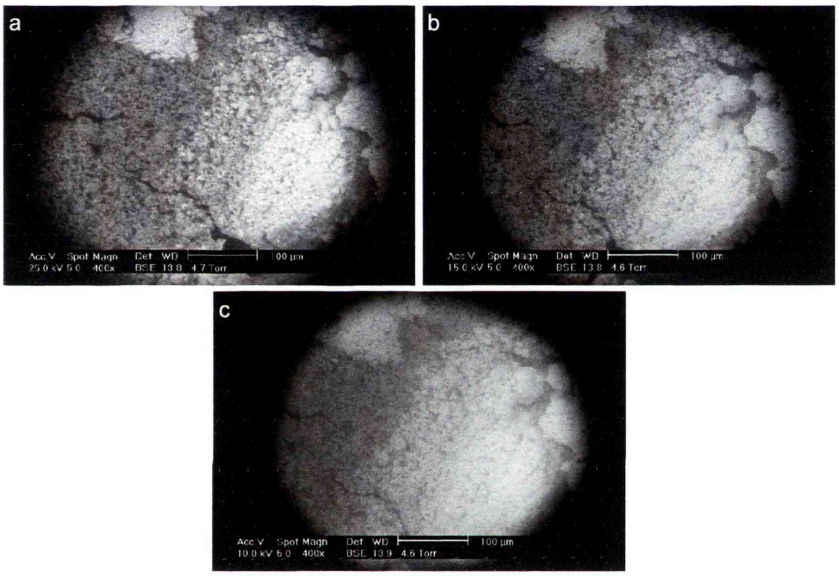

Figure 8.5: Series of back-scattered electron images showing mid-brightness region formed between malachite (left darker region) and cadmium yellow (right bright region) during hydration at accelerating voltages of (a) 25 kV, (b) 15 kV and (c) 10 kV.

8.1.2 Maintaining hydrated samples

An interface between wetted pastes of cadmium yellow and malachite was created in an attempt to produce a discolouration along the interface of the samples at the surface and at greater depths. It was hoped that the region of discolouration would be more visible as a different contrast in back-scattered electron imaging than compared with the potential movement of the pigments across the interface when hydrating dry samples. However, there were difficulties in maintaining the hydration of a paste of pigment with deionised water (Section 4.5.2). In these experiments the pigment pastes were observed to raise and lightly boil. This is most likely due to dissolved gas in the water and to air trapped in the sample paste when being prepared. This bubbling of the pastes caused disturbance of the pigment interface and a drying effect on the pigment pastes. This effect was somewhat reduced by using degassed water to prepare the pigment pastes. In addition, due to the presence of water in the pigment samples, they begin to react when they are placed together as an interface. Usually some formation of discolouration along the interface has already begun by the time the imaging of the sample is possible (normally about 5 minutes from initiating the pump-down sequence). Figure 8.6 is an example of this. In the initial ESEM micrograph (Figure 8.6(a)) after the pump-down sequence there appears to be a mid brightness region between the very bright BSE contrast of the cadmium yellow pigment on the far left and the darker malachite region on the right. The size and shape of this mid-brightness region did not change during the hydration (Figure 8.6(b)). It seems that between hydrated pigments, an interface region is formed before imaging commences and does not broaden significantly during the ESEM imaging of the region. This region is be less dense with pigment particles and the discolouration intensifies as time goes on but more prolonged periods of time would be needed to observe the growth of this mid-brightness interface.

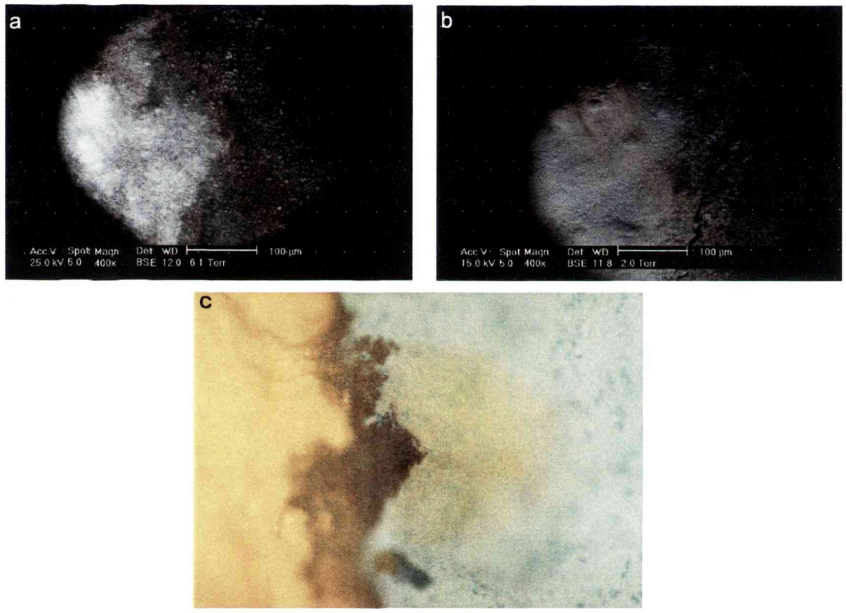

Figure 8.6: BSE images of an interface between hydrated cadmium yellow and malachite pigments. Image (a) is the first image taken of the hydrated sample after pump-down sequence. Image (b) is the dehydrated interface after 80 minutes of maintained hydration. Image (c) is an optical micrograph of the interface after dehydration (WOF = 1mm).

8.2 Summation

The visualisation of the progressive discolouring interaction between cadmium yellow and malachite pigments in the ESEM is problematic. The nature of the interaction requires hydration of the pigments (either in water or linseed oil) for reaction to occur. Examination of this system by interaction in water was selected for this work to complement the hydration capabilities of the ESEM and because the interaction in oil occurs over a larger time frame than is possible for electron microscopy.

The hydration of an interface created between the two dry pigments can result in the shift of less compacted surface particles across the interface causing interaction on the top of the sample and misleading BSE information. This method does hydrate the pigments through the bulk of the sample but achieving a straight plane of interface normal to the electron beam is difficult to achieve as the pigments need to be pressed down. This well-defined interface is somewhat easier with previously hydrated pigments placed in contact as the pigments are not pressed down to ensure contact. However the pigments begin to react immediately when placed in contact with each other and have already undergone some discolouration by the time imaging is possible. Maintaining the hydration of these pigments is also difficult. They tend to boil slightly during the pump-down sequences resulting in disturbance of the interface and slight drying of the pastes.

The interaction between cadmium yellow and malachite pigments is a surface discolouration of cadmium yellow particles by copper ions dissolved from the malachite (Section 2.4.1). This discolouration progresses into the particles over time eventually converting all the cadmium yellow material to a copper sulfide. This process takes several weeks to achieve in the laboratory experiments of the pigments mixed in deionised water and agitated occasionally (Section 4.1.3). The in-situ ESEM experiments are conducted in a matter of four to eight hours. Although discolouration

is achieved in that time frame, the discoloured particles are a core of cadmium yellow surrounded by the copper sulfide produced at the surface. This will have an effect on the BSE contrast of the discoloured regions. They may seem brighter than anticipated. Added to that is the potential of cadmium yellow particles to wash over malachite particles during the hydration of a dry sample. This would lower the overall BSE contrast of that region of the sample and appear as if a mid-brightness region has emerged between the pigments.

It appears that this interaction system is difficult to study accurately using the hydration capabilities of the ESEM. This situation could potentially be improved by the use of mechanical separation of hydrated pigment pastes during the pump-down sequences, or by improved production of a compacted dry pigment interface.

Chapter 9

Discussion of key results

The issue of discolouring interactions between pigments in oil paintings was of considerable concern for artists during the nineteenth century (Carlyle 2001). The scientific and manufacturing advances of the era had brought artists new materials (including pigments) and their commercial production. These factors changed the way that artists produced their work and led to many of the problems that occurred in paintings of the nineteenth century (Mayer 1991). The discolouration of a paint layer due to its pigments was generally suggested to be caused by the interaction between lead or copper based pigments and sulfide-containing pigments. It appears, from an examination of the literature (Section 2.3) and from experimental investigations (Section 5.1), that a discolouring chemical interaction between artistic oil paint pigments occurs between cadmium sulfide pigments and copper-containing pigments. The suggested interactions involving lead white pigment and vermillion pigments are related discolouration due to impure pigments (Gettens & Sterner 1941, Gettens *et al.* 1993a) and environment (Spring & Grout 2002).

The dark discolouring interaction between cadmium yellow and malachite pigments was selected for study as these pigments are readily available examples of cadmium sulfide and copper-containing pigments. The discolouration was observed to occur between the pigments in oil paint and in deionised water (Chapter 5). Cadmium yellow pigment can also be discoloured in contact with copper ions from soluble copper salts (Section 5.3). The x-ray diffraction analyses of the products of the interaction between these pigments (Section 6.3.2) identified the compounds produced to be covellite (cupric sulfide), otavite (cadmium carbonate) and hydrated cadmium sulfate. The covellite is the cause of the dark brown to black colouring that appears between the pigments and predominately on the surface of the cadmium yellow particles. The presence of a copper sulfide after the interaction of these pigments is supported by the findings of Salvadó *et al.* (2003). In that work the discolouring copper sulfides were identified as Chalcocite-Q($Cu_{1.95}S$), Roxbyite (Cu_7S_4) and

Yarrowite (Cu_9S_8). These were produced by interaction between cadmium sulfide pigments and copper ions from a copper metal substrate. Cadmium carbonate and hydrated cadmium sulfate are both white and do not contribute to the discolouration. The hydrated cadmium sulfate is present in the pigments reacted in water and is due to the oxidation of cadmium sulfide in water (Section 6.1.1); thus it is not likely to be a product of the interaction in linseed oil. The development of phases containing copper and sulfur was observed with scatter diagram analyses of x-ray maps of the interaction (Section 7). Scatter diagrams for unreacted pigment mixtures show no significant association between copper and sulfur. However, if the mixture is partially discoloured the scatter diagram shows a phase association for the two elements. A fully discoloured pigment mixture indicated that there are two main common copper- and sulfur-containing phases present as discolouration products. One of these was identified as covellite (CuS) by x-ray diffraction. The other phase, a high-copper copper sulfide, indicated on the scatter diagrams (Figure 7.17), was not identified by the current JCPDS database. The thermal analyses (Section 6.2) also suggest that the discolouration products are more complex than just covellite. As the discolouration reaction is heterogenous, it is likely to produce x-ray amorphous products.

The x-ray diffraction results suggest that a simple dissolution and re-precipitation process is occurring based on the relative solubilities of the reactants and products:

$$CdS + Cu^{2+} \longrightarrow CuS + Cd^{2+}$$

However, the thermal analyses (Section 6.2) indicate the complexity of the range of phases produced by the simple ion exchange mechanism proposed. The identification of these phases, presumably either too small for characterisation by x-ray diffraction or non-stoichiometric and x-ray amorphous, requires investigation beyond the scope of this work.

The interaction has been shown to occur on the surface of the cadmium sulfide

particles (Section 6.3.2). Copper ions diffuse through the oil or deionised water media to the surface of the cadmium yellow particles. These copper ions are liberated by malachite (and other copper-containing pigments) in both linseed oil and deionised water (Gunn *et al.* 2002, Salvadó *et al.* 2003). X-ray diffraction patterns of the progressive discolouration of the cadmium yellow and malachite mixture in deionised water (Section 6.1.3) show that malachite is consumed as the discolouration increases. These ions are transported through the oil or water medium to the surface of the cadmium yellow particles. There is essentially an exchange of cadmium ions for copper ions at the surface which results in the outer part of the cadmium yellow particles being dissolved and copper sulfide precipitated. Initially the entire surface of the particles is converted to copper sulfide. The extent of conversion of the particle to copper sulfide depends on the diffusion of copper ions within the particle and the particle size. For the finely divided cadmium yellow particles (75 to 100 nm diameter), the surface-to-volume ratio is high. This provides a greater surface area to react with and a shorter time to complete conversion than for larger particles. A similar interaction, involving cuprous (Cu(I)) rather than cupric copper, is part of the production of solar cells and that interaction has undergone extensive study (Section 2.4.1).

The discolouring process has been examined in this work as it occurs in aqueous media rather than in linseed oil. This is because the interaction between cadmium yellow and malachite occurs more rapidly in deionised water than in oil. As it is a more easily removable medium, water allows the analyses of products and processes without the presence of linseed oil. The reaction in water allows the interaction to be examined using the hydration capabilities of the ESEM. The difference in behaviour of the interaction in the two mediums is that in oil the discolouration occurs slowly due to the viscosity of the medium and continues to occur until the paint film is completely dry. In aqueous media, the interaction is rapid but will only occur while

liquid water is present.

The information from experimental observations, characterisation techniques and literature (Section 2.4) can be condensed into the following interaction model:

Malachite pigment produces copper ions when in aqueous solution and linseed oil. These copper ions diffuse through the water or oil medium to the surface of cadmium yellow particles. Here they precipitate cuprous sulfide (CuS) with sulfur available from the dissolution of the cadmium sulfide structure at the surface of the particles. After the surface of the particles has reacted, copper ions migrate further into the particles until they are completely converted to copper sulfide. This process is slower than the initial surface discolouration and explains the observation of the dark olive green colour that the reaction mixture takes on in both oil and water before it blackens. The following reaction scheme represents this. The presence of zinc in cadmium yellow is omitted from this reaction scheme as it only contributes colour to the cadmium pigment and is not involved in the discolouration.

$$CdS + Cu^{2+} \longrightarrow CuS + Cd^{2+}$$

The discolouration between the cadmium yellow and malachite pigments in water also produces cadmium carbonate and hydrated cadmium sulfide (previously identified as due to oxidation of pigment in water). It would appear that the cadmium ions released by the conversion of the cadmium yellow particles to copper sulfide combine with carbonate ions (from the dissolution of malachite in water) to form cadmium carbonate. If any cadmium hydroxide was formed with hydroxide ions (also from malachite dissolution), it was not detectable by x-ray diffraction. This interaction model is represented as a schematic diagram in Figure 9.1.

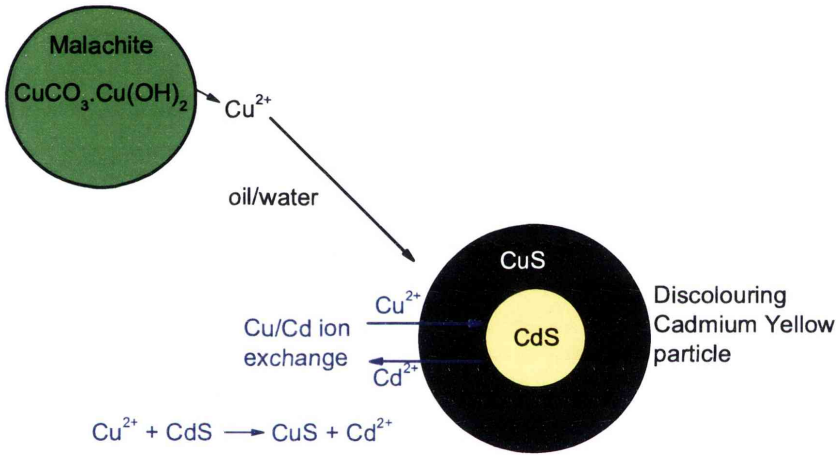

Figure 9.1: Interaction model for the discolouration of cadmium yellow pigment by malachite pigment.

It is possible that the discolouration products of this interaction in linseed oil could be different. The copper sulfide produced may not be covellite (CuS) but other copper sulfides such as those found by Salvadó *et al.* (2003). Hydrated cadmium sulfate is unlikely to occur in an oil paint layer as a result of this pigment interaction as it is due to oxidation of cadmium yellow in water. The production of cadmium carbonate is possible but would be dependant on whether or not cadmium ions migrate through oil paint layers in the same manner as copper ions (Section 2.4). For the reaction between cadmium yellow and malachite pigments in water, the formation of cadmium carbonate occurs by the following reaction:

$$Cd^{2+} + 2CO_3^{2-} \longrightarrow CdCO_3$$

The change in phase associations of the constituent copper, cadmium and sulfur elements during discolouration was evident in the x-ray mapping experiments. The scanning electron microscope was used to scan selected areas of a range of samples and produced micrographs of the detected x-ray signals. These maps were then analysed using scatter diagrams. The association between the copper and sulfur species changes from no association in the unreacted sample to common phases in the reacted sample, reflecting the results of the other techniques. These changes were visualised on the corresponding micrographs to represent the distribution of the emerging phases. These experiments also highlighted the artifacts that can be produced by non-ideal samples. The pigment samples were pressed to avoid surface-related x-ray intensity changes and the resultant spreading of phase nodes in the scatter diagrams. X-ray spatial resolution was improved by using a lower beam energy.

The discolouring interaction was produced in the ESEM either by hydration-dehydration cycles on interfaces of the dry pigments or by maintaining the hydration of an interface of the wet pastes (Chapter 8). In order to exploit this capability, the interaction required the use of water as the reacting medium rather than linseed

oil. A linseed oil medium would have been impractical for these experiments as the interaction takes several weeks to appear to the naked eye and the microscopic changes occur too slowly for dynamic experimentation. The visualisation of the discolouration was achieved by using the back-scattered electron signal to provide compositional contrast images of the interfaces. The discolouration products are seen as a mid-brightness region between the dark malachite and bright cadmium yellow. Figures 8.3, 8.4 and 8.5 are all back-scattered electron images of interfaces of cadmium yellow and malachite that have been through a number of hydration-dehydration cycles. All exhibit a mid-brightness region between the two pigments. Despite the initial surface reaction of the discolouration, this technique can be successfully used to show the formation of the discolouration products at the interface between cadmium yellow and malachite pigments. One of the original aims of this project was to determine if a technique for examining pigment discolouration in oil paints using the low vacuum capabilities of the Environmental Scanning Electron Microscope could be developed. Although the discolouring system was successfully observed, there are a number of challenging practical problems with using the instrument's hydrating capabilities for the examination of interacting pigments. Movement of individual pigment particles or cracking can occur during the hydration-dehydration cycles. The formation of water on the sample can occur in such a way that a layer of water flows across the surface of the sample which can disturb the surface pigment particles. The hydration can also lead to water forming between the pressed pigments and the sample holder, occasionally lifting the sample out of its holder or cracking along the interface between the two pigments. All of these can prevent the continuation of an experiment.

The other hydration technique was less successful. Figure 8.6 shows the mid-brightness region of an interface sample initially made up of wet pastes of cadmium yellow and malachite pigments. The hydrated state of this sample was maintained over a period of 80 minutes. However, it appears that the discoloured mid-brightness

region is present from the initial imaging and it does not broaden over time. This indicated that the discolouration of the interface between the wet pastes of the pigments is too rapid for examination using the ESEM, unless they can be separated until imaging can commence. To compound this issue, wet pastes of samples frequently boiled despite very careful control of chamber evacuation, chamber pressure and sample temperature (Section 8.1.2). However, the boiling of these samples might be a factor of the particular compounds used in this experiment.

Chapter 10

Conclusions

10.1 Interaction between cadmium yellow and malachite pigments

The interaction between historic oil paint pigments was found to be limited to cadmium sulfide pigments (including cadmium yellow) and copper-containing pigments (malalchite is the example in this case). The discolouring interaction occurs by an exchange of ions, via a dissolution and reprecipitation process, at the surface of the cadmium sulfide particles producing a black-coloured copper sulfide layer which was found to be covellite. Over time entire particles are converted to copper sulfide. The smaller the pigment particles, the greater the surface-to-volume ratio and the faster the reaction. This discolouration occurs both in linseed oil and in water, more rapidly in the latter. The effect of the discolouration in an oil painting is a darkening of a region of the paint layer where these pigments are present in the same or adjacent layers. Whether this discolouration visually affects the painting is dependant on the depth and the size of the painted area where this pigment combination was used. The potential for this discolouration to occur in modern oil paintings exists as cadmium sulfide and copper-containing pigments and paints are still available to artists. Encapsulating copper pigments in separate oil paint layers will not prevent the discolouration from occurring as the copper ions are mobile between paint layers.

10.2 Suitability of SEM as a pigment analysis technique

Two main scanning electron microscope techniques were used to examine the interaction between malachite and cadmium yellow pigments. These were x-ray mapping with scatter diagram analyses and ESEM. The x-ray mapping experiments and subsequent analyses clearly show the formation of common copper- and sulfur-containing phases as the pigments are discoloured, from the separate phases of the unreacted pigment mixture. The surface roughness of the dry ground pigment does cause x-ray intensity fluctuations which, along with voids present in the sample, result in spreading of phase nodes and accumulation of nodes at the origin in the scatter diagrams. The effect of this artifact can be minimised by pressing the sample into a pellet to achieve a flat solid surface. X-ray spatial resolution, an issue in all x-ray mapping analyses, was improved by reducing the accelerating voltage. This technique is useful for examining pigment interaction as the changes in phase association can be clearly visualised. However, care needs to be taken when preparing dry pigment powder samples to minimise artifacts.

The discolouration between cadmium yellow and malachite pigment interfaces was successfully created and visualised in-situ in the ESEM (Section 8.1.1). Discolouration occurred due to successive hydration and dehydration cycles on an interface of the two pigments. The interaction products were observed as a mid-brightness backscattered electron signal between the dark malachite and bright cadmium yellow pigments. However, samples can be damaged during hydration, preventing further examination of the interaction.

10.3 Significance for painting conservators

The discolouration that results from the chemical interaction between cadmium sulfide and malachite cannot be reversed. It is a permanent change to the cadmium sulfide pigment and at best could be removed mechanically (Salvadó *et al.* 2003) depending on its placement and extent. It may even be possible to remobilise copper ions in oil paint layers by placing them in contact with fresh oleoresinous materials (Gunn *et al.* 2002). There is some potential for an interaction to occur due to solvent action. Of the solvents examined (Section 5.2.3), both deionised water and acetone result in the discolouration of cadmium yellow paint chips in the presence of malachite paint chips. Discolouration of the cadmium yellow paint also occurs in deionised water with copper metal and occurs immediately in copper sulfate solution. The likelihood of these solvents being in contact with both cadmium yellow and copper-containing pigments or copper metal for enough time during conservation treatments to cause significant discolouration is remote, unless high humidity is a factor. It is even less likely that a cadmium sulfide paint layer would come into contact with a copper sulfate solution. However, conservators should be aware that this kind of discolouring interaction could be activated on a painting's surface and cause visual damage. Other solvents may have the same effect but an extensive study of all solvents that conservators use on paintings, age of paint layer, length of solvent contact with the paints and possible discolouration was beyond the scope of this project.

The occurrence of discolouration in oil painting has become less of a concern to artists during the twentieth century. Production methods for oil paint pigments have improved and impurities are less common; some of the toxic and coincidentally discolouring pigments (emerald green and vermillion) have been removed from general artistic use; and artists have begun to employ other mediums and pigments for their work. Despite these effects significant discolouration of an oil paint layer could still

occur in modern paintings. Both cadmium sulfide and copper-containing pigments are available to today's artists in both pigment and paint form. Perhaps more importantly, this interaction can potentially discolour paintings that are being restored. In-painting of an area of paint loss tends to be performed using traditional pigments and mediums. If a section of a painting was to be repainted using a combination of cadmium sulfide and copper-containing pigments, in the same or an adjacent oil paint layer, then the resulting interaction could adversely effect the appearance of the painting. It is important for painting conservators and artists to appreciate the discolouring potential of this interaction so they may reduce its effect on current and future artworks.

Bibliography

Barnes S.H., Electron Microscopy and Analysis at the Natural History Museum, *Microscopy and Anlaysis* 25, 29–31 (1991)

Bhide V.G., Salkalachen S., Rastogi A.C., Rao C.N.R. & Hegde M.S., Depth profile composition studies of thin film CdS:Cu2S solar cells using XPS and AES, *Journal of Physics D: Applied Physics* 14, 1647–1656 (1981)

Biernacki L. & Pokrzywnicki S., On the pyrolytic decomposition of cadmium carbonate: Thermogravimetry and exoemission of electrons, *Journal of Thermal Analysis* 47 (1996)

Boon J., Keune K., van der Weerd J., Geldof M. & van Asperen de Boer J., Imaging Microspectroscopic, Secondary Ion Mass Spectrometric and Electron Microscopic Studies on Discoloured and Partially Discoloured Smalt in Cross-sections of 16th Century Paintings, *Chimica* 55, 952–960 (2001)

Bower N., Stulik D. & Doehne E., A critical evaluation of the environmental scanning electron microscope for the analysis of paint fragments in art conservation, *Fresenius Journal of Analytical Chemistry* 348, 402–410 (1994)

Bright D., Measurement of chemical components using scatter diagrams with principal component analysis, in *29th Annual Conference of the Microbeam Analysis Society*, 403–404, National Institute of Standards and Technology (1995)

Bright D. & Newbury D., Concentration histogram imaging: A scatter diagram technique for viewing two or three related images, *Analytical Chemistry* 63, 243A–250A (1991)

Buckley R.W. & Woods J., The formation of cuprous sulphide on singles crystals of cadmium sulphide, *Journal of Physics D: Applied Physics* 7, 663–667 (1974)

Cam D. & Fan J., Antique Chinese Paintings studied by LM, SEM and Microanalysis, *Microscopy and Analysis* 79, 25–26 (2000)

Cameron R. & Donald A., Minimising sample evaporation in the Environmental Scanning Electron Microscope, *Journal of Microscopy* 173, 227–237 (1994)

Carlyle L., *The Artist's Assistant*, Archetype Publications, London, England (2001)

Cavallo G., The blue pigment used in Vallemaggia (Switzerland) in the half of the 19th century by painters Vanoni and Pedrazzi, *Microchimica Acta* 155, 121–124 (2006)

Church A.H., *The Chemistry of Paints and Painting*, Seeley and Co Ltd., London, England, 2nd edition (1892)

Danilatos G., *In-Situ Microscopy in Materials Research*, chapter 2, Kluwer Academic, The Netherlands (1997)

Doehne E. & Stulik D., Applications of the Environmental Scanning Electron Microscope to Conservation Science, *Scanning Microscopy* 4 (1990)

Doehne E. & Stulik D., Dynamic Studies of Materials using the Environmental Scanning Electron Microscope, in Vandiver P.B., editor, *Materials Research Society Symposia Proceedings*, volume 185, 31–37 (1991)

Doerner M., *The Materials of the Artist and their Use in Painting (revised from the 1934 edition)*, Harcourt, Inc, New York, USA (1984)

Doménech-Carbó M., Casas-Catalán M., Doménech-Carbó A., Mateo-Castro R., Gimeno-Adelantado J. & Bosch-Reig F., Analytical study of canvas painting collection from the *Basilica de la Virgen de los Desamparados* using SEM/EDX, FT-IR, GC and electrochemical techniques, *Fresenius Journal of Analytical Chemistry* 369, 571–575 (2001)

Dredge P., Wuhrer R. & Phillips M.R., Monet's Painting under the Microscope, *Microscopy and Microanalysis* 9, 139–143 (2003)

Fiedler I. & Bayard M., *Artists' Pigments: A Handbook of Their History and Characteristics*, volume 1, chapter Cadmium Yellows, Oranges and Reds, 65 – 108, Oxford Univeristy Press, Oxford, England (1986)

Fiedler I. & Bayard M., *Artists' Pigments: A Handbook of Their History and Characteristics*, volume 3, chapter Emerald Green and Scheele's Green, 219–271, Oxford Univeristy Press, Oxford, England (1997)

Frost R., Ding Z., Kloprogge J. & Martens W., Thermal stability of azurite and malachite in relation to the formation of mediaeval glass and glazes, *Thermochimica Acta* 390, 133–144 (2002)

Gettens R. & Sterner F.W., Compatibility of Pigments in Artists' Oil Paints, *Technical Studies in the Field of the Fine Arts* 10, 18–28 (1941)

Gettens R. & Stout G.L., *Painting Materials: A Short Encyclopedia (reprinting of 1942 edition)*, Dover Publicaions, New York, USA (1966)

Gettens R.J., Feller R.L. & Chase W.T., *Artists' Pigments: A Handbook of Their History and Characteristics*, volume 2, chapter Vermillion and Cinnabar, 159–182, Oxford Univeristy Press, Oxford, England (1993a)

Gettens R.J., Khn H. & Chase W.T., *Artists' Pigments: A Handbook of Their History and Characteristics*, volume 2, chapter Lead White, 67–81, Oxford Univeristy Press, Oxford, England (1993b)

Goldstein J.I., Newbury D.E., Echlin P., Joy D.C., Romig-Jr A.D., Lyman C.E., Fiori C. & Lifshin E., *Scanning Electron Microscopy and X-Ray Microanalysis*, Plenum Press, New York, USA, 2nd edition (1992)

Green M.A., *Solar Cells: Operating Principles, Technology and System Applications*, University of New South Wales, Kensington Australia (1986)

Grön J. & Beghello L., Cracking and roughening of coated paper surfaces, *Paperi Ja Puu* 78, 121–127 (1996)

Gunn M., Chottard G., Rivire E., Girerd J.J. & Chottard J.C., Chemical reactions between copper pigments and oleoresinous media, *Studies in Conservation* 47, 12–23 (2002)

Hadley-Jr H.C. & Tseng W.F., Materials Aspects of Cu_2S for CdS/Cu_2S Solar Cells, *Journal of Crystal Growth* 39, 61–72 (1977)

Isarov A.V. & Chrysochoos J., Optical and Photochemical Properties of Nonstoichiometric Cadmium Sulfide Nanoparticles: Surface Modification with Copper(II) Ions, *Langmuir* 13, 3142–3149 (1997)

Ives S., John Peter Russell's Vue d'Antibes: A problem with purity, *artonview* 14–16 (1996)

JCPDS, *Powder Diffraction File*, Joint Committee For Diffraction On Powder Diffraction Standards, International Centre for Diffraction Data, Swarthmore, PA, USA (2005)

Kanda K. & Joy D.C., Monte Carlo Simulation, freeware (1996)

Katsibiri O. & Boon J., Investigation of the gilding technque in two post-Byzantine wall paintings using microanalytical techniques, *Spectrochimica Acta Part B* 59, 1593–1599 (2004)

Koga N. & Tanaka H., Thermal decomposition of copper(II) and zinc carbonate hydroxides by means of TG-MS: Quantitative analyses of evolved gases, *Journal of Thermal Analysis and Calorimetry* 82 (2005)

Kuisma-Kursula P., Accuracy, Precision and Detection Limits of SEM-WDS, SEM-EDS and PIXE in the Multi-Elemental Analysis of Medieval Glass, *X-ray Spectrometry* 29, 111–118 (2000)

Lahanier C., Scientific Methods Applied to the Study of Art Objects, *Mikrochimica Acta* 2, 245–254 (1991)

Leone B., Burnstock A., Jones C., Hallebeek P., Boon J. & Keune K., The deterioration of cadmium sulphide yellow artist's pigments, in Verger I., editor, *14th Triennial Meeting, The Hague, 12-16 September 2005: Preprints (ICOM Committee for Conservation)*, 803–810, ICOM Committee for Conservation, James and Jamies Ltd (2005)

Lide D.R., *CRC Handbook of Chemistry and Physics*, CRC Press Inc., Florida, USA, 74 edition (1993-1994)

Mayer R., *The Artist's Handbook of Materials and Techniques*, Viking, 5th edition (1991)

Messier P. & Vitale T., Cracking in Albumen Photographs: An ESEM Investigation, *Microscopy Research and Technique* 25, 374–383 (1993)

Mirti P., X-Ray Microanalysis Discloses the Secrets of Ancient Greek and Roman Potters, *X-ray Spectrometry* 29, 63–72 (2000)

Moran K. & Wuhrer R., X-ray mapping and interpretation of scatter diagrams, *Microchimica Acta* 155, 209–217 (2006)

Morgan S., *Gaseous secondary electron detection and cascade amplification in the environmental scanning electron microscope*, Ph.D. thesis, University of Technology, Sydney (2005)

Nylén P. & Sunderland E., *Modern Surface Coatings*, Interscience Publishers, London, England (1965)

Olszak-Humienik M. & Mzejko J., Eyring parameters of dehydration processes, *Thermochimica Acta* 405 (2003)

Roseboom-Jr E., An investigation of the system Cu-S and some natural copper sulfides between 25° and 700°C, *Economic Geology* 61, 641–672 (1966)

Russell G.J. & Woods J., An electron diffraction study of phases in the CuxS system, *Physica Status Solidi A: Applied Research* 46, 433–444 (1978)

Salvadó N., Molera J. & Vendrell-Saz M., Nature and origin of black spots found on Miró paintings: a non-invasive study, *Analytica Chimica Acta* 479, 255–263 (2003)

Scott D.A., *Copper and Bronze in Art: Corrosion, Colorants, Conservation*, Getty Publications, Los Angeles, USA (2002)

Skoog D. & Leary J.J., *Principles of Instrumental Analysis*, Saunders College Publishers, Fort Worth, Texas, USA, 4th edition (1992)

Smith G.D. & Clark R.J.H., The role of H_2S in pigment blackening, *Journal of Cultural Heritage* 3, 101–105 (2002)

Spring M. & Grout R., The Blackening of Vermillion: An Analytical Study of the Process in Paintings, *National Gallery Technical Bulletin* 23, 50–61 (2002)

Standage H.C., *The Use and Abuse of Colours and Mediums in Oil Painting*, Reeves and Sons Ltd., London, England (1892)

Stanley A., Cadmium Sulfide Solar Cells, *Applied Solid State Science* 5, 251–366 (1975)

Stulik D. & Doehne E., Applications of Environmental Scanning Electron Microscopy in Art Conservation and Archaeology, in Vandiver P.B., editor, *Materials Research Society Symposia Proceedings*, volume 185, 23–29 (1991)

te Velde T., The production of the cadmium sulphide-copper sulphide solar cell by means of a solid-state reaction, *Energy Conversion* 15, 111–115 (1975)

te Velde T. & Dieleman J., Photovoltaic efficiencies of copper-sulphide phases in the topotaxial heterojunction copper-sulphide-cadmium-sulphide, *Phillips Research Reports* 28, 573–595 (1973)

Thiel B., Bache I.C., Fletcher A.L., Meredith P. & Donald A.M., An improved model for gaseous amplification in the environmental SEM, *Journal of Microscopy* 187, 143–157 (1997)

Thiel B. & Donald A., The study of water in heterogenous media using Environmental Scanning Elelctron Microscopy, *Journal of Molecular Lquids* 80, 207–230 (1999)

Thiel B.L., Review of electron-gas interactions in the environmental SEM, *Microcopy and Microanalysis* 5, 272–273 (1999)

Thomas P., Hirschausen D., White R., Guerbois J. & Ray A., Characterisation of the oxidation products of pyrite by thermogravimetric and evolved gas analysis, *Journal of Thermal Analysis* 72, 769–776 (2003)

Townsend J.H., Carlyle L., Khandekar N. & Woodcock S., Later nineteenth century pigments: evidence for additions and substitutions, *The Conservator* 19, 65–78 (1995)

Tucker J. & DeGroft A., From Renaissance Art to Contempory Electron Microscopy: DeGroft's Rediscovery of Titan's "Lost" *Portrait of Federico II Gonzaga, Duke of Mantua*, of 1539-40, *Ultrastructural Pathology* 26, 195–201 (2002)

van Loon A. & Boon J., Characterization of the deterioration of bone black in the 17th century *Oranjezaal* paintings using electron-microscopic and micro-spectroscopic imaging techniques, *Spectrochimica Acta Part B* 59, 1601–1609 (2004)

van Overstraeten R.J. & Mertens R.P., *Physics, Technology and Use of Photovoltaics*, 166, Adam Hilger Ltd, Bristol, England (1986)

Wallert A., Deliquesence and recrystallisation of salts in the Dead Sea Scrolls, in Roy A. & Smith P., editors, *Archaeological Conservation and its Consequences*, 198–202 (1996)

Wexler H., Polymerization of drying oils, *Chemical Reviews* 64, 591–611 (1964)

Wieczoreck-Ciurowa K., Shirokov J. & Parylo M., The use of thermogravimetry to assess the effect of mechanical activation of selected inorganic salts, *Journal of Thermal Analysis and Calorimetry* 60 (2000)

Wuhrer R., Moran K. & Moran L., Characterisation of materials through x-ray mapping, *Materials Forum* 57, 17–27 (2006)